Alma Mater Studiorum – Università di Bologna

DOTTORATO DI RICERCA IN

Oncologia, Ematologia e Patologia

Ciclo XXX

Settore Concorsuale: 06/A2

Settore Scientifico Disciplinare: MED/04

The impact of ST6Gal-I in the progression of colorectal cancer

Presentata da: Dott.ssa Giulia Venturi

Coordinatore Dottorato Prof. Pier Luigi Lollini

Supervisore Prof. Fabio Dall'Olio

Esame finale anno 2018

ABSTRACT

One of the hallmarks associated with cancer is an aberrant expression of glycans decorating the plasma membrane due to altered expression of glycosyltransferases. The elevation of sialyltransferase ST6Gal-I and of its cognate glycan structure Sia6LacNAc has been described in colon and other cancers and controversially associated with malignancy. In this study, we investigated the relationship between ST6Gal-I mRNA expression and clinical features in a cohort of over 600 colorectal cancer (CRC) cases on The Cancer Genome Atlas, finding that low ST6Gal-I expression was associated with a microsatellite unstable and mucinous phenotype, and with BRAF mutation, but not with clinical stage or survival.

To investigate the effect of ST6Gal-I overexpression on CRC, we retrovirally transduced with the human ST6Gal-I cDNA or with an empty vector the cell lines SW48 (microsatellite unstable) and SW948 (chromosomal unstable), generating their ST and NC variants respectively. Transcriptomic analysis of the two cell lines revealed a higher number of modulated genes in SW948 ST compared with SW48 ST. SW948 ST (but not SW48 ST) displayed an accelerated apoptotic response compared to NC, while SW948 ST (but not SW48 ST) displayed increased ability to heal the wound than SW948 NC. In soft agar assay, SW948 ST (but not SW48 ST) cells generated fewer clones, although bigger, than SW948 NC. SW48 ST (but not SW948 ST) displayed a reduced capacity to invade Matrigel compared to NC. Treatment with HGF caused an increase of FAK phosphorylation in SW948 NC cells and a decrease in ST cells. Similar results were observed in SW48 NC and ST cells. With ALDH staining we observed a population of cancer stem cells in the two cell lines with no differences derived from ST6Gal-I overexpression. These results indicate a very cell type specific effect of ST6GAL1 and Sia6LacNAc on the phenotype of CRC cells.

List of abbreviations

5'-UTR: 5' untranslated region
ABCG2: ATP-binding cassette sub-family G member 2
Akt: AKR mouse thymoma kinase or protein kinase B
ALDH: aldheyde dehydrogenase 1
ALG: Asparagine Linked Glycosylation
ANOVA: Analysis of Variance
APC: adenomatous polyposis coli
AURKA: Estrogen-Induced Aurora Kinase-A
Bak: BCL2 antagonist/killer
BAX: gene BCL2 Associated X
BCG: Bacillus Calmette-Guerin
Bcl-2: B-cell lymphoma 2
BH3: Bcl-2 homology domain 3
BMYB: B-myeloblastosis virus
BRAF: Rapidly Accelerated Fibrosarcoma B
BSA: bovine serum albumin
CAZy: Carbohydrate Active Enzymes database
CCND1: cyclin D1 gene
CDG: Congenital Disorders of Glycosylation
cDNA: complementary DNA
Chk1: Checkpoint kinase 1
CIMP: hypermethylation phenotype
CIN: chromosomal instability
c-Met: tyrosine-protein kinase Met or hepatocyte growth factor receptor
CMP: Cytidine monophosphate
CRC: Colorectal cancer
CRK: sarcoma virus CT10 oncogene homolog adaptor
CSC: cancer stem cells
DCoH/PCD: dimerizing cofactor for HNF1
DEAB: N,N-diethylaminobenzaldehyde (ALDH inhibio
DISC: death-inducing signalling complex
DNA: deoxyribonucleic acid
DOC: sodium deoxycholate
Dol-P: dolichol phosphate
E2F1: Transcription factor E2F1
EGF: epithelial growth factor
EGFR: epithelial growth factor receptor
EMT: epithelial to mesenchymal transition
EpCAM: Epithelial cell adhesion molecule
ER: endoplasmic reticulum
ErbB: erythroblastic leukemia viral oncogene homolog
ESCs: embryonic stem cells
FACS: fluorescence-activated cell sorting
FAK: focal adhesion kinase
Fas: Fas cell surface death receptor, TNF superfamily)
FasL: Fas ligand
FBS: fetal bovine serum
FdUrd: 5-fluoro-2'-deoxyuridine

FITC: Fluorescein isothiocyanate
FMOD: fibromodulin
FOLR1: folate receptor 1
FTA: phosphotungstic acid
FucT: Fucosyltransferase
GAB1: protein GRB2 associated binding protein 1
Gal: galactose,
GalNAc: N-acetylgalactosamine
GD: gangliosides
GDP: Guanosine diphosphate
Glc: glucose
GlcNAc: N-acetylglucosamine
GlcNAcT: GlcNAc-transferase
GnT: Alpha-Mannoside Beta-1,6-N-Acetylglucosaminyltransferase
GRB2: growth factor receptor bound protein 2
Her2: erb-b2 receptor tyrosine kinase 2
HGF: hepatocyte growth factor
HNF1: hepatocyte nuclear factor 1
HRP: Horseradish peroxidase
IgM: Immunoglobulin M
iPSC: induced pluripotent stem cells ()
IPT domain: immunoglobulin-plexin-transcription domain
IκBα: NFκB inhibitor alpha
JM: juxtamembrane segment
JNK: Janus kinase 1
KLF4: Kruppel-like factor 4
KLK6: Kallikrein-6
KRAS: Kirsten rat sarcoma viral oncogene homolog
LGR5: Leucine-rich repeat-containing G-protein coupled receptor 5
LLO: lipid-linked oligosaccharide
Man: mannose
MAP1B: microtubule associated protein 1
MAPK: mitogen activated protein kinase
MGAT: Alpha-Mannoside Beta-1,6-N-Acetylglucosaminyltransferase
MLH1: MutL homolog 1
MOMP: outer membrane permeabilization
mRNA: messanger ribonucleotide acid
MSH2: MutS homolog 2
MSI microsatellite instability
Msi-h: high microsatellite instability
Msi-l: low microsatellite instability
MSS: microsatellite-stable
MT4: metalloproteinase 4
MYC: Myelocytomatosis viral oncogene
MYEOV: Myeloma Overexpressed
NANOG: Nanog Homeobox
NC: negative control
NFκB: nuclear factor kappa-light-chain-enhancer of activated B cells
NOS2: nitric oxide synthase 2
Oct4: octamer-binding transcription factor 4
OLFM4: Olfactomedin-4
OST: olygosaccharyltransferase
PARP: Poly (ADP-ribose) polymerase

PBS: Phosphate-buffered saline
PCR: polymerase chain reaction
PI3K: phosphatidylinositol 3-kinase
PKC: protein kinase C
PLCγ1: Phospholipase C gamma 1
PolySia: polysialic acids
PSI domain: Plexin-Semaphorin-Integrin domain
PVDF: polyvinylidene fluoride
Ras: Rat sarcoma
RFT1: Requiring Fifty Three 1 homolog
RNAseq: RNA sequencing
RT-PCR: real time PCR
SALL4: Sal-like protein 4
SC: somatic cells
SDS: sodium dodecyl sulphate
Sema: Semaphorin
Ser/Thr: serine/threonine
SH3GL2: SH3 domain containing GRB2 like 2, endophilin A1
SHC: Src homology-2-containing
SHP2: Protein-tyrosine phosphatase 2C
Sia6LacNAc: Siaα2-6Galβ1-4GlcNAc
sLe^a: sialyl Lewis^a
sLe^x: sialyl Lewis^x
Smac/DIABLO: second mitochondrial activator of caspases/direct IAP-binding protein with low pI
SMAD2/4: Mothers against decapentaplegic homolog 2/4
SNA: *Sambucus nigra* agglutinin
SOS: Son of Sevenless
SOX2: (sex determining region Y)-box 2
Src: sarcoma viral oncogene homolog
ST: ST6GAL1 transduced cells
ST3Gal-I: Beta-Galactoside Alpha-2,3-Sialyltransferase 1
ST6Gal-I: β-galactoside α2,6-sialyltransferase 1
ST6GalNAc-I: Alpha-N-acetylgalactosaminide alpha-2,6-sialyltransferase 1
ST8Sia-I, V: alpha-N-acetyl-neuraminide alpha-2,8-sialyltransferase 1, 5
STAT3: signal transducers and activator of transcription 3
TBS-T: tris-buffered saline with Tween 20
TCF: Transcription Factor
TCGA: The Cancer Genome Atlas
TGFβ (TGFB): transforming growth factor β
TKIs: tyrosine kinase inhibitors
TKRs: tyrosine kinase receptors
Tn, sialyl Tn, T, sialyl T: Thomsen-Friedenreich-related antigens
TNF: tumour necrosis factor
TNFR1: tumour necrosis factor receptor 1
TPEN: N,N,N′,N′-Tetrakis(2-pyridylmethyl)ethylenediamine
TRAIL: TNF-related apoptosis-inducing ligand

UDP: Uridine diphosphate
VEGF: vascular endothelial growth factor
VEGFR: vascular endothelial growth factor receptor
Wnt: Wingless-related integration site (Wnt pathway)
αGlcase: α-glucosidases
αManase: α-mannosidase
β1,4 GalT: β-1,4-galactosyltransferase
β1,4GalT: β1,4-Galactosyltransferase
β4GalNAcT-II: Beta-1,4 N-acetylgalactosaminyltransferase 2

INDEX

1. INTRODUCTION

1.1. GLYCOSYLATION

Glycosylation is one of the most important post-translational modifications occurring inside the cell. It consists in the glycosidic linkage of glycans to secretory and membrane-anchored proteins or lipids (*1*). It is known that glycans have important roles in protein folding and stability, cell adhesion, signalling, cell-cell recognition in fertilization and immune response (*2*), apoptosis and cell survival (*3*) as well as in antibody recognition (*4*). The many glycosylated proteins expressed on the plasma membrane contribute to form the glycocalyx. The impairment of the glycosylation process causes the genetic diseases called Congenital Disorders of Glycosylation (CDG), which appear in infants and cause malfunctions of several organs including central nervous system, muscle and intestine (*5*), often incompatible with life.

The glycosylation process occurs in the endoplasmic reticulum (ER) or in the Golgi apparatus, involving many glycosyltransferases, the enzymes that catalyse the transfer of a sugar from an activated nucleotide-sugar donor to another sugar, a protein or a lipid. There are two main types of glycan chains that can be added on proteins, they differ in the amino acid used for the glycosidic linkage and in the sequence of reactions that lead to the synthesis of the glycan: O-linked and N-linked.

O-linked glycosylation is developed in the Golgi apparatus and it is characterized by the addition of sugars to the oxygen atom of serine/threonine (Ser/Thr) residues of the polypeptide chain. Mucins are the most common O-linked glycoproteins and their biosynthesis starts in *cis* Golgi by the addition of a N-acetylgalactosamine (GalNAc) residue operated by the peptide:GalNAc-transferases (*6*) and can be followed by the transfer of galactose (Gal), N-acetylglucosamine (GlcNAc), sialic acid and fucose creating linear or branched chains (*7*). There are also non-mucinous types of O-linked glycoproteins where the sugar linked to Ser/Thr is different from GalNAc and could be fucose, xylose, mannose, GlcNAc, galactose or glucose (Glc) (*8*).

N-linked glycoprotein biosynthesis is more complex and organized than O-linked glycosylation. In fact, it starts in the endoplasmic reticulum where the dolichol phosphate (Dol-P) is used as carrier to build an oligosaccharide comprised of 3 glucose, 9 mannose (Man) and 2 GlcNAc residues (*9*) forming the lipid-linked oligosaccharide (LLO). The first steps occur in the cytoplasmic side of the ER membrane and involve glycosyltransferases encoded by the ALG (*Asparagine Linked Glycosylation*) genes that add two GlcNAc and five mannose residues forming the branched structure $Man_5GlcNAc_2$ (*10*). At this point, the RFT1 enzyme translocates the LLO on the luminal side of the ER where its biosynthesis continues with the progressive addition of four mannose and three glucose residues operated by α-mannosyltransferases and α-glucosyltransferases (*11*). The final structure is conventionally formed by three antennae (a, b and c) and it is terminated by the addition of the "capping" α-1,2-linked glucose on the a-antenna, which determines the substrate recognition by the oligosaccharyltransferase (OST) (*12*). The biosynthesis of the LLO is fundamental for the N-linked glycosylation, in fact, deficiencies in this process result in hypoglycosylation of proteins which is the primary cause for the severe clinical signs observed in CDG (*5*). The OST is the central enzyme of the pathway because it catalyses the addition of the LLO on the asparagine residue of the consensus sequence N-X-S/T (where X could be any amino acid but proline) of a forming polypeptide chain before the protein folding takes place (Fig. 1.1) (*12*).

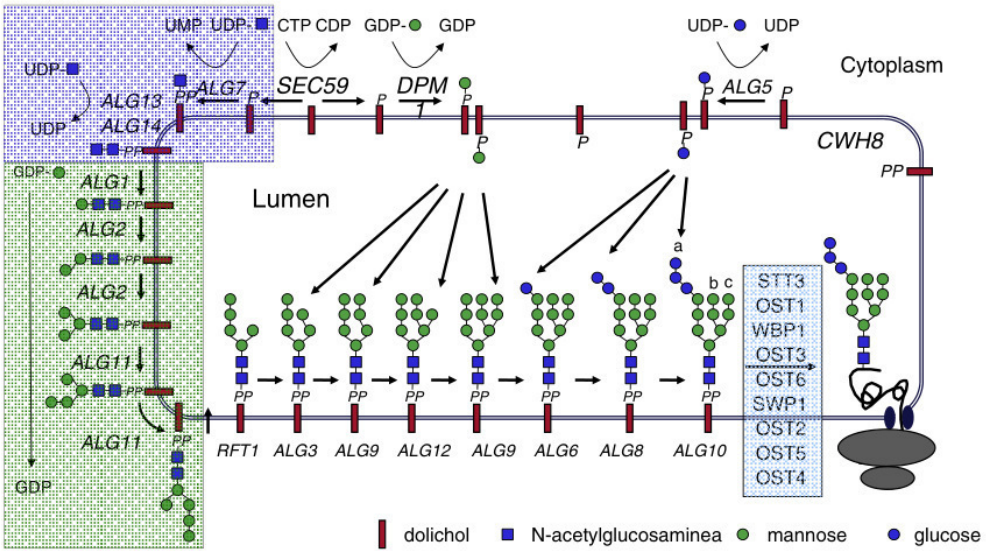

Fig. 1.1 N-linked glycosylation process starts in the ER with the lipid-linked oligosaccharide biosynthesis catalysed by enzymes encoded in the ALG loci. GlcNAc transferases and Man transferases acting in the cytoplasmic side of the ER use UDP-GlcNAc (blue box) and GDP-Man (green box), respectively. The LLO composed by $Man_5GlcNAc_2$ is transferred to the ER lumen and further processed by lumen-oriented glycosyltransferases to obtain $Glc_3Man_9GlcNAc_2$ oligosaccharide. This is then transferred on a selected asparagine residue of a growing polypeptide (*12*).

The N-linked chain undergoes further processing through the action of glycosidases. In fact, the three-terminal glucose are trimmed by α-glucosidase I and II, followed by the removal of four mannose residues catalysed by α-mannosidase I (*13*). Then, the enzyme GlcNAc-transferase I (GlcNAcT-I) transfers the first GlcNAc residue to the chain while the α-mannosidase II removes two additional mannose residues. The successive step is catalysed by the GlcNAc-transferase II (GlcNAcT-II) that adds a second GlcNAc residue to the N-glycan (*14*). This structure can be further implemented in the Golgi apparatus by the action of many glycosyltransferases creating a heterogeneous collection of mature glycoconjugates (*7*). In fact, the N-linked chains can be completed by the addition of galactose residues performed by members of the β-1,4-galactosyltransferase (β1,4 GalT) family, or by the addition of a fucose residue linked to the first GlcNAc of the chain (core-fucose) operated by Fucosyltransferase VIII (FucT-VIII). In addition, a third GlcNAc residue can be linked to the innermost mannose residue by the enzyme GlcNAc-transferase III (GlcNAcT-III) creating the bisecting GlcNAc structure. This sugar residue is not elongated further. Each antenna can be terminated by a α-2,3- or α-2,6-linked sialic acid residue (Fig. 1.2). While the addition of α-2,3-linked sialic acid can be operated by Sialyltransferases

ST3Gal-III (*15*), ST3Gal-IV (*16*) or ST3Gal-VI (*17*), the addition of α-2,6-linked sialic acid can be mediated only by ST6Gal-I (*18*). In fact, the second ST6Gal (ST6Gal-II) shows negligible activity towards glycoprotein substrates (*19, 20*).

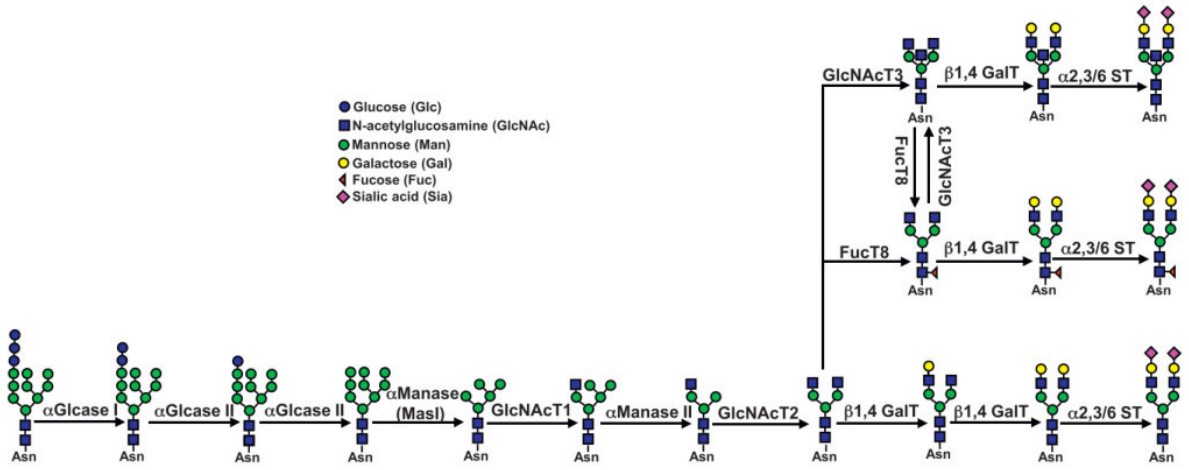

Fig. 1.2 Biosynthesis of N-linked glycans in the Golgi apparatus. The $Glc_3Man_9GlcNAc_2$ oligosaccharide transferred on an asparagine residue undergoes further processing by the sequential removal of 3 Glc residues, mediated by α-glucosidases (αGlcase) I and II, and 4 Man residues, mediated by α-mannosidases (αManase). The first GlcNAc residue is transferred to the chain by the GlcNAcT-I. Then, other 2 Man residues are trimmed by αManase II and the second GlcNAc residue is added by GlcNAcT-II. This structure can be further modified by the addition of galactose residues, by members of the β1,4GalT family or by core-linked fucose (mediated by FucT-VIII) or bisecting GlcNAc (by GlcNAcT-III). The sugar chains are frequently terminated by the addition of sialic acids linked either via α2,3 or α2,6 to galactose (*14*).

Additional branches with similar or different structures can be linked to the two α-linked mannose residues, giving rise to tri- and tetra-antennary structures. The terminal portions of these branches can be decorated by various sugar epitopes. It is important to notice that glycosylation, unlike protein or DNA synthesis, is a stochastic process. In fact, it depends on the abundance of glycosyltransferases, glycosidases and nucleotide-activated sugar donors. Therefore, it is common to find a certain degree of heterogeneity in the sugar chains linked to a specific glycosylation site in a given glycoprotein (*14*).

1.1.1. Glycosyltransferases

Glycosyltransferases are a family of enzymes responsible for transferring a sugar residue from a donor (nucleotide sugar) to polypeptide chains, lipids or other sugars through the formation of α- or β-glycosidic linkage. They are principally located in ER and Golgi membranes. They are defined by the sugar that they transfer, by the type of linkage that they catalyse and by the acceptor of their enzymatic activity. Glycosyltransferases are grouped into 105 families considering their catalytic activity in the Carbohydrate Active Enzymes database (CAZy) (*21*). The glycosyltransferases found in the Golgi are type II transmembrane proteins composed of a short N-terminal cytoplasmic portion, a transmembrane sequence and a globular catalytic domain in the Golgi lumen.

1.1.2. Sialyltransferases

Sialylation consists in the transfer of a sialic acid to the oligosaccharide chain. Sialic acids are constituted of a nine-carbon backbone with a negative charge at physiological pH. Among the different types of sialic acids, the most common in human is N-acetylneuraminic acid (Neu5Ac) that can be linked *via* α2,3- and α2,6-linkage to galactose containing glycans or via α2,6 bond to GalNAc and GlcNAc residues (*22*). In addition, sialic acid can be linked through a α2,8 bond to another sialic acid, forming polysialic acids. These different linkages are catalysed by a family of enzymes called sialyltransferases that share the same sugar donor, CMP-sialic acid (*23*). It has been reported that an increase in sialylation is closely associated with cancer, mainly because of altered expression of sialyltransferases (*24-26*). Basic properties of cancer cells such as reduced intercellular adhesion and increased adhesion to endothelial cells which are crucial for metastatisation can be regulated by sialic acids. In fact, sialic acids could prevent cell-cell interaction because of its negative charge that create a repulsive effect while sialylated glycans can be recognized by cell adhesion molecules such as selectins and siglecs.

1.1.3. β-galactoside α2,6-sialyltransferase 1 (ST6Gal-I)

β-galactoside α2,6-sialyltransferase 1 (ST6Gal-I) is a sialyltransferase that catalyses the transfer of a sialic acid to a galactose with a α2,6-linkage and is comprised of 406 amino acids (UniProtKB P15907) with a predicted molecular weight of 46 kDa. ST6Gal-I belongs to the GT29 family of the CAZy database. ST6Gal-I is a type II membrane protein that resides in the trans-Golgi, but a truncated form of the enzyme can be secreted and found in body fluids (*27*). This protein is comprised of a short N-terminal cytoplasmic tail followed by the transmembrane domain linked to a large luminal catalytic domain (*18*). ST6Gal-I expression is regulated at transcriptional level from tissue-specific promoters resulting in different mRNA species diverging at the 5'end (*28*). Tree major isoforms of ST6Gal-I mRNA have been identified. The first one was isolated from a placenta library (*29*) and is constituted by the exons Y and Z at the 5'-untranslated region (*30*). This isoform is considered the most widely expressed. A second isoform which is mainly expressed by the liver (hepatic form), lacks the Y and Z exons but presents a short sequence in front of exon I (*31*). The third isoform is expressed mainly in B-lymphocytes and contains the 5'-untranslated exon X (X form) (Fig. 1.3) (*32*). It has been reported that the hepatic form is expressed in colon cancer (*33*), this suggests that the malignant transformation alters its transcriptional regulation. Xu et al. demonstrated that the accumulation of the hepatic form in colon cancer was due to the activity of the transcription factor HNF1 (hepatocyte nuclear factor 1) and to its dimerization cofactor (DCoH/PCD). While HNF1 was expressed both in normal and cancer tissue, DCoH/PCD was abundantly expressed only in colon cancer specimens suggesting the idea that the overexpression of this cofactor can be fundamental for ST6Gal-I accumulation in colon cancer (*34*). After these tissue specific exons, the ST6Gal-I gene encodes six exons. Translation starts inside exon two and stops inside exon six. Consequently, the three isoforms generate identical peptides.

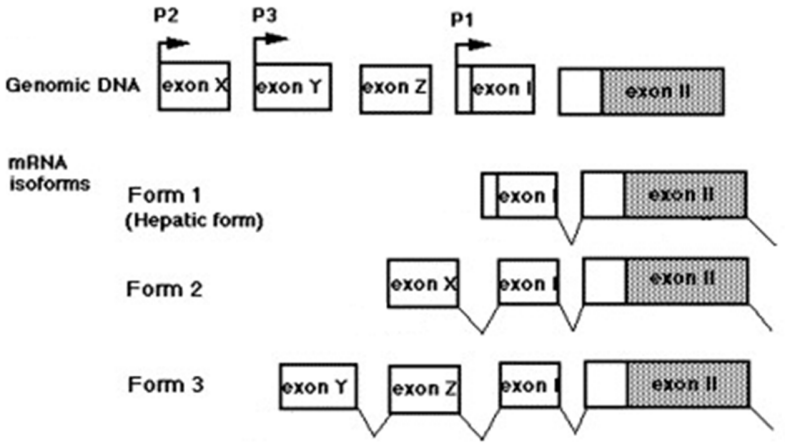

Fig. 1.3 Schematic representation of ST6Gal-I mRNA transcript variants. The three isoforms differ in the 5'UTR sequence. The hepatic form presents a small sequence at the beginning of exon I, the form 2 encodes for exon X in the 5'UTR, while form 3 is characterized by exon Y and Z. These mRNA variants are regulated by three different promoters (*34*).

1.2. COLORECTAL CANCER

Colorectal cancer (CRC) is the third most common type of cancer among men and the second among women worldwide (*35*). It arises usually through a progressive accumulation of genetic and epigenetic alterations. Two main mechanisms are at the basis of the colorectal carcinogenesis. The classical adenoma-carcinoma sequence (*36*) in which both copies of the adenomatous polyposis coli (APC) gene must be inactivated by genetic or epigenetic mechanisms, allowing adenoma growth. β-catenin, which is no longer inhibited by APC, translocates to the nucleus where it forms a transcriptional complex with TCF (transcription Factor), promoting the expression of proliferation-promoting genes, such as cyclin D1 and MYC (myelocytomatosis viral oncogene). A second mutational event of this pathway consists in the activation of KRAS (Rat sarcoma), while the inactivation of SMAD2 and SMAD4, which are effectors of transforming growth factor β (TGF-β) signalling, is usually a third event. It should be emphasized that TGF-β normally behaves as a cell cycle inhibitor. Loss of TP53 function and other tumour-suppressor genes leads to cancer development. This pathway is usually associated with instability of the number and structure of chromosomes and is consequently referred to as chromosomal instability (CIN) phenotype (Fig. 1.4).

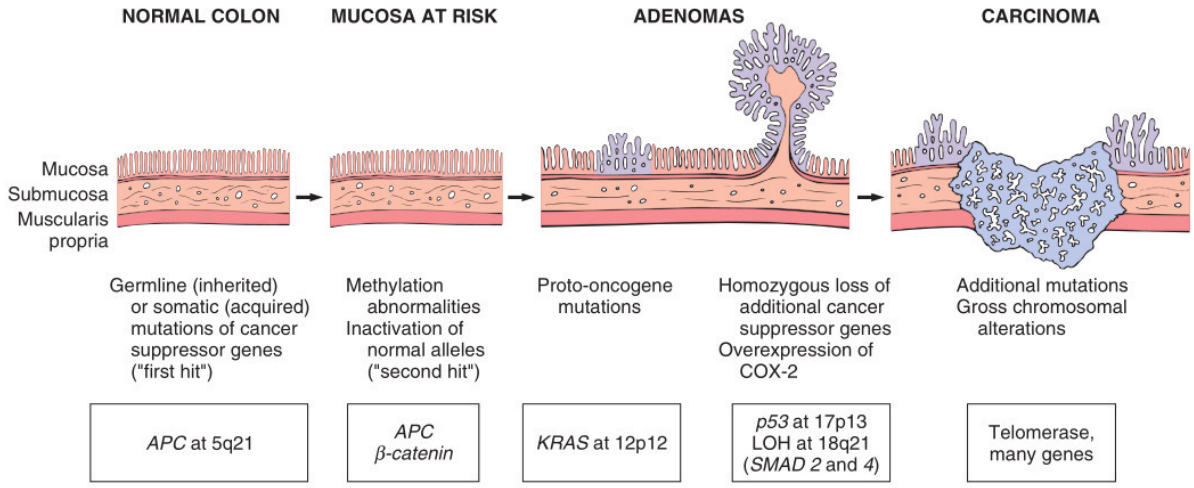

Fig. 1.4 Molecular and morphological alterations that lead to carcinogenesis in the classical adenoma-carcinoma sequence. The first mutation occurs in one allele of the APC gene (first hit), followed by the second allele (second hit). Other mutations affecting KRAS, TP53, SMAD2/4 or telomerases, lead to the formation of adenoma and then carcinoma (*37*).

The second main mechanism is based on the inactivation of genes involved in the DNA repair process known as "mismatch repair" (Fig. 1.5) (*38*). These genes, which include MLH1 (mutL homolog 1) and MSH2 (mutS homolog 2), can be inactivated in the germline, leading to Lynch syndromes, or sporadically. In both cases, their inactivation leads to the instability of short repeated DNA sequences known as microsatellites. Tumours displaying this phenotype are referred to as microsatellite instable (MSI). Although the microsatellite regions are often confined in non-coding regions of the genome, in a few cases there are short repeated sequences inside the coding regions of genes controlling cell growth and apoptosis. Examples are provided by the TGF-β receptor, whose mutation leads to loss of TGF-β signalling and by the pro-apoptotic gene BCL2 Associated X (BAX). A subgroup of the MSI cancer in which the inactivation of the mismatch repair genes is due to their promoter hypermethylation rather than mutation is referred to as CIMP (hypermethylation phenotype) (*39*). Usually, these cases are characterized by mutations of BRAF (Rapidly Accelerated Fibrosarcoma B) and wild type RAS and TP53. From a morphological point of view, it is possible to describe two different ways: the classical adenoma-carcinoma sequence starting with premalignant lesions such as adenomas, and the serrated neoplasia pathway that

begins with serrated adenomas or hyperplastic polyps (*40*). CIN and MSI are usually responsible for the classical adenoma-carcinoma pathway and for the serrated neoplasia, respectively.

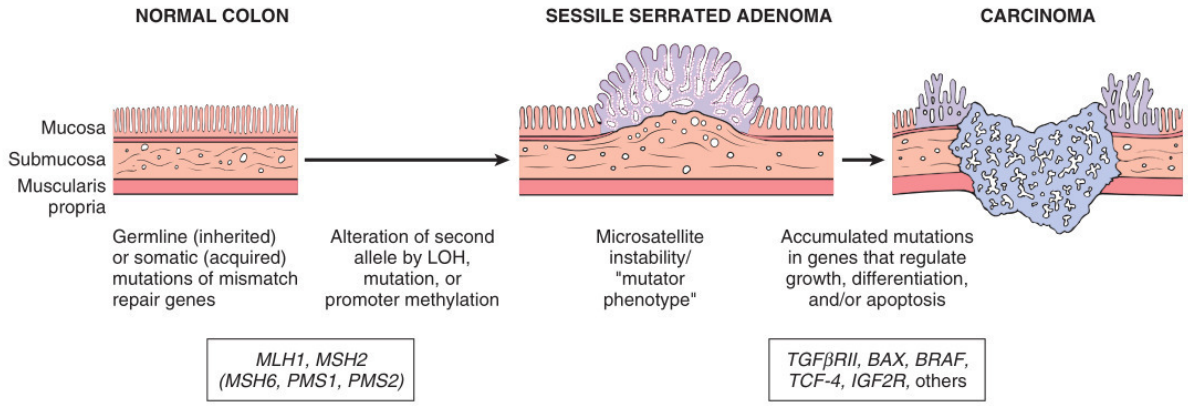

Fig. 1.5 Molecular and morphological modifications associated with microsatellite unstable pathway which is caused by mutation in mismatch repair genes (MLH1, MSH2). This permits the accumulation of mutations in various genes leading to carcinogenesis (*37*).

Although the mutational events which characterize the two main transformation pathways are different, their functional consequences can be partially overlapping. For example, instead of having the loss of function in APC, CRC aroused by MSI have mutations in β-catenin (*41*). Moreover, inactivation of the growth inhibitory pathway based on TGF-β signalling can be achieved by SMAD2 and SMAD4 inactivation or by TGF-β receptor inactivation.

1.3. GLYCOSYLATION IN CANCER

Alterations in glycan display has become a well-known hallmark of cancer cells. In fact, cancer cells express a variety of glycan-structures that are different from the ones present in normal tissue (*42*). In their work Hakomori and Kannagi defined two main mechanisms responsible for the tumour-associated alteration of carbohydrate chains: the incomplete synthesis and the neo-synthesis process (*43*). The incomplete synthesis is more frequent in early stage tumours and is driven by the impairment of the normal synthesis process of complex glycans (*44*). This leads to the biosynthesis in cancer cells of truncated structures. On the other hand, the neo-synthesis is typical of advanced stage tumours and it is due to the cancer-associated expression of specific glycosyltransferases (*44*). Various factors are responsible for the altered glycosylation present in

cancer cells: the under- or overexpression of glycosyltransferases, due to dysregulation at the transcription level; changes in the tertiary structure of the acceptor protein; availability of the acceptor substrate or of the sugar nucleotide donors and the correct expression and localization of the glycosyltransferases in the Golgi apparatus (*45*). The most common cancer-associated modifications in glycans structures regard sialylated and fucosylated structures, O-linked glycans truncation and N- and O-linked chains branching (*45*). In the following sections, some of the most relevant cancer-associated structures will be briefly reviewed.

1.3.1. Truncated O-linked glycans

The T or Tn antigens and their sialylated forms are examples of shortened or truncated glycans (*45*). In particular, the expression of peptide:GalNAc transferases is often altered in cancer leading to aberrant O-linked glycosylation or synthesis of truncated chains (*46*). A single GalNAc residue linked to serine or threonine is referred to as Tn antigen. Its α2,6-sialylated counterpart, synthesized mainly by sialyltransferase ST6GalNAc-I (*47*), is referred to as sialyl-Tn and is a well-known cancer-associated structure, widely expressed in cancer such as pancreas, stomach, colorectal, breast, bladder and ovary correlating with poor prognosis (*45, 48*) and malignancy (*49*). Therefore, it has been proposed as prognostic marker and as a target for the development of anti-cancer vaccines (*50*). Elongation of the Tn antigen by a β1,3-linked galactose (Fig. 1.6) leads to the biosynthesis of the Thomsen-Friedenreich (T) antigen, while the further addition of α2,3-linked sialic acid, mediated by ST3Gal-I, forms the sialyl-T antigen. Collectively, T, Tn and their sialylated variants are often referred to as Thomsen-Friedenreich-related antigens (*51*) (for the structure refer to fig. 1.6). In breast epithelium, the neoplastic transformation increases the presence of T and sialyl-T structures, probably due to a down-regulation of the competing enzyme core 2 β1,6GlcNAcT and up-regulation of ST3Gal-I(*52*). However, data on mice suggested that the responsible for cancer progression could be ST3Gal-I and its tumour-promoter activities, but not the expression of the cognate sT antigen. Both, ST3Gal-I (*53*) and ST6GalNAc-I (*54*) are involved in bladder cancer. In particular, high ST6GalNAc-I and sTn expression correlate with a better response to the adjuvant therapy with Bacillus Calmette-Guerin (BCG) (*55*). Probably this is due

to a down-regulation of genes preserving genomic stability in ST6GalNAc-I expressing cells resulting in increased sensitivity to the oxidizing agents released by BCG (*56*).

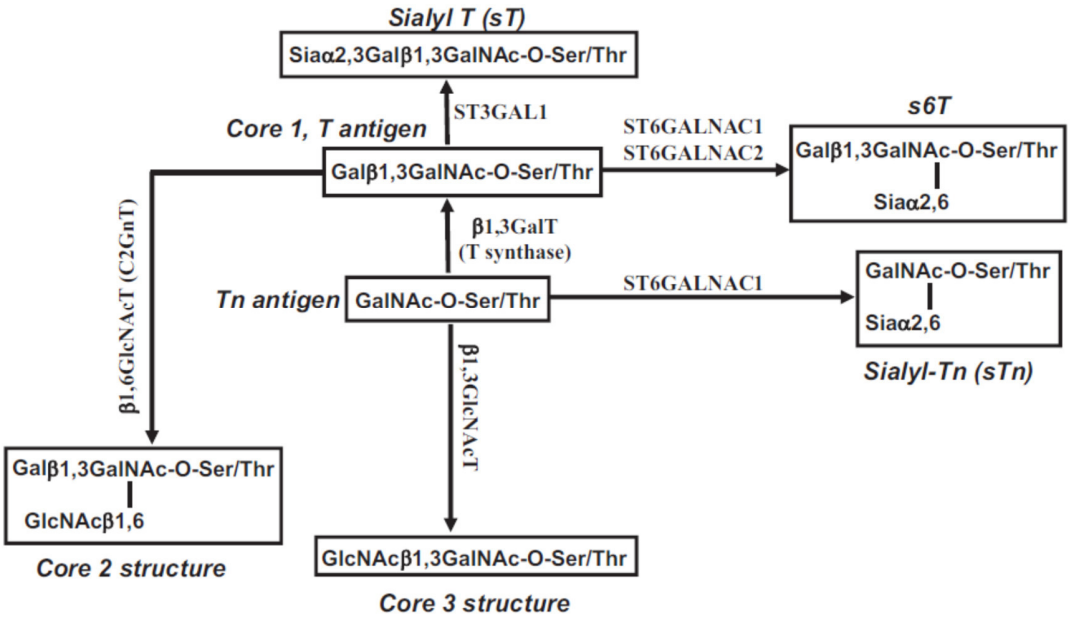

Fig. 1.6 Structure and biosynthesis of Thomsen-Friedenreich-related antigens. The Ser/Thr-linked GalNAc (Tn antigen) can be elongated by the addition of either β1,3 linked Gal (T antigen) operated by β1,3GalT or α2,6-linked sialic acid (Sialyl-Tn antigen) by ST6GalNAc-I. The elongation of the Tn antigen with a β1,3-linked GlcNAc by β1,3GlcNAcT leads to the formation of a core 3 structure. The T antigen can be elongated by the addition of a α2,3-linked sialic acid forming the Sialyl T antigen or by the addition of a β1,6 GlcNAc leading to the formation of a core 2 structure. (*25*)

1.3.2. Core fucosylation

Core fucosylation is catalysed by FucT-VIII and consists in the addition of a fucose residue to the innermost residue of GlcNAc on N-linked chains. It has been reported that FucT-VIII is up-regulated in lung and breast cancer (*57, 58*) and that the fucosylated form of α-fetoprotein is a good marker for early detection of hepatocellular carcinoma (*59*). Moreover, in breast cancer the core fucosylation of epidermal growth factor receptor (EGFR) triggers dimerization and phosphorylation of the receptor, thus increasing EGFR-mediated signalling (*57*).

1.3.3. Branching and bisecting GlcNAc glycans

Many cancer cells express on their surface complex β1,6-branched N-linked glycans due to an increased activity of the enzyme GnT-V encoded by MGAT5 gene (*45*). Interestingly, MGAT5 expression is regulated by the Ras signalling pathway, which is commonly activated in cancer (*60*). Its overexpression in lung epithelial cell lines induces increased cell motility and tumour formation in athymic mice (*61*). Moreover, GnT-V seems to be responsible for early events in the formation of breast carcinoma in Her2-transgenic mice (*62*). The data are confirmed by the suppression of tumour growth and metastasis in mice deficient for MGAT5 (*63*).

On the other hand, bisecting GlcNAc is synthetized by the enzyme GnT-III encoded by the gene MGAT3. It has been reported that MGAT3 acts as a tumour-suppressor gene in cancer, reducing metastasis (*64*). In fact, it regulates the glycosylation of EGFR, integrins and cadherins (*60*).

1.3.4. Sialyl-Lewis antigens

Sialyl Lewis antigens sialyl Lewis^a (sLe^a) and sialyl Lewis^x (sLe^x) (for the biosynthetic pathway refer to fig. 1.7) derive from the α2,3 sialylation followed by the α1,4 (in sLe^a) or α1,3 (in sLe^x) fucosylation of a type 1 or a type 2 chain, respectively. The enzyme responsible for the α2,3 sialylation in sLe^a antigen is ST3Gal-III, while ST3Gal-III, -IV or -VI catalyse the reaction in sLe^x antigen. The final step of sLe^a and sLe^x biosynthesis consists in the addition of α1,3- or α1,4-linked fucose catalysed by FucT-III (sLe^a) or FucT-III, -IV, -V, -VI, -VII (sLe^x). When expressed by leukocytes, the original function of these structures is to bind to E- and P-selectins expressed on activated endothelial cells. However, they can be ectopically expressed by cancer cells, conferring the capacity to spread and metastasise (*65*). In particular, their expression is reported in lung carcinoma, colon, stomach and kidney (*66*). The sLe^a tetrasaccharide is a cancer-associated marker widely used in clinical practice because it is the epitope of the Ca19-9 antigen (*67*). The aberrant expression of sLe^a and sLe^x is probably multifactorial and strongly tissue-specific. The expression of sLe^x in adult T cell leukaemia cells is reported to be dependent on FucT-VII activity because the etiologic agent of this pathology (the human T-lymphotropic virus 1) encodes a transcriptional activator protein that regulates the transcription of FucT-VII (*68*). At the same time, in breast

tumour its expression is regulated by FucT-VI (*69*) and in lung cancer by a coordinate up-regulation of FucT-III and -VI (*70*). The antigen sLe^x is overexpressed also in colon cancer but the enzyme responsible for its biosynthesis, FucT-VI, does not result upregulated (*71*). The aberrant expression of sLe^x and sLe^a in gastric cancer has been associated with the activation of the β1,3GlcNAc transferase that is an upstream enzyme in their biosynthetic pathway (*72*). On the other hand, the low sLe^x expression in normal colonic mucosa is at least partially due to the concomitant high expression of the competing enzyme β4GalNAcT-II, synthesizing the Sd^a antigen (*73*).

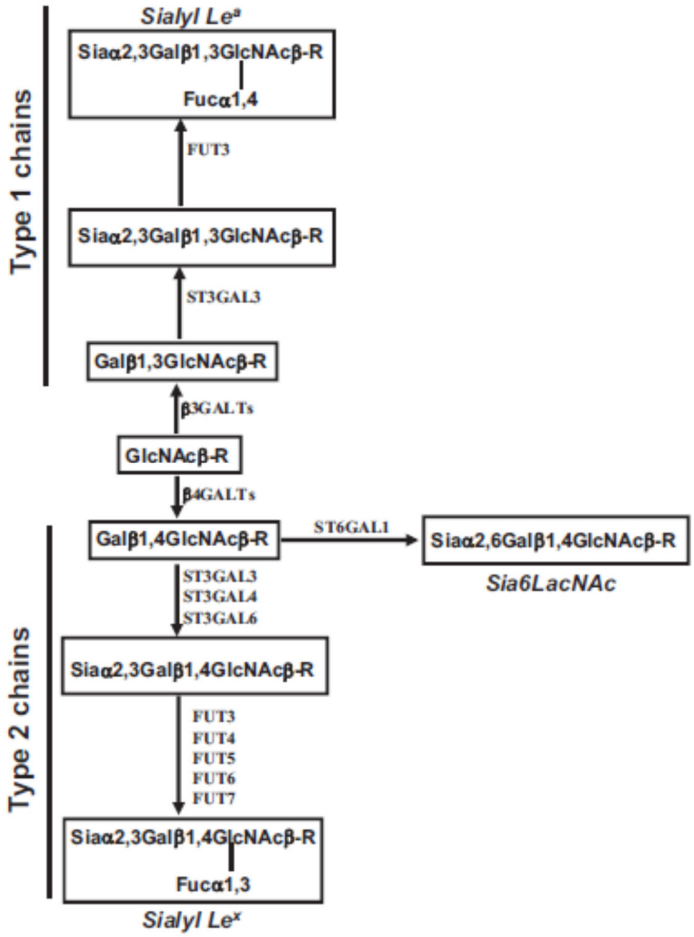

Fig. 1.7 Structure and biosynthesis of sialyl Lewis antigens and Sia6LacNAc. The binding of a β1,3 Gal to the GlcNAc forms the basic unit of the type 1 chain, while the binding of β1,4 Gal leads to the formation of lactosamine, the basic structure of type 2 chain. The addition of a α2,3 sialic acid to both chains operated by different sialyltransferases creates the substrate for the action of FucT-III or FucT-III, -IV, -V, -VI, -VII that form sialyl Lewis^a or sialyl Lewis^x, respectively. The lactosamine can also be elongated by the addition of a α2,6 sialic acid by ST6Gal-I, forming Sia6LacNAc (*25*).

1.3.5. Polysialic acids

The increased level of sialylation in tumours can also be due to the expression of polysialic acids (polySia). They are long linear arrays of sialic acids linked with a α2,8 bond to N-linked chains. The enzymes involved in the biosynthesis of polysialic acids are ST8Sia-II and ST8Sia-IV (*74*). Recent studies report that the presence of polySia on N- and O-glycans are essentials for cell migration and plasticity during nervous system development (*75, 76*), for regeneration of damaged neurons (*77*) and for liver development and regeneration (*78*). In cancer, they are frequently expressed in high grade tumours (*79*) mainly from neuroectodermal origin (*80*) and are correlated with high aggressiveness and poor prognosis (*81*).

1.3.6. Gangliosides

Gangliosides are sialic acid-containing glycosphingolipids. Their biosynthesis starts in the *cis* Golgi by the enzymatic activity of ST3Gal-V, ST8Sia-I and ST8Sia-V that show high specificity towards glycolipids (*82*). After the synthesis of the precursors, other glycosyltransferases can further elongate the chains by the addition of GalNAc, Gal or sialic acid in a stepwise manner (*83*). Gangliosides are often aberrantly expressed in tumours such as melanoma, neuroblastoma and breast cancer (*84*). In particular, the ganglioside GD3, highly expressed in cancer tissue (*85*), can promote tumour progression due to interaction with integrins (*86*), growth factor receptors (*87, 88*) and Src kinase (*89*). GD1α is reported to be a crucial mediator of breast cancer metastasis to the brain, because the aberrant expression of this antigen usually restricted to the brain enables breast cancer cells to pass through the blood-brain barrier (*90*).

1.3.7. Sia6LacNAc

The sialylated cancer-associated antigen that will be the focus of this work is Sia6LacNAc. It is synthetized by the enzyme β-galactoside α2,6 sialyltransferase (ST6Gal-I) by the transfer of a α2,6-linked sialic acid to lactosaminic chains. It is recognized by the lectin *Sambucus nigra* (SNA) which has been widely used to detect the antigen in normal and cancer tissues (*33, 91, 92*). ST6Gal-I is

considered a cancer-associated glycosyltransferase, in fact its elevation was detected by our and other groups in colon cancer tissues (*93-95*), and confirmed in many other malignancies (*24*). It has been reported that SNA reactivity and ST6Gal-I expression in colon cancer is associated with poor prognosis (*96, 97*). Moreover, Gebert *et al.* reported that increased SNA reactivity was mainly associated with microsatellite stable (MSS) colon cancer phenotype (*98*). This is probably due to the fact that ST6Gal-I expression is regulated by Ras oncogene, which is commonly mutated in MSS colon cancer (refer to section 1.2.). In fact, it has been demonstrated that both oncogenic N-ras and H-ras stimulate ST6Gal-I expression (*99*), and that Ras triggers β1-integrins sialylation through the overexpression of ST6Gal-I in a colonocyte cell line (*100*).

A recently published study reported that ST6Gal-I is markedly upregulated in hepatocellular carcinoma tissue and cells. Moreover, its high values correlate with aggressiveness and poor prognosis (*101*). These findings agree with the elevated presence of ST6Gal-I in rodent hepatoma (*102*) but disagree with previous data showing that only a small group of liver cancer patients displayed increased ST6Gal-I expression (*103*). Moreover, in prostate cancer tissues ST6Gal-I expression was higher compared to normal prostate tissue. In fact, high ST6Gal-I expression positively correlated with Gleason scores, seminal vesicle involvement and poor survival (*104*). *In vitro*, the overexpression of ST6Gal-I promoted cell proliferation, migration and invasion in cell lines from hepatocellular carcinoma (*101*), pancreatic ductal adenocarcinoma (*105*), prostate cancer (*104*) and osteosarcoma (*106*). Previous studies demonstrated that ST6Gal-I is responsible for the α2,6-sialylation of β1-integrins resulting in increased binding to extracellular matrix in epithelial cancers (*100, 107-110*) and in integrin-based signal transduction (focal adhesion kinase signalling) providing survival signals. Moreover, α2,6 sialylated β1-integrins can reduce the binding of galectin-3 (*111*) a lectin that can have a pro-apoptotic effect (*112*), inhibiting apoptotic death and, thus, increasing malignancy. On the other hand, ST6Gal-I expression in the colon cancer cell line SW948 reduced its tumorigenic potential and its multilayer growth (*109*), its expression reduced also the invasive growth of glioma cells (*113-116*). Moreover, loss of ST6Gal-I, due to epigenetic regulation of the promoter, reduced invasiveness in prostate cancer tissues (*117*). In addition, St6gal1-null mice present normal development and defects mainly in IgM production (*118*) and granulopoiesis (*119*). Mammary tumours developed by St6gal1-null mice displayed

higher differentiation, but the same growth rate and a selectively altered expression of genes associated with focal adhesion signalling with a reduced phosphorylation of focal adhesion kinase, compared with the wild-type (*120*). Interestingly, the α2,6-sialylation of VEGFR (vascular endothelial growth factor receptor) prevented angiogenesis and tumour progression. In hypoxic conditions ST6Gal-I was downregulated while MGAT5 was upregulated, this leads to an altered expression of the N-linked glycans on VEGFR2 and consequent binding to galectin 1 activating vascular endothelial growth factor (VEGF) signalling (*121*). More importantly, ST6Gal-I expression is associated with resistance to radiations and drugs. In fact, it has been reported that ST6Gal-I confers cisplatin resistance to ovarian cancer cells (*122*), multidrug resistance in leukaemia cells (*123*) and resistance to gefitinib resistance in a colon cancer cell line due to sialylation of the receptor (*124*). However, in human T lymphoblastic leukaemia cells the resistance to desoxyepothilone B correlates with reduced expression of ST6Gal-I (*125*). In addition, ST6Gal-I is involved in resistance to radiations as the exposure to ionizing radiation resulted in higher expression of the enzyme in animal models and cell lines (*126*), while the overexpression of ST6Gal-I in colon cancer cells results in radiation resistance (*127*).

1.4. APOPTOSIS

Apoptosis is a programmed pathway for cell death and occurs in many tissues of the body to maintain homeostasis. It is well known that the impairment of the apoptotic machinery is a hallmark of malignancy giving the cancer cells the ability to survive with severe damages to their DNA (*128*). Apoptosis occurs through two different pathways: the intrinsic and the extrinsic pathway. The intrinsic pathway is characterised by the release of cytochrome c and Smac/DIABLO (second mitochondrial activator of caspases/direct IAP-binding protein with low pI) from the mitochondria into the cytoplasm (*129*). This follows the mitochondrial outer membrane permeabilization (MOMP) which is controlled by stress sensor that alters the interactions of the Bcl-2 proteins (B-cell lymphoma 2) (*130*). The BH3-only proapoptotic proteins (part of the Bcl-2 family) promote Bax and Bak oligomerization at the mitochondrial outer membrane inducing MOMP. In the

cytoplasm, cytochrome c triggers the assembly of the apoptosome complex containing the initiating caspase-9 that is able to activate the effector caspases (*129*).

The extrinsic apoptosis pathway involves the binding of death ligands on death receptors on the surface of the cell and the transmission of the signal to the effector caspases (*131*). The most studied family of death ligands is the tumour necrosis factor (TNF) family which includes TNF, Fas ligand (FasL), and TRAIL (TNF-related apoptosis-inducing ligand). The binding with the death ligand triggers death receptor trimerization and the formation of the death-inducing signalling complex (DISC) with subsequent activation of the initiator caspase-8 and the effector caspase-3 (*131*). Both these pathways result in the typical phenotype of apoptotic cells which consist in plasma membrane "blebbing," cell shrinkage, chromatin condensation, and internucleosomal DNA fragmentation (*131*).

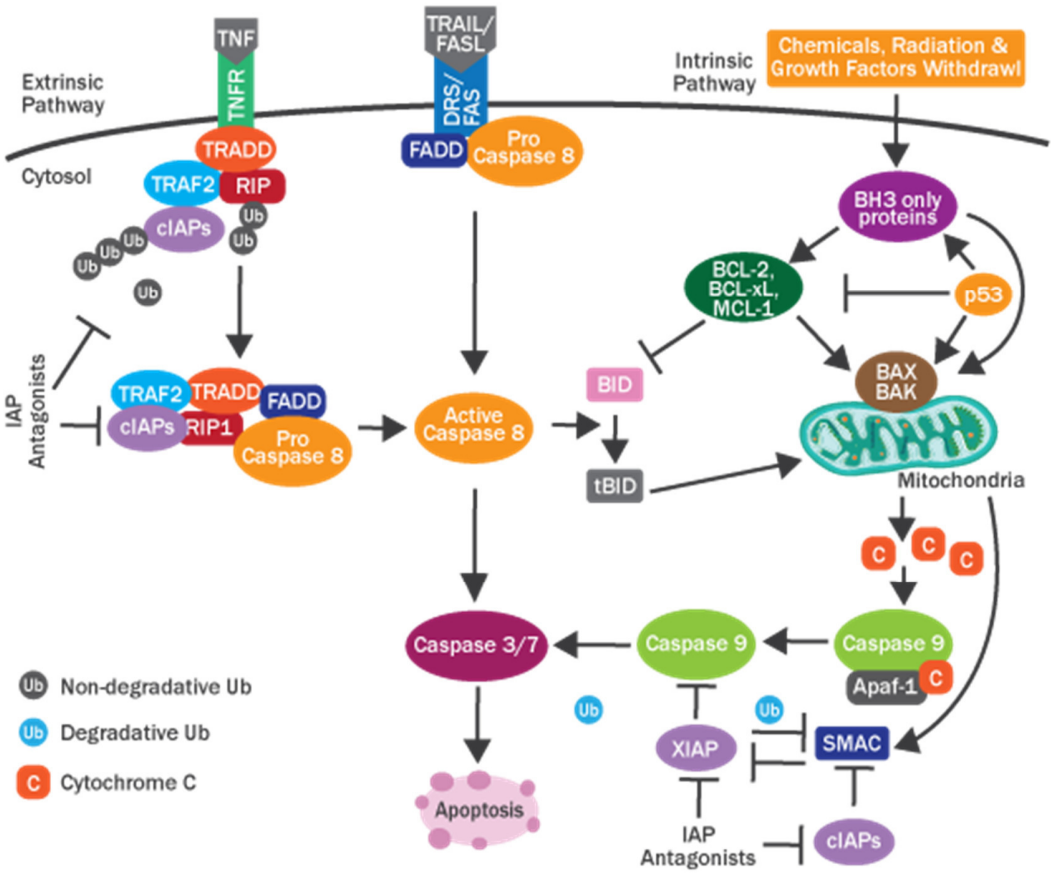

Fig. 1.8 Extrinsic and Intrinsic pathways of apoptosis. The extrinsic pathway starts with the binding of death ligands (TNF, TRAIL, FASL) to death receptors. Then, receptor oligomerisation and formation of the DISC (death induced signalling complex) triggers the activation of the initiator caspase-8 and the effector caspase-3. In the intrinsic pathway the stress sensor proteins BH3-only (part of the Bcl-2 family) promote Bax and Bak oligomerization at the mitochondrial outer membrane inducing permeabilization (MOMP) and release of cytochrome c and Smac/DIABLO that activates the initiating caspase-9 and the effector caspase-3/7 (*132*).

1.4.1. ST6Gal-I and apoptosis

According to some studies, ST6Gal-I could have a role in protection from apoptosis. In fact, it is known that in colon tumours β1-integrin is a substrate for the enzyme ST6Gal-I and therefore presents α2,6-linked sialic acid at the end of its glycans (*100*). Secreted galectin-3, a tumour-associated lectin, induces apoptosis via the binding with β1-integrin. However, sialylated β1-integrin by ST6Gal-I impairs galectin-3 binding and therefore protects from apoptosis (*133*). Moreover, ST6Gal-I can shield the cells from apoptosis also by sialylation of death receptors. In

fact, the α2,6-sialylation of the tumour necrosis factor receptor 1 (TNFR1) in macrophages impairs TNFα induced apoptosis (*134*). In addition, Fas death receptor sialylation by ST6Gal-I confers protection against Fas-mediated apoptosis, therefore promoting tumour cell survival (*135*).

A very recent study reported that ST6Gal-I could protect tumour cells against serum growth factor withdrawal. In fact, it shows that in ovarian and pancreatic cancer cell lines the overexpression of ST6Gal-I induces the activation of pro-survival signalling molecules, pNFκB (nuclear factor kappa-light-chain-enhancer of activated B cells) and its tumour-promoting transcriptional factors, and the apoptosis inhibitor cIAP2. Therefore, this could increase tumour cells survival in a microenvironment depleted of growth factors (*136*).

1.5. GROWTH FACTOR RECEPTORS

Growth factor receptors are transmembrane proteins with an extracellular portion that binds growth factors and a cytoplasmic portion conveying the signal. Many of these receptors are tyrosine kinase receptors (TKRs) that dimerize after binding their ligand and trigger the signal through autophosphorylation of tyrosine residues in their cytoplasmic portion. They are often aberrantly expressed or activated in cancer, providing the cells with proliferative signals (*128*). Glycosylation plays an important role in growth factor receptors turn-over and activity. In fact, the presence of particular oligosaccharide chains can alter the binding between the receptor and the ligand and in general the signalling of the receptor (*137, 138*). Moreover, galectins can bind the glycans present on growth factor receptors and form a lattice that can control the receptors' turn-over on the plasma membrane usually potentiating their signalling (*139*).

1.5.1. HGF receptor

Hepatocyte growth factor (HGF) receptor, also known as c-Met, is a heavily glycosylated transmembrane protein, which is expressed on epithelial cells of many organs including liver, pancreas, kidney and prostate (*140*). It is present also in normal colon, but its expression significantly increases in malignant tissue (*141*). C-Met receptor is composed of an extracellular

portion with three domains, one transmembrane helix and the catalytic domain in the cytoplasmic portion (Fig. 1.9). The α- and β-subunits form the Semaphorin (Sema) domain on the extracellular portion, which binds HGF and is necessary for receptor dimerization (*142*). Below, is localized the PSI domain responsible for the correct positioning of the ligand-binding site of the receptor (*143*). This domain is connected with the underlying transmembrane domain through the four immunoglobulin-plexin-transcription (IPT) domains. Intracellularly, the receptor is comprised of a tyrosine kinase catalytic domain, containing the catalytic tyrosines, and of a docking site that binds to signalling effectors (*140*).

Upon HGF binding, the receptor undergoes homodimerization and autophosphorylation of the two tyrosines in the catalytic domain followed by the phosphorylation of the tyrosines on the C-terminal tail. This recruits effector proteins such as the adaptor protein GRB2 associated binding protein 1 (GAB1), the growth factor receptor bound protein 2 (GRB2) and Src homology-2-containing (SHC), the effector molecules phosphatidylinositol 3-kinase (PI3K), and v-src sarcoma viral oncogene homolog (SRC), and transcription factor signal transducer and activator of transcription (STAT-3). These effector proteins could propagate the signal through different pathways (*140*). The mitogen activated protein kinase (MAPK) pathway is activated via rat sarcoma viral oncogene homolog (RAS) and Son of Sevenless (SOS) signalling resulting in cell proliferation (*144*). Furthermore, c-Met signalling activates PI3K/Akt pathway inducing cell survival and resistance to apoptosis (*145*). Another signalling pathway activated by HGF receptor is the one leading to cell transformation. This pathway involves the phosphorylation of Janus kinase 1 (JNK), via binding to CRK (*146*), and STAT3 (signal transducers and activator of transcription 3) (*147*).On the other hand, cell migration is promoted downstream c-Met by the focal adhesion kinase (FAK) through the phosphorylation of Src, in this way the cell acquires the ability to growth in absence of anchorage (*148*). FAK is localized at cellular adhesion complexes and is associated with integrin related signalling, therefore playing an important role in cellular migration and adhesion (*149*).

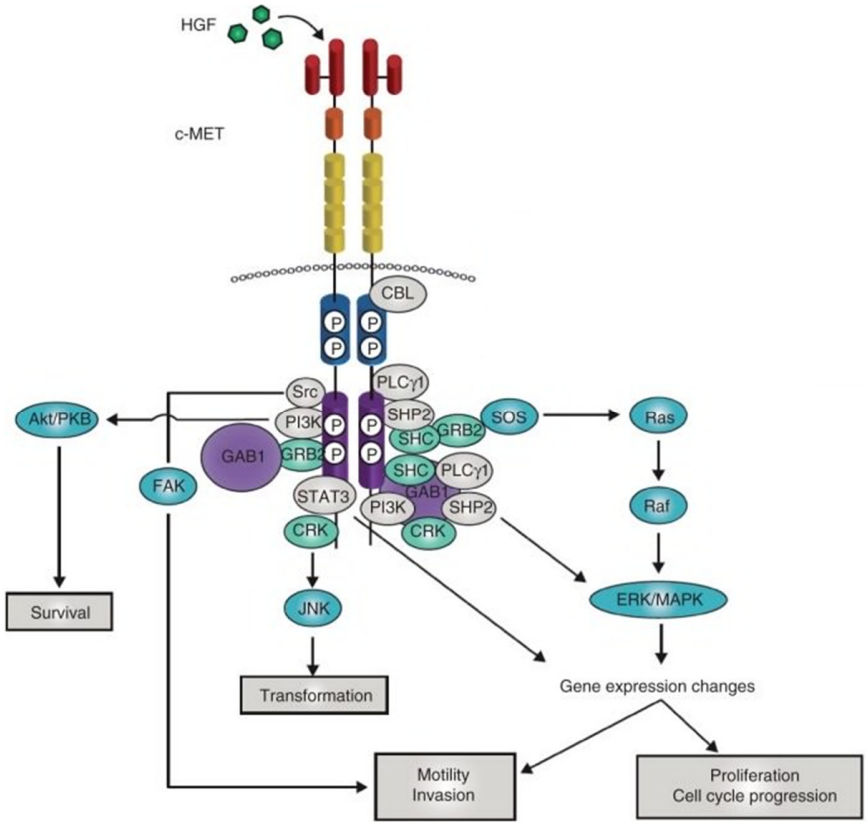

Fig. 1.9 c-MET signalling pathway. HGF binding triggers receptor dimerization and autophosphorylation of the tyrosines within the multifunctional docking site. They recruit signalling effectors and adaptor proteins such as GRB2, SHC, CRK and CRK-like, PI3K, PLCγ1, SRC, STAT3. In addition, GAB1, a multi-adaptor protein, can bind directly to c-MET or through GRB2. c-MET signalling activates the MAPK cascade through the activation of RAS via binding with SHC and GRB2. The activation of this pathway leads to cell proliferation, cell motility and cell cycle progression. Also SHP2, which is recruited by GAB1 to the receptor, can activate the MAPK pathway. PI3K can bind directly to the receptor or via GAB1 and activated the AKT/protein kinase B pathway leading to cell survival response. The transformation signalling of c-MET is mediated by phosphorylation of JNK, which occurs via binding to CRK and STAT3. The direct binding of STAT3 to the receptor cause SAT3 phosphorylation, dimerization and translocation to the nucleus where it promotes the transcription of genes involved in tubulogenesis and invasion. c-MET through the direct binding of SRC kinase activated FAK signalling resulting in cell migration. Adapted from Organ *et al*. 2011 (*140*).

1.5.2. EGF receptor

Epidermal growth factor (EGF) receptor ErbB-1 is part of the ErbB (erythroblastic leukaemia viral oncogene homolog) family which is comprised also by ErbB-2, ErbB-3 and ErbB-4. Their structure is similar and consists of an heavily glycosylated extracellular portion containing the ligand-binding domain, a single transmembrane helix and a cytoplasmic portion comprising the catalytic

domain (*150*). The extracellular portion of ErbB1 is composed of three domains: domain 1 and 3 recognize the ligand and domain 2 is necessary for dimerization (*151*). The intracellular portion contains a juxtamembrane (JM) segment, a protein kinase domain, and a carboxy-terminal tail (*152*). EGF binding triggers receptor homo or heterodimerization, in particular ErbB-1 interacts with ErbB-2, resulting in kinase activation through transphosphorylation (*150*). The binding to the terminal tail by Grb2, SOS or by the adaptor molecule Shc activates the MAPK pathway via Ras, resulting in the activation of transcription factors involved in cell proliferation. Moreover, the PLCγ interacts with the receptor and catalyses the hydrolysis of phosphatidylinositol 4,5-diphosphate to inositol 1,4,5-triphosphate, that releases intracellular calcium, and 1,2-diacylglycerol that activates protein kinase C (PKC) signalling pathway, resulting in MAPK and c-Jun pathway activation (*153*). On the other hand, the dimerization of EGFR and ErbB-3 allows the direct binding of PI3K to the phosphorylated tyrosines of the receptors' tail. This activates the PI3K/Akt pathway involved in cell survival, invasion, migration and resistance to apoptosis (*154*). In addition, also STAT proteins bind to EGFR and, after their dimerization, translocate to the nucleus and promote the expression of specific target genes (*153*). Another signal transducer that binds to EGF receptor is Src that activates FAK, PI3K and STAT regulating cell proliferation, migration and adhesion (*155*). EGF receptor can be internalized via endocytosis resulting in receptor degradation, recycling or nuclear translocation contributing to signalling. In the nucleus EGFR can induce DNA replication, DNA damage repair, transcription and cell proliferation because of the gene transactivation activity at the C-terminal portion (*154*). In particular, nuclear EGFR binds to the promoter of the cyclin D1 gene (CCND1) increasing its transcription (*154*). EGFR can also behave as a cofactor for STAT3 and E2F1 transcription factors (*153*). Other target genes for nuclear EGFR are NOS2 (inducible nitric oxide synthase), which catalyse the formation of nitric oxide necessary for inflammation signalling; AURKA (Estrogen-Induced Aurora Kinase-A), a protein kinase associated with microtubules, and the transcription factor BMYB (B-myeloblastosis virus), responsible for cell differentiation, proliferation and survival (*156*).

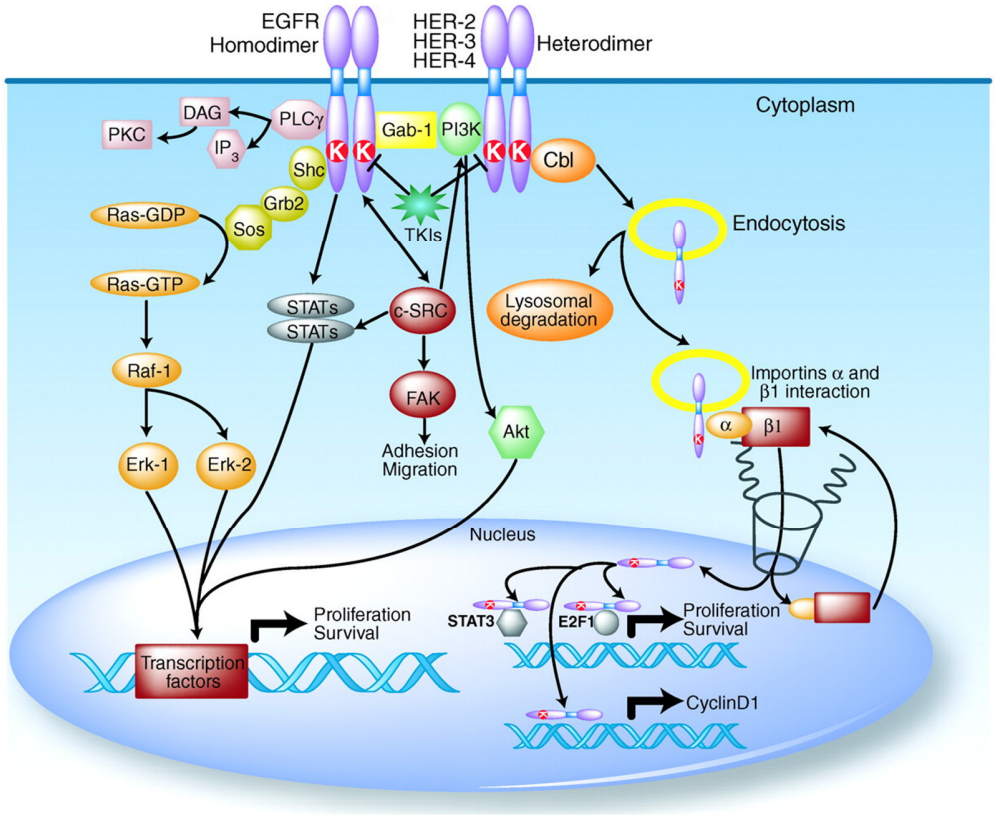

Fig. 1.10 EGFR signalling pathway. EGF binding cause receptor homo/heterodimerization and to phosphorylation of specific tyrosine residues. This recruits to the receptor several effector proteins such as PLCγ, STAT and PI3K, or adaptors as Shc, GRB2. Their activation results in the signalling through PKC, AKT and MAPK pathways that induce cell proliferation and survival, and through FAK pathway that cause cell migration. EGFR can also be internalized by endocytosis and can either behave as a transcription factor or as a co-regulator of other gene transactivators. Both pathways result in transcription of genes involved in cell proliferation, survival, invasion and metastasis. Adapted from Scaltriti *et al.* 2006(*153*).

1.5.3. ST6Gal-I and growth factor receptors

Among the glycosyltransferases that can act on growth factor receptors, ST6Gal-I plays an important role on receptor activation and can exert an inhibitory or activator effect. In fact, it has been reported that sialylation of EGFR in colon cancer cells reduces the receptor activation due to EGF binding, but in contrast it decreases the cytotoxic effect of gefitinib, therefore inducing resistance to chemotherapy (*157*). Moreover, in lung cancer cells the overexpression of ST6Gal-I suppresses EGFR dimerization and phosphorylation upon EGF treatment, reducing EGFR-

mediated invasion (*158*). On the other hand, sialylation of EGFR could enhance EGFR sensitivity to tyrosine kinase inhibitors (TKIs) in lung cancer cell lines (*159*). Furthermore, sialylation of the VEGFR operated by ST6Gal-I prevents galectin 1 binding and VEGF-signalling, resulting in anti-VEGF drug sensitivity (*160*). However, ST6Gal-I exerts an activator effect on the hepatocyte growth factor receptor (c-Met). In fact, in a colon cancer cell line, the knockdown of ST6Gal-I induces hyposialylation of c-Met and reduces cell motility (*161*). Moreover, in a breast cancer cell line the overexpression of ST6Gal-I promotes TGFβ-induced epithelial to mesenchymal transition (EMT) and the maintenance of the mesenchymal state, which can promote malignant progression (*162*).

1.6. CANCER STEM CELLS AND PLURIPOTENCY

Stem cells are defined as a population of cells able to self-renew indefinitely, form single cell derived populations and differentiate into various cell types (*163*). Stem cells found in human tissues are generally multipotent and can originate a restrict number of cell types unlike embryonic stem cells (ESCs) that are pluripotent and can originate any cell type. Recently, great emphasis has been given to the discovery that somatic cell can undergo de-differentiation through the expression of specific transcription factors such as Oct4 (octamer-binding transcription factor 4), SOX2 (sex determining region Y box 2), c-Myc and KLF4 (Kruppel-like factor 4) (*164*). These reprogrammed cells have been called induced pluripotent stem cells (iPSC) and share many characteristics with ESCs but present also differences (*165*), for example different DNA methylation (*166*). Stem cells have been recognized also in cancer tissues where they acquire the ability to survive from conventional treatment and escape from the immune system (*167*). Therefore, they can cause recurrence of cancer because even few surviving cancer stem cells (CSC) are sufficient to form a new tumour (*168*). At present, the mechanism of CSC development is still controversial. One theory suggests that they can be due to oncogenic mutations accumulating within adult stem cells, which leads to their uncontrolled proliferation, retaining stemness. The second theory considers cellular dedifferentiation from a cancer cell into a stem-like state (*169*). Regardless the mechanism of development, markers have been identified to recognise cancer stem cells. In particular, in colon cancer Oct4, SOX2, c-Myc, and KLF4 (that can dedifferentiate cells in iPSC) together with

NANOG (Homeobox protein NANOG) are overexpressed, conferring the cells a stem cell like phenotype (*170*). Other most used markers for CSC identification are CD133 and CD44. CD133 is a well-known stem cell marker and it has been reported that cells $CD133^{+}$ isolated from primary CRC were able to originate tumours in mice (*171*). CD44 is overexpressed since early events of colorectal cancer development because its expression is regulated by the Wnt pathway, often altered in CRC (*172*), single $CD44^{+}$ cells are able to form tumour spheres with stem cell characteristics that give rise to tumours when injected in mice (*172*). There are other markers under study for the identification of colorectal CSCs. SALL4 (Sal-like protein 4) controls self-renewal and pluripotency in embryonic stem cells, evidences suggest that it is regulated by the Wnt pathway (*173*); moreover, it has been found in plasma of patients with local CRC (*174*). ABCG2 is part of ATP binding cassette superfamily, therefore involved in drug resistance (*175*), and is associated with proliferation and maintenance of CSCs, as well as tumour formation (*176*). STAT3 is a transcription factor correlated with increased proliferation and invasion of cancer cells (*177*), its presence has been reported in tumour-initiating $CD133^{+}$ cells (*178*). In addition, other potential markers that can be used to identify CSCs are EpCAM and LGR5. EpCAM (Epithelial cell adhesion molecule) is principally expressed on tumours of epithelial origin and is enriched in colon tumours relative to normal colon. $EpCAM^{High}/CD44^{+}$cells can originate tumours if injected in mice (*179*). LGR5 (Leucine-rich repeat-containing G-protein coupled receptor 5) is a newly identified marker whose knockdown causes tumour regression, while its recovery induces tumour growth and recurrence (*180*). Finally, aldehyde dehydrogenase 1 (ALDH) is considered a typical marker of normal and cancer stem cells. Its expression is increased in CRC correlating with poor prognosis. In fact, $ALDH^{High}$ cells display properties of CSCs, such as self-renewal, *in vivo* tumour growth potential and chemoresistance (*181*). Moreover, it has been reported that patients with high ALDH before chemoradiation present recurrence after surgery, thus ALDH can predict the prognosis of patients receiving post-surgery chemoradiation (*182*).

1.6.1. ST6Gal-I involvement in cancer stem cells

In the attempt of defying the phenotypic characteristics of iPSCs and CSCs, many studies have considered the role of glycans in these cell types because of their known functions in cell-cell

interactions in normal cell differentiation and embryogenesis. The glycomic analysis performed by Hasehira *et al.* (*183*) on iPSC highlights differences on the glycan profile between iPSC and somatic cells (SC). In fact, they report that upon induction of pluripotency high mannose-type N-linked glycans increased and that α-1–2 fucose and Galβ1,3GlcNAc type 1 structures became evident. Moreover, they observed a shift from α2,3- to α2,6-linked sialic acid in iPSCs compared to SC. This correlates with data showing increased expression of ST6Gal-I obtained with microarray analysis. The increased expression of ST6Gal-I and thus the presence of α2,6-linked sialic acid in iPSCs was also confirmed in other studies (*184, 185*). In a more recent study it has been proposed that ST6Gal-I could contribute to the regulation of pluripotency (*186*). In fact, downregulation of ST6Gal-I induces a reduced Oct4 expression, significantly modulated the expression of genes involved in cell differentiation and impaired the induction of cellular pluripotency in somatic cells. In addition, ST6Gal-I colocalizes with ALDH staining at the base of crypts in colon normal tissue, or in the basal epidermal layers of the skin, where progenitor cells are found, and its expression is up-regulated in CSCs derived from colon cancer cell lines $ALDH^{High}$ and $CD133^{+}$ (*187*). Furthermore, the work of Schultz *et al.* points out that the downregulation of ST6Gal-I in pancreatic and ovarian cancer cell lines impaired CSC spheroid formation, and that cells from primary ovarian cancer sorted for α2,6 sialylation were able to grow as spheroids in comparison with cells lacking α2,6 sialylation (*188*) confirming that this sialyltransferase could induce a CSC state.

1.7. PREVIOUS RESULTS

In the literature it has been reported that ST6Gal-I activity and SNA reactivity increase in colon cancer specimen compared to normal mucosa. These data were first reported by our group (*91, 93*) and confirmed later by others (*95*). In particular, the enzymatic activity of ST6Gal-I in cancer tissue was always higher than that of normal samples but the extent of its activation was different among patients (Fig. 1.11A) (*189*). Moreover, SNA reactivity to Sia6LacNAc was higher in colorectal cancer specimens (Fig. 1.11 B.1-B.4) but partially correlated with enzymatic activity data of corresponding samples. Real time PCR performed on normal and cancer tissues showed the presence of two ST6Gal-I transcripts, the housekeeping variant that present Y and Z exons, and the

hepatic form, the latter one increased in neoplastic tissue. Subsequent studies demonstrated that the expression of ST6Gal-I is controlled by Ras oncogene, explaining its upregulation in different types of cancer (*99*). On the other hand, studies performed on a colorectal cancer cell line (SW948) transfected with cDNA of rat ST6Gal-I indicated that the overexpression of the enzyme could attenuate the neoplastic phenotype of the cells (*109*). In fact, ST6Gal-I-transfected clones showed increased binding to collagen IV and fibronectin, compared to mock-transfected cells (Fig. 1.11 C.1-C.4). This was probably due to the increased level of expression of β1-integrins, often reported as substrate for this enzyme. In addition, when ST6Gal-I-transfected and mock-transfected cells were mixed and injected together in nude mice, only mock cells were able to develop tumours (Fig. 1.11 D).

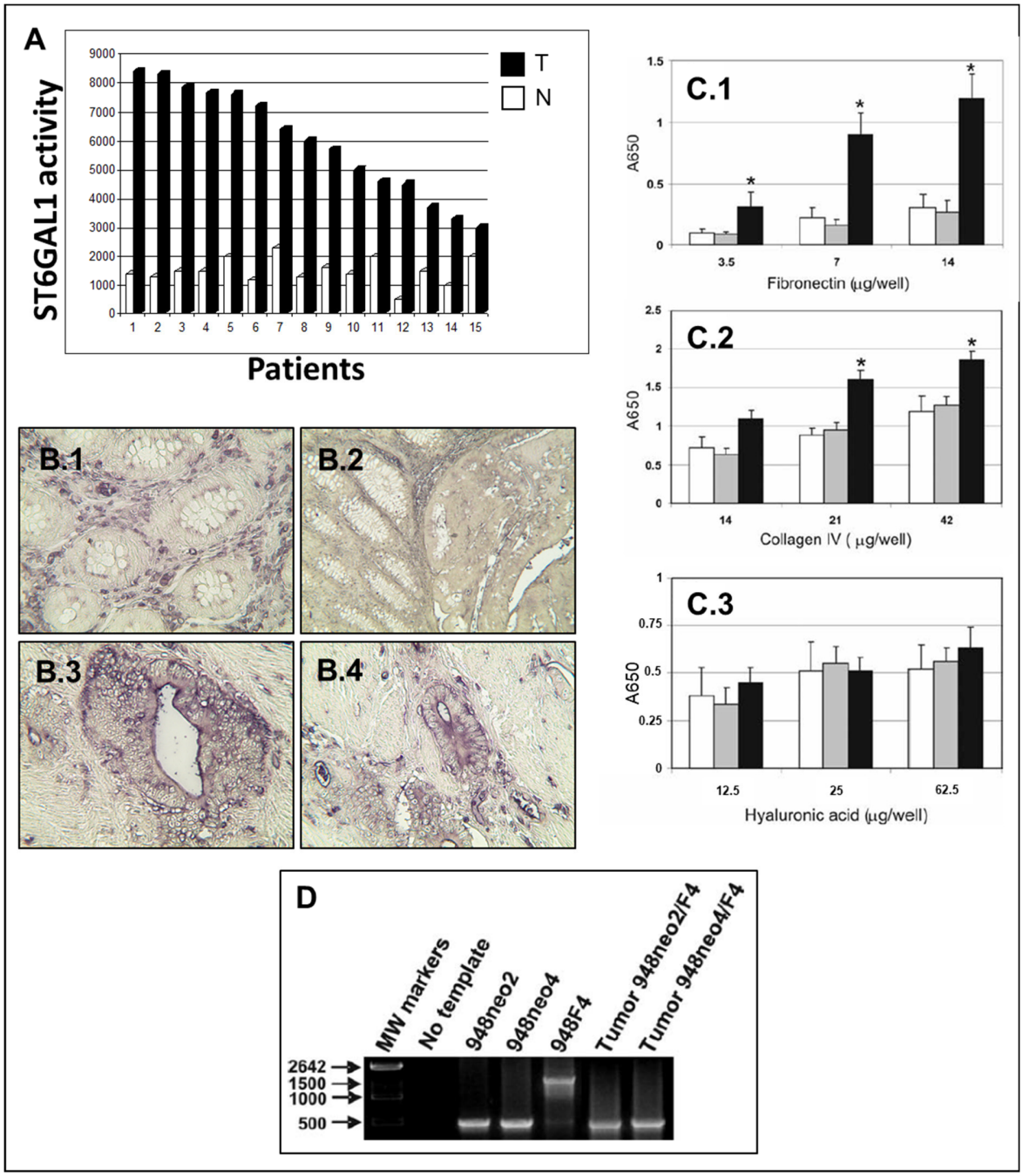

Fig. 1.11 Previous results obtained from our group. **A:** ST6Gal-I activity in normal (N) and tumour (T) tissue **B:** SNA staining of four histological section: **B.1** normal colon tissue, **B.2-B.4** colon cancer tissue. **C** Adhesion of untransfected SW948 (white), mock-transfected clones (grey) and ST6Gal-I transfected clones (black) to fibronectin (**C.1**), collagen IV (**C.2**) and hyaluronic acid (**C.3**). **D** ST6Gal-I transfected cell (948F4) and mock (948neo2-4) were mixed in the same number and injected together in mice. The genomic DNA was extracted from the tumour and amplified with a primer pair specific for the regions of the vector flanking the insert. In the tumours was present only an amplification product corresponding to the empty vector of the 948neo clones.

2. AIM OF THE PROJECT

From the literature and from previous observations obtained by our group, it is evident that the sialyltransferase ST6Gal-I and its cognate antigen Sia6LacNAc are associated with cancer, but it is still unclear their role in tumour development and progression. This project is aimed to:

a) elucidate possible correlations between the expression of ST6Gal-I mRNA and clinical data from The Cancer Genome Atlas (TCGA) database. This database contains mRNA expression values obtained from microarray and RNAseq experiments on cancer specimens and normal tissue together with clinical data such as survival, stage of the tumour, mutations and response to conventional treatment.
b) Evaluate the impact of ST6Gal-I overexpression in two colon cancer cell lines, SW948 and SW48, representing chromosomal instability and microsatellite instability respectively. These cells have been transduced with the cDNA of ST6Gal-I, originating SW948 and SW48 ST, or with an empty vector resulting in SW948 and SW48 negative control (NC). In particular, we will investigate whether ST6Gal-I expression in our models can alter gene expression profiles and the typical hallmarks of cancer, such as anchorage independent growth, migration and invasion capacity, apoptosis and stemness.

3. MATERIALS AND METHODS

3.1. TCGA DATABASE

Data regarding gene expression and clinical information of 623 cancer and 51 normal tissues from a cohort of colorectal-adenocarcinoma patients were downloaded from TCGA database while data regarding mutations were downloaded from cBioPortal (*190*). Data of TCGA database were downloaded from http://firebrowse.org/ considering only the cohort of colon adenocarcinoma (COADREAD). We downloaded separately the file with clinical data and mRNA expression and we removed the genes with average expression lower than five. Finally, we matched the clinical information with the gene expression results. ST6Gal-I mRNA expression values were analysed in comparison with tumoural/normal status, stage of the tumour, the presence of MSI phenotype (MSI-high or -low), response to treatment, the histological type, survival, and with KRAS, BRAF, APC and TP53 mutations. The samples do not present a normal distribution; therefore, it has been necessary to use non-parametric tests. Mann Whitney test was used to analyse ST6Gal-I expression in tumoural/normal status, mucinous/non-mucinous histological type, and in correlation with KRAS, BRAF, APC or TP53 mutations. Kruskal-Wallis test was used to evaluate ST6Gal-I mRNA expression, with respect to cancer stages and presence of MSI phenotype. The survival curve was calculate using the Mantel-Cox test for log-rank.

3.2. CELL CULTURES

SW948 (ATCC® Number: CCL-237™) and SW48 (ATCC® Number: CCL-231™) cell line were cultured in Leibovitz's L-15 Medium supplemented with 10% fetal bovine serum (FBS), 1% L-Glutamine and 1% Penicillin/Streptomycin. Cells were kept at 37°C in absence of CO_2 (L-15 is phosphate buffered) in a humidified incubator.

As reported in Malagolini *et al.* (*191*) SW948 ST and SW48 ST were transduced with the cDNA of the whole coding sequence of human ST6Gal-I obtained from Caco2 cells. The entire coding

sequence without 5'-untranslated regions (5'-UTR) was PCR amplified using the following primer pair: the forward primer (hST6Gal-I.L1) consisting of the nucleotide sequence CACCATGATTCACACCAACCTGAAGAAAAAGTTCAGCTGCTGC and the reverse primer (hST6Gal-I.R1) consisting of the sequence TTAGCAGTGAATGGTCCGGAAGCCAGGCAGTGTG. The underlined sequence included in the forward primer is necessary for the directional cloning in the TOPO vectors and is not gene specific. The PCR product was cloned in the pLenti6/V5 directional TOPO vector (Invitrogen, Carlsbad, CA) and used to transfect the 293FT cell line, according to the instruction manual of the Vira Power Lentiviral Expression System (Invitrogen). The conditioned medium, containing the virions, was centrifuged to remove cell debris, filtered on a 0.45 μM membrane, diluted with 9 volumes of fresh culture medium, added to SW948 cells, and left for 48 h. Cells were selected by the presence of 10 μg/mL blasticidin. A mock transduction was run in parallel with a lentivirus lacking the ST6Gal-I insert, originating SW948 and SW48 NC (Negative control) cells.

3.2.1. Cell treatments

Both apoptosis inducer and growth factors were added directly to the culture medium at a concentration determined as follows:

- TPEN (N,N,N′,N′-Tetrakis(2-pyridylmethyl)ethylenediamine) is resuspended in water to a final stock concentration of 10 mM and used on cell at 10 μM.
- Recombinant HGF (hepatocyte growth factor) is resuspended in PBS and bovine serum albumin (BSA) 0.1% to a final stock concentration of 10 μg/ml and used on cells at 25 ng/ml.
- Recombinant EGF (epidermal growth factor) is reconstituted in water to a final stock concentration of 1 μg/μl and used on cells at 5 and 20 ng/ml.

3.2.2. Induction of apoptosis

To evaluate the propensity of SW948 and SW48 NC and ST to undergo apoptosis through the intrinsic pathway, $2*10^6$ SW48 or $1.5*10^6$ SW948 cells were plated per well in a multiwell 6 plate. After 2 days they were treated with TPEN at a final concentration of 10 μM and collected at different time points by trypsinization or by direct lysis in the wells, depending on the downstream analysis.

3.2.3. Treatment with HGF and EGF

SW948 and SW48 NC and ST were plated respectively at a concentration of $2*10^6$ and $1.5*10^6$ per well in a multiwell 6 plate and they were let adhere for 24-48 hours. Then, they were starved in serum-free medium for 24 hours and treated with HGF or EGF at a final concentration of 25 ng/ml or 20ng/ml respectively, for 15, 30 minutes and 2 hours. The samples thus treated were collected by scraping the surface of the plate.

3.3. ANALYSIS OF ST6Gal-I-TRANSDUCED CELLS

3.3.1. Sample collection and cell lysis

Cells were collected either by trypsinization or by scraping the surface of the plate. In the first case, cells were detached using trypsin and collected using complete L-15 to inactivate the enzyme. Then, the cells were centrifuged to collect the pellet, washed once with PBS, to remove any trace of serum and trypsin, and finally stored at -80°C as dry pellet until needed. The cells were then homogenized in water.

In the second case, the cells were washed with PBS, lysed for 15 minutes in ice by directly adding the lysis buffer to the plate. The cells were then collected by scraping the plate surface, incubated in ice for 15 minutes and centrifuged for 20 minutes at 4°C at 10000x*g*. As lysis buffer we used

Ripa Buffer (50 mM Tris-HCl pH 8, 150 mM NaCl, 1%NP-40, 0.5% DOC, 0.1% SDS) supplemented with protease inhibitor and phosphatase inhibitor cocktail (100x).

3.3.2. Determination of protein concentration

Protein concentration was determined by using Lowry assay or Bradford assay. The sample concentration was calculated by interpolating the absorbance value to a standard curve obtained with known concentration of BSA.

3.3.3. Western Blot

Samples were prepared with an equal amount of proteins and made up to the desired loading volume by adding H_2O and sample buffer 4x (0.5 M Tris HCl pH 6.8, 10% SDS, 30% Glycerol, 6% β-Mercaptoethanol and 0.012% Bromophenol Blue), boiled for 5 minutes and separated in 8% to 12% acrylamide gel, depending on the molecular weight of the protein of interest in denaturing and reducing conditions. We used the PageRuler Prestained Protein Ladder as protein molecular weight markers. The proteins were then transferred to an activated PVDF membrane for 10 minutes using the BioRad Transblot turbo system.

After the transfer, membranes were incubated for 1 hour at room temperature with 1-2% BSA in TBS-T (tris-buffered saline and 0,05%Tween20) as blocking solution, then incubated overnight at 4°C with primary antibody on an orbital shaker. The following day, the membranes were washed with TBS-T and incubated for 1 hour at room temperature with a secondary antibody conjugated with Horseradish peroxidase (HRP). Detection was performed using Super Signal West pico as a chemiluminescent substrate. Pictures of the films were taken using EDAS 290 camera (Kodak). Densitometric analysis was performed using Kodak 1D software and statistical analysis with two-way ANOVA followed by Holm-Sidak's multiple comparisons test.

The following primary antibodies were used in Western Blots: mouse monoclonal anti-phosphotyrosine (Cytoskeleton) and anti-vinculin (Sigma), rabbit polyclonal anti-β-Actin (Sigma)

and anti-FAK [pY397] (Life Technologies), goat polyclonal anti-ST6Gal-I (R&D systems). As secondary antibodies, polyclonal rabbit anti-mouse (Sigma), goat anti-rabbit (Sigma) and donkey anti-goat (R&D system) conjugated to HRP were used. To evaluate apoptosis, we used Apoptosis Western Blot Cocktail (pro/p17-caspase 3, cleaved-PARP, muscle Actin) (abcam). Both primary and secondary antibodies were diluted in TBS-T 0.05% + 0.1% BSA.

3.3.4. Stress and apoptosis pathway protein array

To evaluate apoptosis with the PathScan® Stress and Apoptosis Signaling Antibody Array Kit (Cell Signaling), SW948 and SW48 NC and ST were plated respectively at a concentration of $2*10^6$ and $1.5*10^6$ per well in a multiwell 6 plate and they were let adhere for 24-48 hours. They were treated with TPEN 10 μM at different time points and lysed directly on the plate with the lysis buffer of the kit following manufacturer's instructions. Protein concentration was measured as previously described with Bradford assay. 50 μl of cell lysates were then incubated for 2 hours on the slide at a final concentration of 1 mg/ml after blocking the non-specific sites with Array Blocking Buffer. The slide was washed with Array Wash Buffer and incubated with the Detection Antibody Cocktail for 1 hour. Then, it was washed again and incubated for 1 hour with HRP-linked Streptavidin and the chemiluminescent signal was obtained by incubation of the slide with LumiGLO and Peroxide and read through a ChemiDoc Imaging System (BioRad).

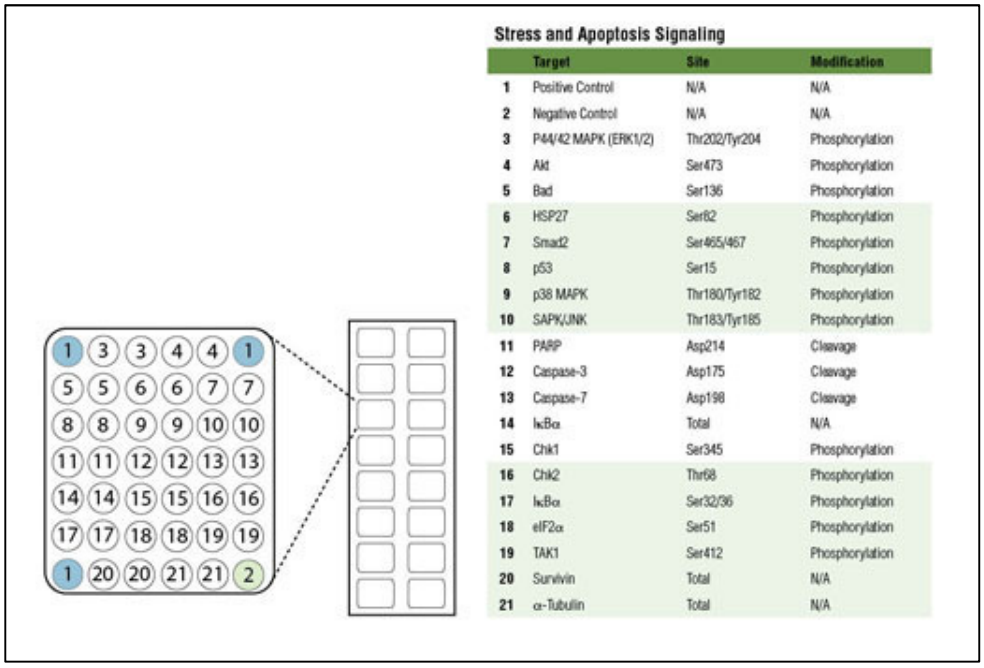

Fig. 3.1 Target map of the PathScan® Stress and Apoptosis Signaling Antibody Array Kit (Chemiluminescent Readout) #12856.

3.3.5. Sialyltransferase activity

Sialyltransferase activity was measured in whole cell homogenate by incorporation of [^{3}H] sialic acid on asialotransferrin. Radioactivity incorporated on endogenous acceptors was subtracted. A solution containing 80mM Na-cacodylate buffer pH 6.5 and 0.5% Triton X-100 was incubated with 300 µg asialotransferrin, 30 µM CMP-sialic acid, 1 µl CMP-[^{3}H] sialic acid (1x10^5 dpm/µl) and 100 µg of cell homogenate in a final volume of 50 µl for 3 hours at 37°C. After incubation the reaction was stopped by adding 500 µl of phosphotungstic acid (FTA) (1% phosphotungstic acid in 0.5 M HCl) and then washed twice with FTA. Then, the samples were boiled for 20 minutes with 300 µl of 1 M HCl. After the addition of 3.5 ml of liquid scintillation cocktail, the radioactivity of the samples was determined with the Guardian 1414 Liquid Scintillation Counter (PerkinElmer).

3.3.6. Evaluation of SNA reactivity

Flow cytometry (FACS) analysis

Approximately $5x10^5$ SW948 and SW48 NC and ST cells were washed with PBS containing 1 mg/ml BSA and incubated 20 minutes with 50 µg/ml FITC-conjugated SNA at 4°C in the dark. The samples were then washed with PBS/BSA and then resuspended with 500 µl of PBS supplemented with 2% formaldehyde. The analysis was performed using FACSCalibur (BD) and CellQuest Pro software (BD), the fluorophore was read with FL1 channel.

Immunofluorescence

A number of $8x10^5$ SW948 and SW48 NC and ST cells were plated on a glass coverslip and let adhere for 24-48 hours. The coverslips were washed in PBS and then fixed with 2% formaldehyde for 20 minutes and then stained with FITC-conjugated SNA lectin for 20 minutes. After staining, they were washed and mounted on microscope slides. Images were taken with a Nikon Eclipse E600 microscope and DXM1200F digital camera.

3.3.7. RNA extraction and cDNA reverse transcription

Total RNA was extracted according to Chomczynski e Sacchi (*192*) and suspended in 50 µl of RNase free water. RNA concentration was determined using the Nano Genius Photometer ONDA, measuring absorbance at 260 nm with a 260:280 ratio of 2.1+/-0.5. RNA integrity was determined running RNA samples on a 1% agarose gel.

RNA samples were reverse transcribed using the High Capacity cDNA Reverse Transcription Kit (Applied Biosystems) following manufacturer's instructions.

3.3.8. Transcriptomic analysis

Transcriptomic analysis of RNA extracted from SW948 and SW48 NC and ST was carried out in duplicate at LTTA Microarray Facility, Università di Ferrara with Agilent Technologies. Statistical analysis was performed using two-way ANOVA for repeated measures and the false discovery rate was controlled with two-stage linear step-up procedure of Benjamini, Krieger and Yekutieli with Q=0.05. P values and q values are listed in table 4.1 and 4.2.

3.3.9. Real-Time PCR

Real time PCR was carried out in triplicate using SsoAdvanced™ Universal SYBR® Green Supermix (BioRad) containing the fluorescent SYBR Green reagents, nucleotide mix and Sso7d fusion protein polymerase. To this mix, forward/reverse primers (details can be found in Table 1) at a concentration of 0.25 µM and sample cDNA (20ng) were added forming a total reaction volume of 10µl. The PCR reaction was carried out with a CFX96 machine (BioRad), using the following protocol: 98°C hold step for 2 minutes and 40 cycles of 98-60°C for 5 and 30 seconds respectively.

Gene	Forward 5'-3'	Reverse 5'-3'
BACT	GCGAGCACAGAGCCTCGCCTTT	GCACATGCCGGAGCCGTTGTCG
KLK6	ACCTGGTGTCCCGTGAGGAGT	CCACATACCAGCGGACCCCC
MYEOV	CATACACCCCAGCTCTCCCGA	GCAACGAGTCCCTGTCCCCA
OLFM4	GGCTTCAGCTCTTTCCCAGGTGT	GGTCCCACGGTCATCCACGG
TGFB2	CGCGAGAGGAGCGACGAAGA	AGAAAGTGGGCGGGATGGCA
FOLR1	ATGGCACCTGCCTGCAAACG	GGGCACGTTCAGTACCCGCT
SH3GL2	CGGCCTCAAGAAGCAGTTCCAT	GCCCTGCTGGTGACATCCACTTTC
FMOD	CCCCCAGTCAACACCAACCTGG	ACGTCCACCACGGTGCAGAA
MAP1B	TCAAAGCTGCACGTGGGGAAGA	CCTGGGGGCACAGCAGATGAC
MT4	GGACCCCAGGGAATGTGTCTGC	CCCCGGGCACATTTGGCACA
WNT16	TCGGAAACACCACGGGCAAAGA	GGAGCCGGAAACTCCGTGGC

Table 3.1 Primers' sequences.

To evaluate ST6Gal-I mRNA expression in SW948 and SW48 transduced cells we performed real time PCR in triplicate with TaqMan® Fast Universal PCR Master Mix (Applied Biosystems) supplemented with the sample (20 ng) and TaqMan probes and primers for ST6Gal-I (assay identification Hs00949382_m1) or β-ACTIN (Hs99999903_m1) in a final volume of 10 µl. The reaction was conducted with the same protocol used for SYBR® Green real time PCR.

3.3.10.Soft agar growth assay

A 3,3% solution of agar in water was diluted to a final concentration of 0,5% in complete L-15. 1 ml of this solution was dispensed per well in a multiwell 6 plate. On the top of this first layer of agar we distributed a 0.3% agar solution in complete L-15 medium, containing 1 $x10^4$ cells per well in triplicate. The plates were then incubated for two weeks at 37°C in a humidified incubator without CO_2. To evaluate the number of colonies formed, the plates were fixed and coloured for one hour with a solution containing formaldehyde 4% and Crystal Violet 0.005% in PBS. Pictures were taken using a Nikon Eclipse TS100 inverted microscopy a 5x magnification and a Digital C-Mount camera Sony Colour. Then the colonies were counted, and statistical analysis was performed using non-parametric Kolmogorov-Smirnov test.

3.3.11. Wound healing assay

The wound healing assay was performed using Culture-Insert 2 Well (Ibidi). This consists in a 2 well silicone insert with a defined cell-free gap which gives the possibility to plate the cells in the two wells and to evaluate their ability to close the wound once the insert has been removed. We prepared a solution with $1x10^6$ cells/ml, in case of SW48, and $7x10^5$ cells/ml, in case of SW948, in complete medium and plated 70 µl per well. When the cells reached confluency, we removed the insert and evaluated the capacity to migrate taking pictures with Nikon Eclipse TS100 inverted microscopy a 10x magnification and a Digital C-Mount camera Sony Colour. The area was then measured using the MRI Wound Healing Tool in ImageJ. Statistical analysis was performed using two-way ANOVA and Tukey's multiple comparisons test.

3.3.12.Transwell invasion assay

The transwell invasion assay was performed using Matrigel-coated polycarbonate filters (8 mm pore size, Corning BioCoat Matrigel Invasion Chamber). $3x10^6$ SW948 cells were plated in T25 flasks, while $5x10^6$ SW48 cells were plated in T75 flasks and starved for 24 hours. Then they were detached and plated at a density of $2x10^5$ for SW948 and $4x10^5$ for SW48 in the upper chamber of the well in serum-free medium. Complete L-15 with 10% FBS or serum-free L-15 + HGF 25ng/ml were used as chemoattractant and placed in the lower chamber of the well. The plates were then incubated for 24 hours at 37°C in a humidified incubator without CO_2. Following manufacturers' instructions, the membranes were fixed in methanol and stained with toluidine blue. Finally, they were mounted on slides and the cells were counted using an optical microscope at a 10x magnification. Statistical analysis was performed using two-way ANOVA and Sidak's multiple comparisons test.

3.3.13.ALDEFLUOR assay

For the ALDEFLUOR (Stem Cell technologies) assay for stemness, we activated ALDEFLUOR following manufacturer's instructions. For the samples preparation, the cells were detached with trypsin, counted using a Neubauer Chamber and collected in order to have $2x10^5$ cells/ml per sample. Then we added ALDEFLUOR to our samples and we transferred half of the cell suspension to the tube containing DEAB, a specific ALDH inhibitor used for negative control. The samples were then incubated for 30 minutes at 37°C and centrifuged at 250 x g. Cell pellets were then suspended in ALDEFLUOR buffer. For the acquisition of the fluorescent signal we used a FACSCalibur and CellQuest Pro software. We opened a dot plot with the physical parameters and a second one representing FL1 (green fluorescence) on the X axis and SSC on the Y axis. On this second dot plot we set the fluorescence of the DEAB sample and defined the area for ALDH positive cells, then we acquired the sample with ALDEFLUOR reagent. Cells beyond the threshold established with DEAB sample were considered ALDEFLUOR positive.

3.3.14.Statistical analysis

The GraphPad Prism 7 software was used to perform statistical analysis, using the different tests described above.

4. RESULTS

4.1. THE IMPACT OF ST6Gal-I EXPRESSION ON THE PROGRESSION OF CRC: A SURVEY OF THE TCGA DATABASE

The Cancer Genome Atlas (TCGA) is a public database, which contains data obtained from a high number of cancer patients. From interrogation of this database, it is possible to correlate data on gene expression with clinical data. We evaluated the mRNA expression levels of ST6Gal-I in CRC specimens and normal tissues. We noticed that the gene expression level was relatively constant in normal tissues, whereas it was extremely variable among CRC specimens (Fig. 4.1A). Surprisingly, the median mRNA level of our gene of interest in cancer tissue was similar to that of normal tissue (Fig. 4.1B), in contrast with enzymatic activity data reporting higher ST6Gal-I activity in tumour tissue compared to normal tissue (*93*). The expression of ST6Gal-I in the cohorts of patients showing the 15% higher or 15% lower expression was correlated with clinical parameters. Low ST6Gal-I expression was correlated with high microsatellite instability (Msi-h) (Fig. 4.1D), mucinous phenotype (Fig. 4.1E) and BRAF mutations (Fig. 4.2B). On the other hand, no correlation was observed between ST6Gal-I expression and clinical stage (Fig. 4.1C), mutations in KRAS (Fig. 4.2A), APC (Fig. 4.2C) and TP53 (Fig. 4.2D), response to therapy (Fig. 4.1F) and overall survival (Fig. 1K). Collectively, these data are not consistent with a strong impact of ST6Gal-I level on the progression of CRC, as suggested by previous clinical and experimental data (refer to introduction).

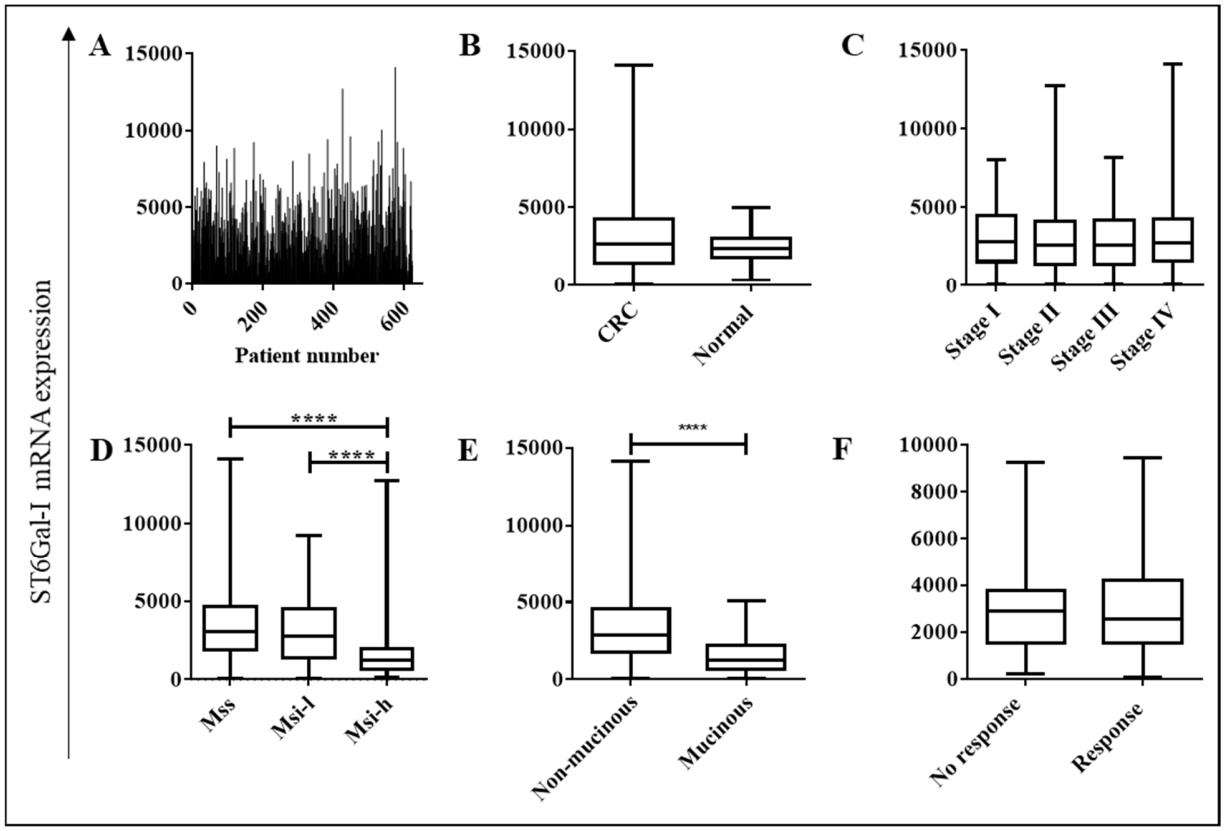

Fig. 4.1 Data from TCGA database. Evaluation of ST6Gal-I mRNA in patients (**A**), and in cancer and normal tissue (**B**). Correlation of ST6Gal-I expression with tumour stage (**C**), microsatellite phenotype: microsatellite stable (Mss), low microsatellite instability (Msi-l) and high microsatellite instability (Msi-h) (**D**), mucinous or non-mucinous type (**E**) and with response to therapy (**F**).

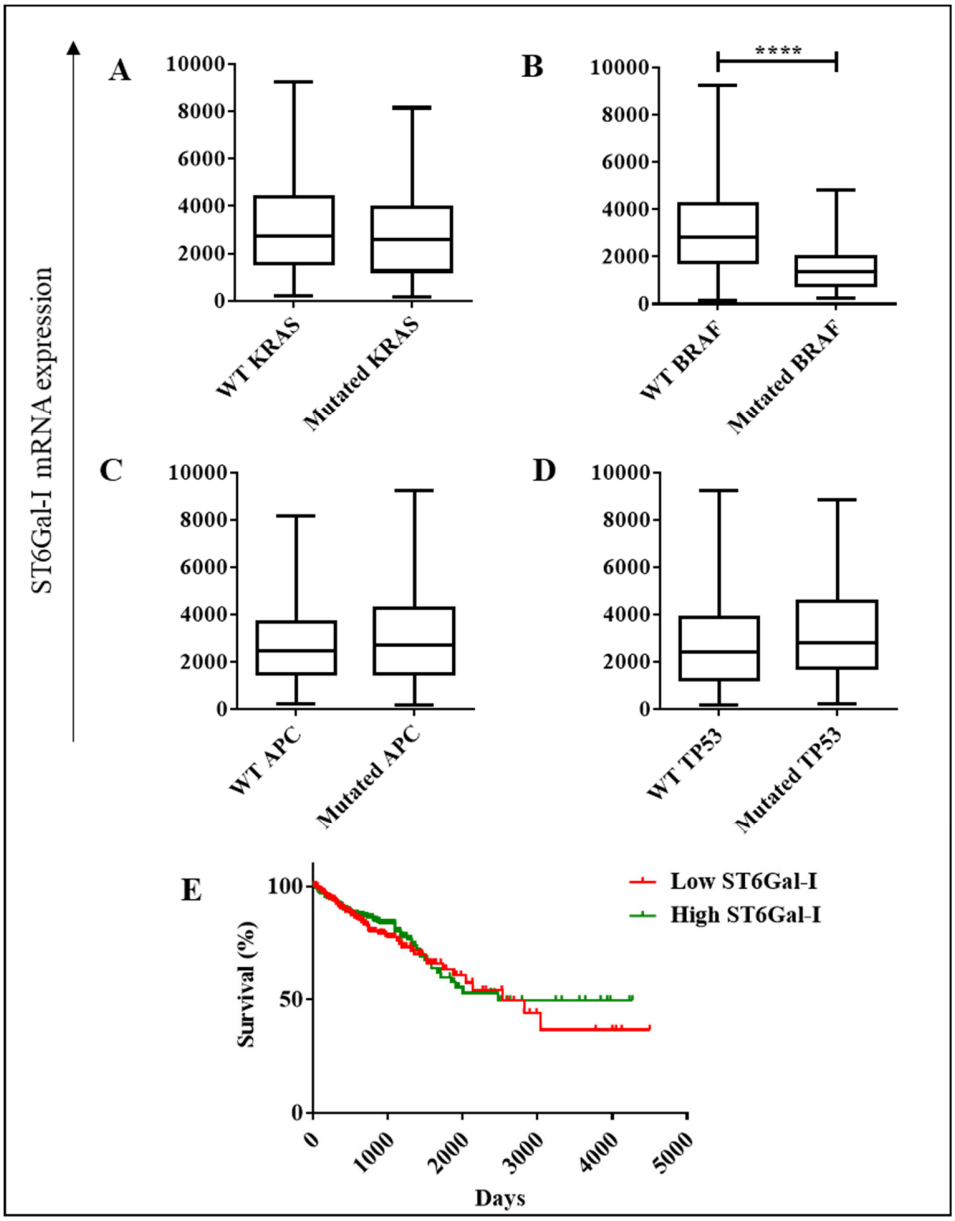

Fig. 4.2 Data from TCGA database. ST6Gal-I expression in colorectal cancer is correlated with mutation in KRAS (**A**), BRAF (**B**) APC (**C**) and TP53 (**D**). **E** shows the survival curve for patients expressing high or low ST6Gal-I.

4.2. THE IMPACT OF ST6Gal-I EXPRESSION ON THE PHENOTYPE OF CRC CELL LINES

4.2.1. SW948 and SW48 cell lines

To fully understand the role of ST6Gal-I overexpression in colon cancer, we selected two colon cancer cell lines, SW948 and SW48. These cell lines lack ST6Gal-I expression and enzyme activity and, in addition, they represent the two principal ways of colorectal cancer pathogenesis: chromosomal instability, in case of SW948, and microsatellite instability, in case of SW48. The two cell lines had been previously transduced with a lentivirus containing the cDNA of ST6Gal-I, obtaining ST cells, or with an empty vector, resulting in negative control (NC) cells (*191*). A characterization of these cell lines with regard to ST6Gal-I expression is reported in Fig. 4.3. By RT-PCR, we noticed a high expression of ST6Gal-I mRNA in both SW948 and SW48 ST cells compared with NC cells (Fig. 4.3A). In addition, we analysed protein expression in western blot and we observed the presence of ST6Gal-I band only in transduced cells and not in NC cells (Fig. 4.3B). Then, we analysed the enzymatic activity measuring the incorporation of radioactive sialic acid on asialotransferrin and we registered a higher activity in both ST6Gal-I transduced cell lines compared to their negative control (Fig. 4.3C). We evaluated also SNA reactivity, both by immunofluorescence and FACS analysis and we confirmed that SW948 and SW48 ST cells were more reactive with the lectin compared to NC cells (Fig. 4.3D, E).

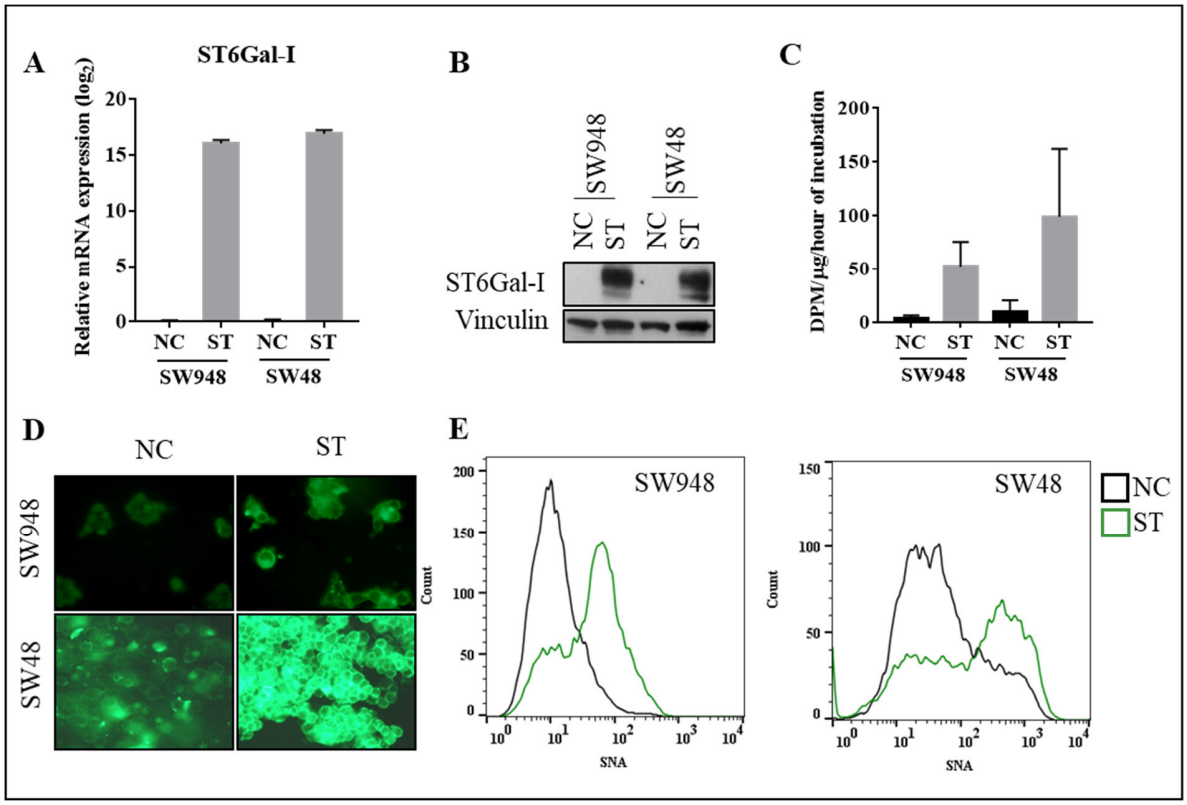

Fig. 4.3 Characterization of SW948 and SW48 transduced with ST6Gal-I. We evaluated ST6Gal-I mRNA expression (**A**), protein level (**B**) and enzymatic activity (**C**); and SNA reactivity in immunofluorescence (**D**) and FACS analysis (**E**).

4.2.2. Transcriptomic analysis

To investigate whether and how the overexpression of ST6Gal-I could modify the gene expression profile of the colorectal cancer cell lines that we use as models, we performed a microarray analysis using Agilent Technologies. Fig 4.4 shows scatter plots representing gene expression of the two cell lines transduced with ST6Gal-I compared to their negative control (NC). We noticed that the overexpression of ST6Gal-I caused a more pronounced modulation of the transcriptome in SW948 cells than in SW48 cells. In particular, the number of modulated genes and the extent of their modulation was higher in SW948 than in SW48 cells. In table 4.1 and 4.2 we report the list of modulated genes in SW948 and SW48 cells, respectively. Surprisingly, none of the differentially expressed genes displayed the same behaviour in both cell lines.

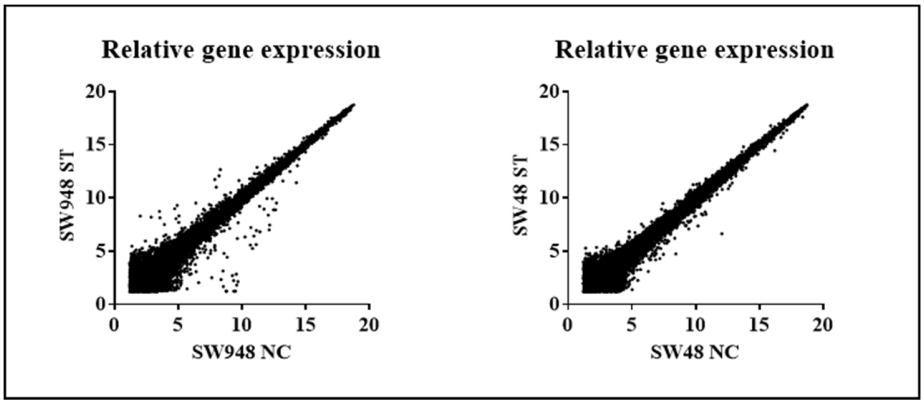

Fig. 4.4 Transcriptomic analysis. The two scatter plots show the relative gene expression of SW948 ST and NC cells and of SW48 ST and NC cells.

Gene Symbol	ST - NC	q value	p value	Gene Symbol	ST - NC	q value	p value
OLFM4	4.4	0.0009	<0.0001	C1orf229	-2.0	0.0372	0.0589
DUSP5	3.9	0.0031	0.0003	TSPEAR-AS2	-2.0	0.0367	0.0573
RYBP	3.9	0.0031	0.0003	FLNA	-2.0	0.0364	0.0565
SH3GL2	3.6	0.0071	0.0008	CDCA5	-2.0	0.0364	0.0561
SLC1A3	3.5	0.0074	0.0009	KLK6	-2.0	0.0364	0.0553
TCL6	3.4	0.0105	0.0016	POLH	-2.0	0.0363	0.0535
MYEOV	3.3	0.0118	0.0022	DSCR9	-2.0	0.0362	0.0525
CAPSL	3.1	0.0144	0.0033	ATXN8OS	-2.0	0.0362	0.0520
ANKRD1	3.1	0.0147	0.0036	DSCAS	-2.1	0.0362	0.0494
REG1A	3.1	0.0164	0.0042	LOC389602	-2.1	0.0362	0.0489
FLNC	3.0	0.0173	0.005	SIM1	-2.1	0.0362	0.0487
LRRD1	3.0	0.0173	0.0054	CTF1	-2.1	0.0362	0.0458
DPY19L2P1	3.0	0.0173	0.0055	LEP	-2.1	0.0356	0.0431
SLIT1-AS1	2.9	0.0175	0.006	lnc-IL37-1	-2.1	0.0356	0.0423
SLC14A1	2.8	0.0208	0.0081	LINC01239	-2.1	0.0356	0.0417
ZNF439	2.8	0.0208	0.0084	DLC1	-2.2	0.0356	0.0415
BST2	2.8	0.0217	0.0092	lnc-SYT4-1	-2.2	0.0356	0.0407
H2AFY2	2.7	0.0220	0.0102	lnc-CRYGS-1	-2.2	0.0356	0.0407
SMAD5-AS1	2.7	0.0232	0.0115	LINC01431	-2.2	0.0356	0.0395
MMP7	2.7	0.0232	0.0115	FAM230B	-2.2	0.0356	0.0391
CALD1	2.7	0.0233	0.0119	LINC00520	-2.2	0.0356	0.0380
THEG	2.6	0.024	0.0133	TRAM1L1	-2.2	0.0356	0.0343

MIP	2.6	0.0248	0.0149	FGF13	-2.2	0.0356	0.0342
CNTN5	2.6	0.0248	0.015	PPP1R17	-2.2	0.0356	0.0334
GGNBP1	2.6	0.0248	0.0157	MBD2	-2.2	0.0356	0.0327
PHACTR3	2.6	0.0248	0.0158	ZNF345	-2.3	0.0349	0.0281
DQX1	2.6	0.0248	0.016	OTOP2	-2.3	0.0334	0.0242
WFDC21P	2.5	0.0248	0.0162	WNT4	-2.4	0.0333	0.0234
PLA2G3	2.5	0.0264	0.0176	IQCF3	-2.4	0.0248	0.0142
TGFB2	2.4	0.0315	0.0215	AKT1S1	-2.6	0.0240	0.0133
CCDC148	2.4	0.0333	0.0237	CXCL12	-2.6	0.0240	0.0131
SULT1C2P1	2.3	0.0349	0.0264	TCAF2	-2.6	0.0220	0.0103
PCDHGB1	2.3	0.0349	0.0268	MIR4500HG	-2.7	0.0220	0.0099
ORAOV1	2.3	0.0349	0.0276	KLK6	-2.7	0.0208	0.0086
MEDAG	2.3	0.0349	0.0276	LINC00643	-2.8	0.0208	0.0085
EVI2A	2.3	0.0349	0.0283	USP17L1	-2.8	0.0198	0.0070
FAM229B	2.3	0.0354	0.0292	GNAT2	-2.9	0.0173	0.0057
LOC100506175	2.3	0.0356	0.0313	FMOD	-2.9	0.0173	0.0048
ACE2	2.3	0.0356	0.0327	PLAC4	-3.0	0.0144	0.0033
CACNA1C-AS4	2.2	0.0356	0.0349	HBB	-3.1	0.0119	0.0024
DMBT1	2.2	0.0356	0.0352	SPTB	-3.2	0.0109	0.0019
MAPT-AS1	2.2	0.0356	0.0354	FAM230A	-3.3	0.0090	0.0013
TIMP3	2.2	0.0356	0.0368	FAT3	-3.4	0.0013	<0.0001
RIMS3	2.2	0.0356	0.0368	EML5	-4.2	0.0009	<0.0001
LOC550113	2.2	0.0356	0.0382	EIF4G3	-4.4	0.0001	<0.0001
C20orf85	2.2	0.0356	0.0388	lnc-MYB-1	-5.1	<0.0001	<0.0001
ATP2B2	2.2	0.0356	0.0413	PEG3	-5.4	0.1476	0.0062
LOC440300	2.2	0.0356	0.0414				
APOBEC3C	2.1	0.0356	0.0426				
EDA2R	2.1	0.0356	0.0427				
SEMA7A	2.1	0.0356	0.043				
BST2	2.1	0.0358	0.0437				
IFIT2	2.1	0.0362	0.0453				
MYBL1	2.1	0.0362	0.0453				
EPB41L3	2.1	0.0362	0.0480				
CELF4	2.1	0.0362	0.0480				
LOC100506974	2.1	0.0362	0.0486				
PRB2	2.1	0.0362	0.0496				
GGT8P	2.1	0.0362	0.0503				
GPR110	2.1	0.0362	0.0514				

TGFB2-AS1	2.1	0.0362	0.0515
IL4R	2.1	0.0362	0.0520
PTAFR	2.1	0.0363	0.0537
PRO1082	2.0	0.0364	0.0545
LINC01234	2.0	0.0364	0.0560
IL1RN	2.0	0.0393	0.0635
FOLR1	2.0	0.0393	0.0636

Table 4.1 List of genes up- or down-regulated in SW948 ST cells in comparison with NC cells. The table reports on the left hand-side genes up-regulated in SW948 ST, whereas on the right hand-side genes down-regulated in SW948 ST cells.

Gene Symbol	ST - NC	q value	p value	Gene Symbol	ST - NC	q value	p value
OVAAL	3.3	0.0176	0.0007	NME8	-2.0	0.0419	0.0399
BPI	3.1	0.0176	0.0013	PROM2	-2.0	0.0419	0.0396
GLDC	3.0	0.0183	0.0024	DACT1	-2.0	0.0419	0.0374
SLC7A4	2.6	0.0339	0.0080	ITGBL1	-2.0	0.0419	0.0366
HRCT1	2.5	0.0339	0.0107	DCLK3	-2.0	0.0419	0.0362
ATP6V0E2-AS1	2.4	0.0339	0.0120	IGFL4	-2.0	0.0419	0.0360
MZF1-AS1	2.4	0.0339	0.0122	INSC	-2.0	0.0419	0.0348
FBXO3-AS1	2.3	0.0357	0.0159	NTRK2	-2.0	0.0413	0.0316
CGA	2.3	0.0357	0.0165	RIMS2	-2.1	0.0413	0.0310
CYS1	2.2	0.0357	0.0193	CALCA	-2.1	0.0385	0.0273
MASP2	2.2	0.0357	0.0207	ITGBL1	-2.1	0.0380	0.0263
ATXN3	2.2	0.0360	0.0217	UGT2B7	-2.1	0.0373	0.0248
F11	2.2	0.0360	0.0229	HILS1	-2.2	0.0360	0.0226
ST3GAL4	2.1	0.0373	0.0251	lnc-WNT1-3	-2.2	0.0357	0.0205
AMICA1	2.1	0.0408	0.0297	TSPAN3	-2.2	0.0357	0.0201
MTUS2-AS1	2.0	0.0419	0.0333	KLHL14	-2.2	0.0357	0.0198
MZB1	2.0	0.0419	0.0392	GALNT5	-2.2	0.0357	0.0198
THTPA	2.0	0.0419	0.0399	PARP11	-2.3	0.0357	0.0181
				IGFL2	-2.3	0.0350	0.0144
				DOC2B	-2.3	0.0350	0.0144
				ZGRF1	-2.4	0.0339	0.0127
				KRT14	-2.4	0.0339	0.0123
				C1QA	-2.4	0.0339	0.0119
				ATRN	-2.4	0.0339	0.0114

MAP1B	-2.5	0.0339	0.0105
NUDT12	-2.5	0.0339	0.0086
SMIM22	-2.8	0.0230	0.0043
CALCA	-2.8	0.0230	0.0042
PHGR1	-2.8	0.0230	0.0038
WNT16	-3.0	0.0183	0.0024
IFNA14	-3.0	0.0183	0.0019
MT4	-3.2	0.0176	0.0011
MAP1B	-3.2	0.0176	0.0011

Table 4.2 List of genes up- or down-regulated in SW48 ST cells in comparison with NC cells. The table reports on the left hand-side genes up-regulated in SW48 ST, whereas on the right hand-side genes down-regulated in SW48 ST cells.

Considering the genes showing the stronger modulation, in SW948 the overexpression of ST6Gal-I drives gene expression mainly towards up-regulation. In fact, we counted 67 up-regulated and 47 down-regulated genes. Among them, we validated by RT-PCR seven genes with a potential role in tumour development or progression: OLFM4, SH3GL2, FOLR1, TGFB2, MYEOV, FMOD and KLK6 (Fig 4.5). We examined other genes potentially important in cancer biology, but the validation did not confirm their modulation.

The more consistently up-regulated gene in SW948 ST cells resulted to be OLFM4 and its increase was confirmed also in RT-PCR. OLFM4 is a glycoprotein overexpressed in many tumours, including colorectal cancer, but its biological role seems to be strictly tissue specific (*193*). In mice, OLFM4 seems to regulate the Wnt/beta-catenin and NFκB pathways inhibiting colon-cancer development (*194*). Another highly modulated gene in SW948 ST cells validated in RT-PCR is SH3GL2, which is a tumour suppressor frequently deleted or methylated in breast, lung, head and neck cancer and glioblastoma (*195*). FOLR1, folate receptor 1, is reported to be overexpressed in breast and ovarian cancer with poor prognosis (*196*), it is expressed in colorectal cancer tissue as well, where it seems to increase the cytotoxicity of 5-fluoro-2'-deoxyuridine (FdUrd) treatment (*197*). We reported also the up-regulation of TGFB2 in SW948 ST cells compared to NC. Its role in tumour biology is still controversial but recent studies reported that TGFB2 expression is increased in advanced and poorly differentiated CRC and correlates with poor prognosis (*198*).

The last up-regulated gene in SW948 ST is MYEOV, which has a tumour promoting role in colon by increasing cell proliferation and invasion (*199*). Among the down-regulated genes in SW948 ST compared to NC we selected for validation FMOD and KLK6. FMOD encodes fibromodulin protein, a collagen fibrillogenesis modulator that is highly expressed in cancer stroma increasing collagen fibril thickness (*200*). KLK6 is highly expressed in colorectal cancer cells and promotes cell migration and invasion (*201*). In conclusion, from this analysis we demonstrated the necessity to validate with RT-PCR the results obtained with microarray to better understand the biological significance underlying our data. In the analysis of the more consistently modulated gene in SW948 ST cells, we reported the up-regulation of two tumour suppressing genes (OLFM4 and SH3GL2) and the downregulation of two tumour promoting transcripts (FMOD and KLK6) which may suggest an anti-tumorigenic potential of ST6Gal-I in colorectal cancer. On the other hand, TGFB2, MYEOV and FOLR1, with a pro-tumorigenic effect, are up-regulated after ST6Gal-I overexpression. Therefore, at present it is not possible to define if the effect of ST6Gal-I overexpression results in a tumour promoting or tumour suppressing function in SW948 cell line.

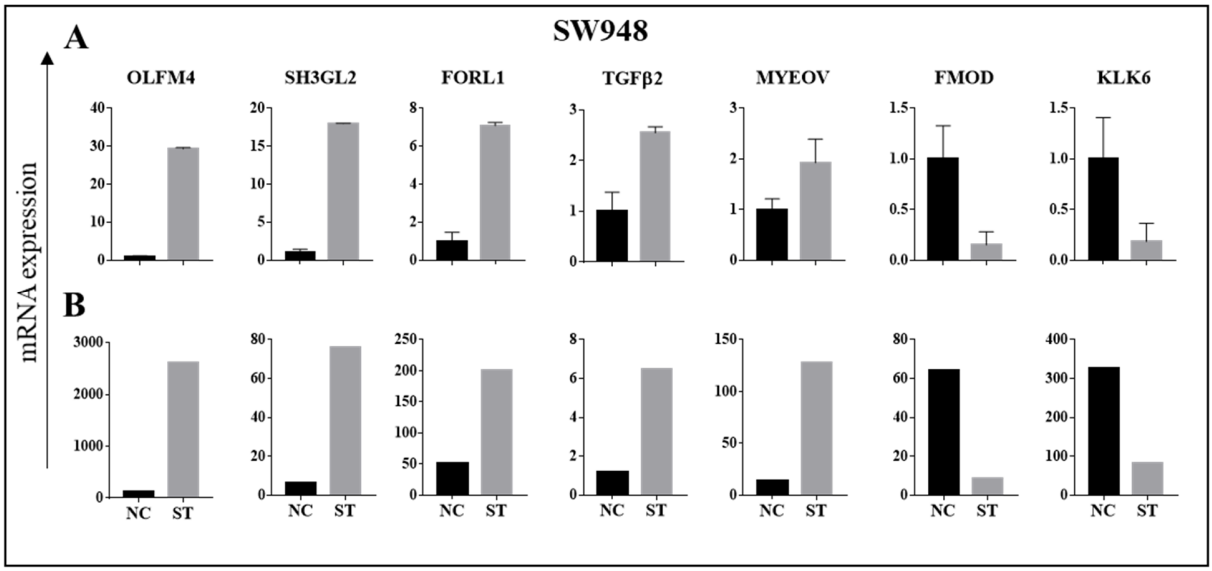

Fig. 4.5 mRNA quantification by real time PCR (**A**) or microarray analysis (**B**). RNA was extracted from SW948 NC and ST cells. The mRNA level determined by RT-PCR was expressed in fold change and normalised on β-Actin expression level. The mRNA level evaluated by microarray analysis was expressed in arbitrary units and calculated as RNA expression= 2^(log2E-1.3) Where 1.3 is the lowest log2E value of the evaluated genes.

In SW48 cells transduced with ST6Gal-I, we found only a few genes reaching a log 2E change higher than +/-3; the majority of these were down-regulated. In fact, SW48 ST displayed 18 up-regulated and 33 down-regulated genes. However, very few of these differentially expressed genes are reported to be involved in cancer biology. Among the genes that we validated, only three showed a consonant modulation in qPCR; they are MAP1B, MT4 and WNT16 (Fig. 4.6). MAP1B is a microtubule associated protein which seems to be important for microtubule stability in response to microtubule-targeting anti-cancer drugs (*202*); moreover, it is involved in cancer cell invasion and migration (*203*). MT4 is a membrane type matrix metalloproteinase and is involved in cancer cell invasion and metastasis (*204*). Eventually, WNT16 is part of WNT family involved in cell proliferation. It has been reported that WNT16 is upregulated in gastric adenocarcinoma (*205*) and promotes resistance to chemotherapy in prostate tumour (*206*). In conclusion, the small number of modulated genes suggests a trend towards a tumour suppressive effect of ST6Gal-I overexpression in SW48 cell line. These findings show that the effect of ST6Gal-I overexpression on the transcriptome of the two colorectal cancer cell lines is very different and strongly cell-type specific.

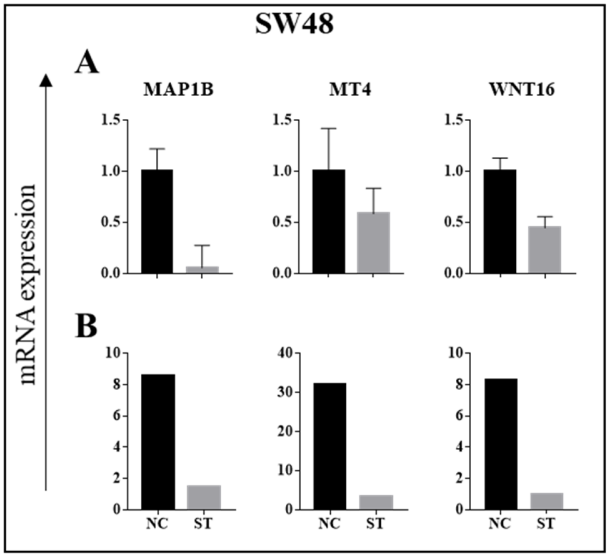

Fig. 4.6 mRNA quantification by real time PCR (**A**) or microarray analysis (**B**). RNA was extracted from SW48 NC and ST cells. The mRNA level determined by RT-PCR was expressed in fold change and normalised on β-Actin expression level. The mRNA level evaluated by microarray analysis was expressed in arbitrary units and calculated as RNA expression= 2^(log2E-1.3) where 1.3 is the lowest log2E value of the evaluated genes.

4.3. PHENOTYPIC CHANGES INDUCED BY ST6Gal-I OVEREXPRESSION

To assess if the overexpression of ST6Gal-I could alter the phenotype of cancer cells, with special focus on the typical hallmarks of cancer, we characterized the ST6Gal-I transduced cells for their basic properties.

4.3.1. Anchorage-independent growth

The ability to grow without adhesion to a solid substrate is a basic hallmark of malignancy. To test such ability, we performed soft agar growth assay. In this assay (Fig. 4.7), the cells are plated as a single cell within a layer of agar to mimic the growth in absence of adhesion. After two weeks of incubation we were able to count the colonies at the microscope. With SW948 ST6Gal-I transduced cell line we observed the formation of fewer colonies but of larger dimension compared with their negative control (NC). On the other hand, SW48 ST cell line could form a higher number of colonies compared with SW48 NC, with no significant difference in colonies dimension.

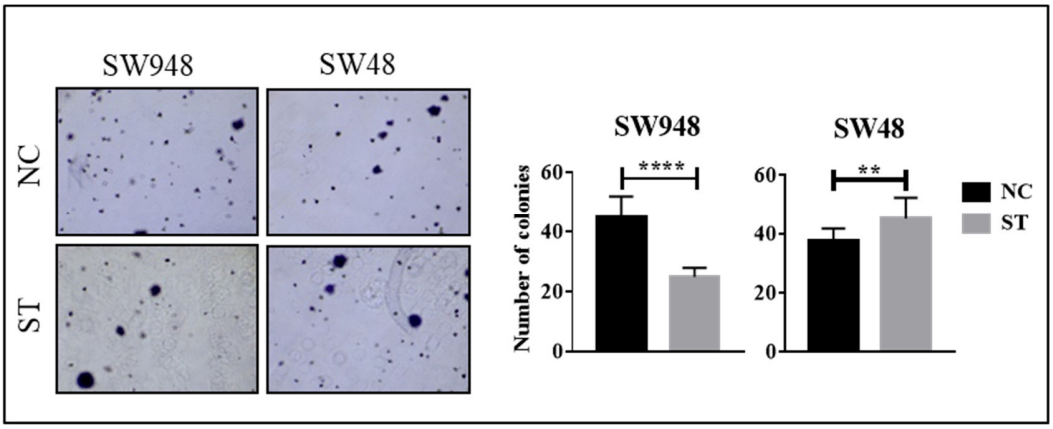

Fig. 4.7 Reduced adhesion-independent growth of SW948 ST in absence of adhesion compared to NC cells, increased colony formation in SW48 ST compared with NC cells. On the left-hand side an example of soft agar growth assay. The histogram represents the colonies counted in three biological replicates.

4.3.2. Wound healing assay

To evaluate if ST6Gal-I transduction could alter the ability of the cells to proliferate and migrate, we performed wound healing assay using Ibidi culture insert (Fig. 4.8). We observed that ST6Gal-I overexpression conferred on SW948 ST the ability to heal the wound more rapidly than SW948 NC, as it is shown in the graph representing the area of the wound. However, a close look to the pictures revealed that SW948 ST cells close the wound more rapidly because they tend to proliferate first in monolayer and only in a second time as a multilayer. On the contrary, NC cells showed a stronger tendency to multi-layer growth. The expression of ST6Gal-I produced an opposite effect in SW48. In fact, SW48 NC cells closed faster the wound than SW48 ST6Gal-I transduced cells.

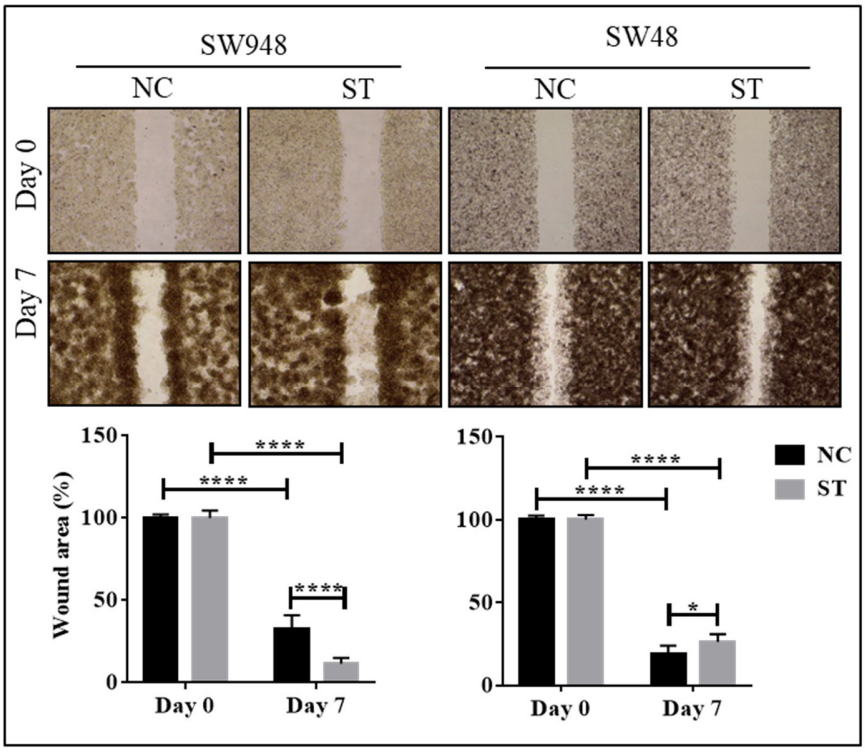

Fig. 4.8 SW948 ST close more rapidly the wound compared with NC cells, while SW48 ST are less effective in closing the wound compared to NC cells. The upper part shows representative pictures of wound healing assay taken at day 0 and day 7 from the creation of the wound. The histograms show the percentage area of the wound in three biological replicates and it is expressed in percentage of the day 0 NC sample.

4.3.3. Invasion assay

With invasion assay we studied the capacity of the two cell lines used as models to invade the extracellular matrix. After 24 hours of serum starvation, SW948 and SW48 cells were plated in the upper chamber of the transwells. As chemoattractant in the lower chamber we used either complete medium supplemented with FBS or serum-free medium with HGF. In both cell types the chemiotactic activity of HGF was lower than that of complete medium. However, while in the SW948 cell type the expression of ST6Gal-I did not affect the ability of complete medium to drive the invasion of the extracellular matrix, the ST6Gal-I expressing SW48 cells displayed reduced extracellular matrix invasion (Fig. 4.9).

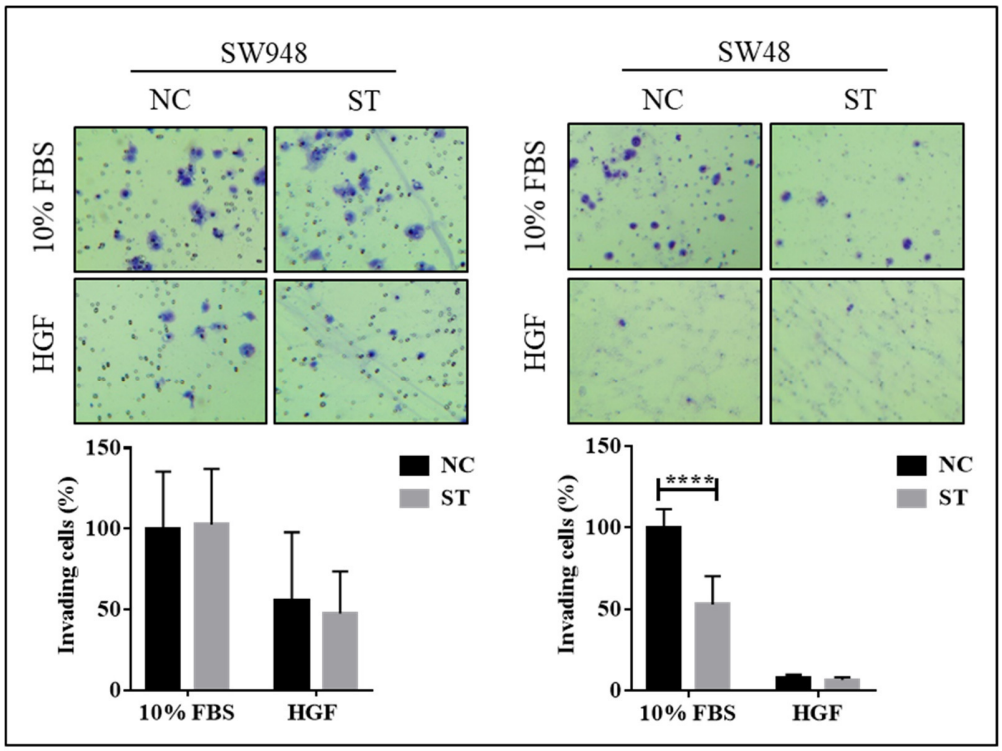

Fig. 4.9 SW948 NC and ST present the same capacity to invade Matrigel, while SW48 ST display a reduced capacity to invade Matrigel compared to NC cells. The upper part shows representative pictures of cells that passed through the porous membrane of the transwell and invaded Matrigel. The histograms represent the number of invading cells in three biological replicates.

In conclusion, the experiments reported in this section showed a different response of the two cell lines SW948 and SW48, supporting the hypothesis that the effects of ST6Gal-I overexpression can be evaluated only in a cell line specific context.

4.3.4. Propensity to apoptosis

Propensity to apoptosis is a crucial aspect of cancer cell biology. To understand if ST6Gal-I expression could modify the response to apoptotic stimuli, we used TPEN, a zinc chelator, to activate the intrinsic pathway of apoptosis. To monitor the response, we detected cleaved-PARP at 0, 4, 8, 16, 24 and 48 hours. Cleaved-PARP is one of the most known markers of apoptosis (*207*). In Western Blot (Fig. 4.10 A), we observed the presence of cleaved-PARP in SW948 ST shortly after treatment (4 hours), while it appeared only at 8 hours in SW948 NC. This suggests that the transduction with ST6Gal-I in SW948 accelerates the apoptotic response.

To further investigate how ST6Gal-I overexpression could impact on the apoptotic pathway, we used an antibody array kit able to detect 19 proteins involved in the regulation of the stress response and apoptosis. We treated again the cells with TPEN, but we considered only short time points: 0, 4, 8 and 16 hours. After the incubation of the protein extract and the antibody mix on the array (refer to methods) we analysed the intensity of the spots resulted by chemiluminescence. Of the 19 proteins detected by the protein array, we reported only those significantly modulated. In the SW948 cell type (Fig. 4.10 B), ST6Gal-I expression results generally in an upregulation of several apoptotic stress markers which include p53 (a tumour-suppressor that regulates the cell cycle and activates apoptosis in presence of stress) and IκBα phosphorylated on Ser 32/36 (which controls NFκB activation in response to different stimuli (*208*)). The executioner caspases -3 and -7 displayed similar low level of expression in early time points, reaching a significant higher expression in ST6Gal-I expressing SW948 cells only 16 hours after the administration of the apoptotic stimulus. The anti-apoptotic P44/42 MAPK (*209*), appeared to be poorly responsive to the apoptotic stimulus. However, its slightly higher constitutive expression in SW948 ST is probably due to a subtle stimulation of this pathway. It appears that in the SW948 cell type, the

overexpression of ST6Gal-I caused an up-regulation of some apoptotic markers even in absence of apoptotic stimulus and an acceleration of the apoptotic response to the stimuli.

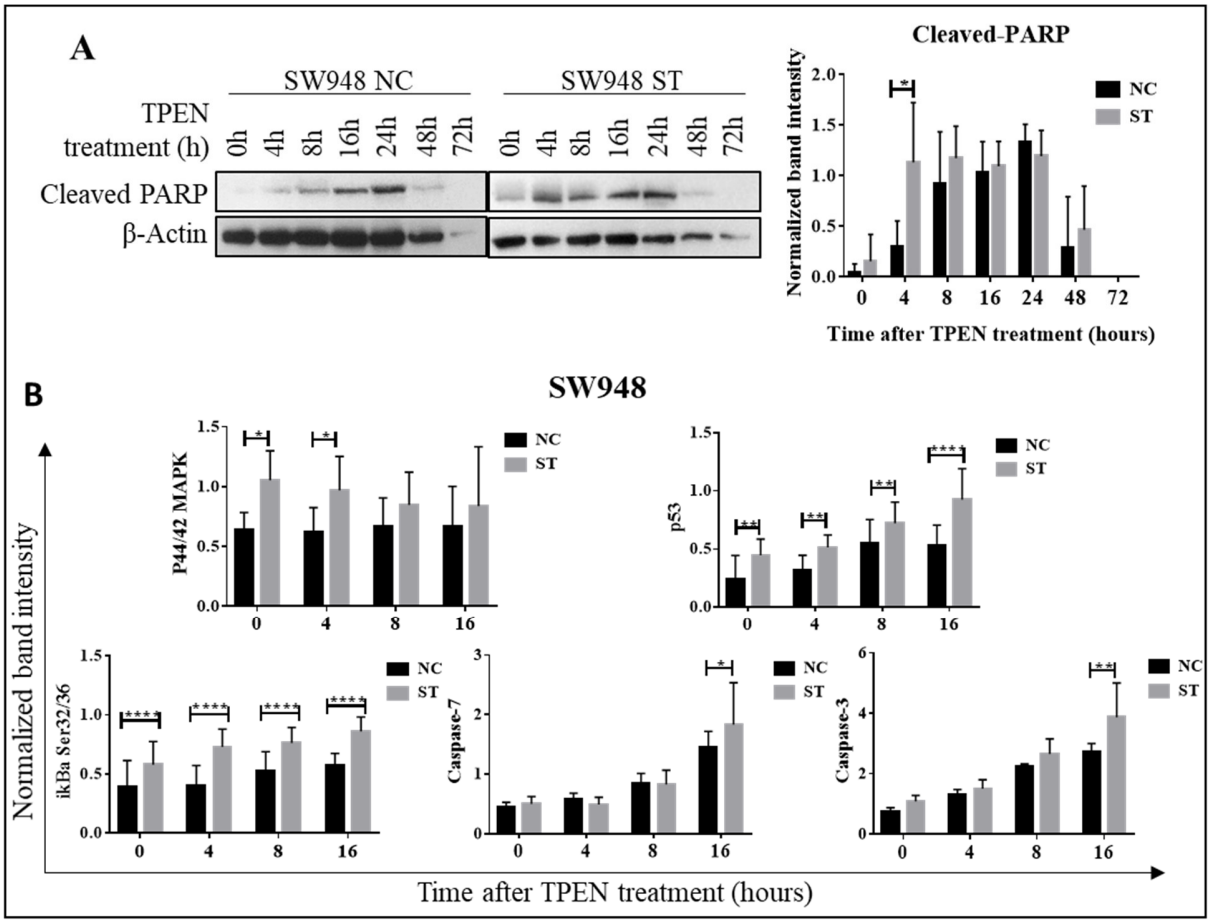

Fig. 4.10 SW948 cells show an accelerated response to the apoptotic stimulus and increased expression of apoptosis and stress markers. SW948 NC and ST were treated with TPEN and collected at different time points. **A** Western blot showing a more rapid increase of cleaved-PARP in ST compared to NC cells. The histogram represents the band intensity of cleaved-PARP normalized on β-Actin of three replicates. **B** Incubation of protein extracts of SW948 NC and ST cells after treatment with TPEN resulted in up-regulation of stress and apoptosis markers. The graphs report the band intensity normalized on β-Tubulin of three biological replicates.

In the SW48 cell type, ST6Gal-I failed to induce acceleration of PARP cleavage, as detected by Western blot analysis (Fig. 4.11 A). Analysis with the antibody array kit (Fig. 4.11 B) revealed a similar basic level of expression in ST6Gal-I-transduced and control cells of most apoptotic markers, with the exception of IκBα phosphorylated on Ser 32/36. It was found only an increased

expression of the antiapoptotic P44/42 MAPK at the 4 h time point, of p53 at 8h and 16h time points and of Chk1 (which plays an important role in DNA damage checkpoint control (*210*)) at 8h time point. Overall these data indicate that the effect of ST6Gal-I expression on the propensity to undergo apoptosis along the intrinsic pathway is nearly undetectable in SW48 cells. These findings suggest that the protein array is a more sensitive technique, compared with Western Blot, in fact is able to detect even slight differences in the level of activation of proteins involved in the apoptosis pathway. Furthermore, with these results we proved that the effect of ST6Gal-I overexpression on the propensity to apoptosis is specific for the cell line analysed.

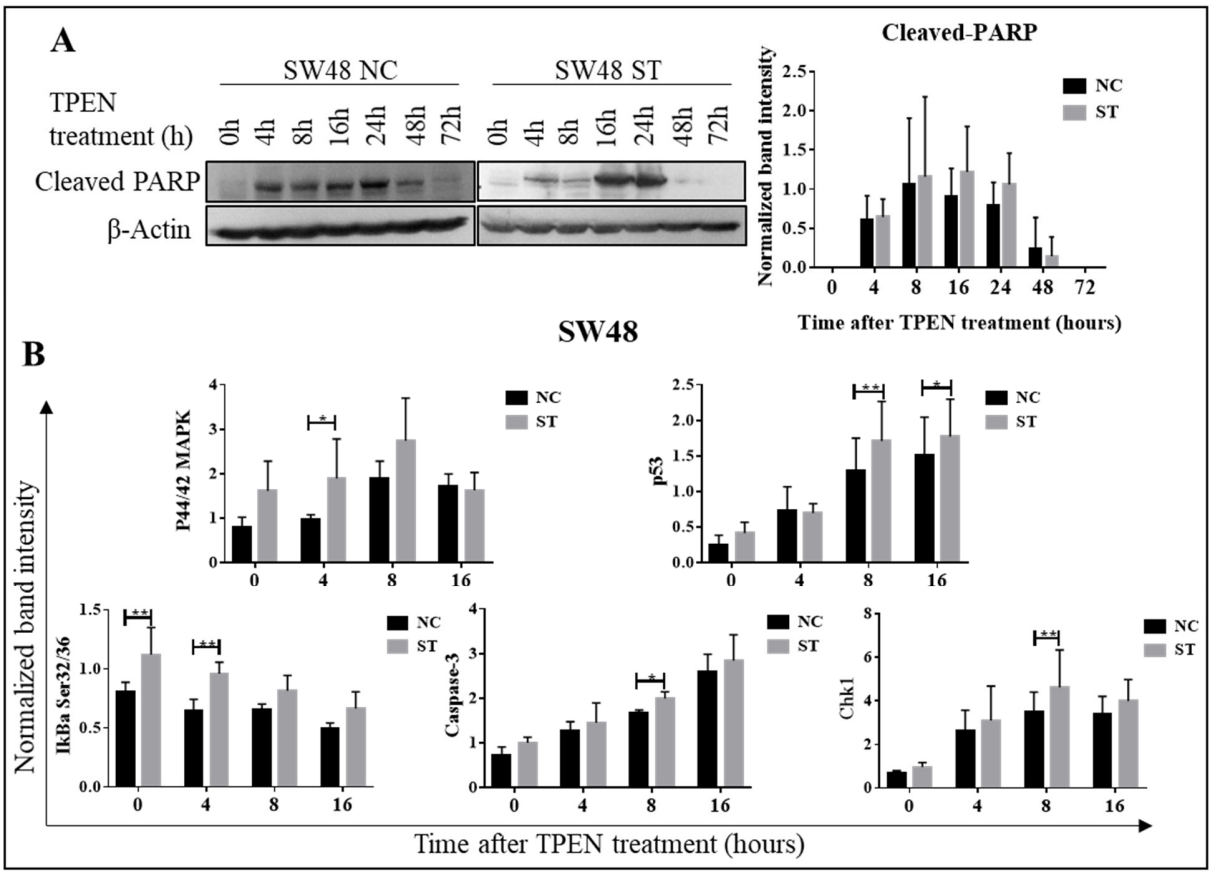

Fig. 4.11 In SW48 the expression of ST6Gal-I does not alter the apoptotic response compared to NC cells. Similar modulation of stress and apoptosis markers in SW48 NC and ST. SW48 NC and ST were treated with TPEN and collected at different time points. **A** Western blot showing a similar kinetics of cleaved-PARP in ST and NC cells. The histogram represents the band intensity of cleaved-PARP normalized on β-Actin of three replicates. **B** Incubation of protein extracts of SW48 NC and ST cells after treatment with TPEN resulted in an unaltered expression of stress and apoptosis markers. The graphs report the band intensity normalized on β-Tubulin of three biological replicates.

4.3.5. HGF-induced substrate phosphorylation

To investigate if the overexpression of ST6Gal-I could affect the intracellular signalling in response to growth factors, we treated SW948 and SW48 cells with HGF that stimulates cell proliferation and migration. Cells were serum starved for 24 hours to minimize the effects of growth factors contained in serum and treated with HGF for short times. We analysed the intracellular signalling using anti-pFAK (Tyr397) and anti-phosphotyrosine antibodies (Fig. 4.12) by Western blotting. We noticed that pFAK (Tyr397) levels were significantly higher in untreated SW948 ST than in untreated SW948 NC. In SW948 NC, cells pFAK decreased progressively during HGF treatment, reaching the lowest value at 120 minutes, while in SW948 NC it rose gradually during treatment time. We evaluated also the changes in the tyrosine phosphorylation induced by HGF, choosing phosphoproteins of 125, 60 and 25 kDa as they were the most abundant in our extracts. Although the differences did not reach statistical significance, the trend was similar to that observed for pFAK (Tyr397): an increased level in ST without HGF treatment, an increase of the phosphorylation levels in SW948 NC and a decrease in SW948 ST from 0 to 120 minutes.

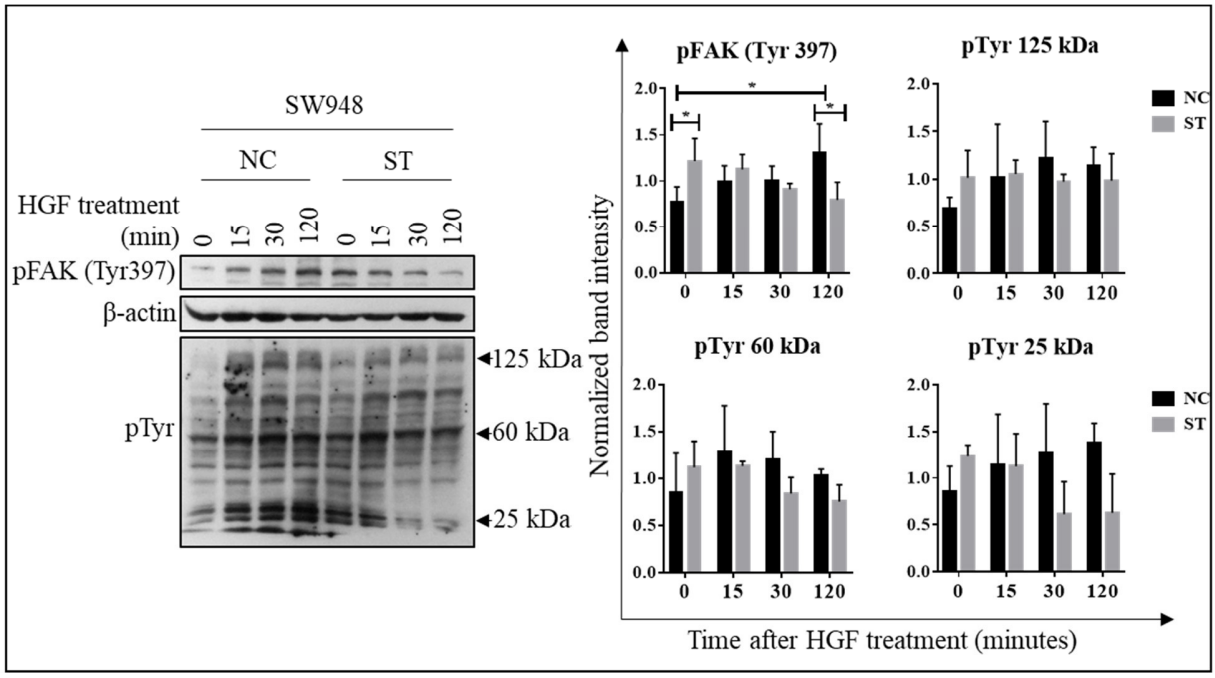

Fig. 4.12 FAK phosphorylation at Tyr397 is higher in SW948 ST compared with NC in the untreated samples. Then, during treatment with HGF it increases in SW948 NC cells and decrease in ST cells. SW948 NC and ST were treated with 25 ng/ml HGF for 0, 15, 30 and 120 minutes. The histograms represent pFAK (Tyr397) and phosphoproteins at 125, 60 and 25 kDa band intensity normalized on β-Actin of three independent experiments.

On the other hand, treatment of SW48 NC and ST with HGF failed to induce significant changes of the levels of pFAK (Tyr397), and of the 125 and 60 kDa phosphoproteins which were similar in the two cell lines (Fig. 4.13). We observed only a modulation in the phosphorylation levels of the 25 kDa phosphoproteins which increased gradually during time in SW48 NC, but not in SW48 ST, without reaching statistical significance.

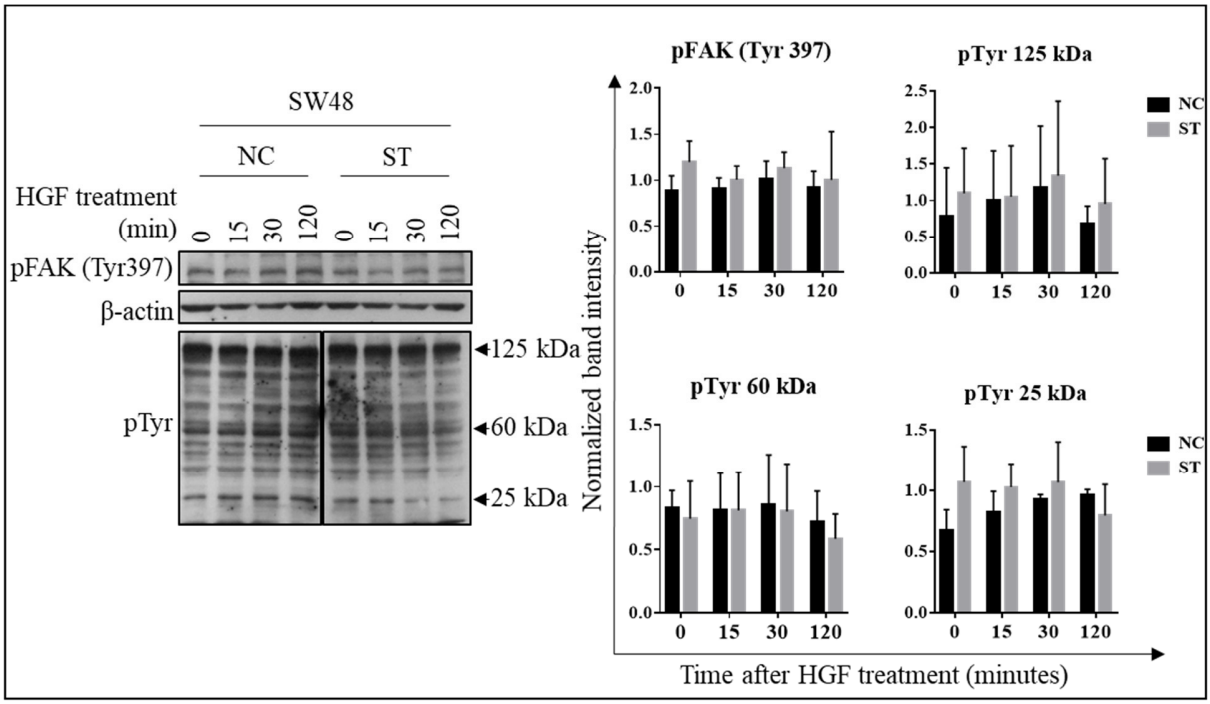

Fig. 4.13 FAK phosphorylation at Tyr397 is similar in SW48 ST compared with NC cells with and without HGF treatment. SW48 NC and ST were treated with 25 ng/ml HGF for 0, 15, 30 and 120 minutes. The histograms represent pFAK (Tyr397) and phosphoproteins at 125, 60 and 25 kDa band intensity normalized on β-Actin of three independent experiments.

Treatment with EGF according to the same protocol did not induce significant changes.

4.3.6. ST6Gal-I overexpression and stemness

Recent studies reported that ST6Gal-I could be involved in the regulation of pluripotency (*186*) and that it correlated with stem cell markers in colon cancer cell lines (*187*). Therefore, we investigated if in our models the overexpression of ST6Gal-I could induce the expression of stem cell markers. We used ALDEFLUOR to detect the activity of aldehyde dehydrogenase (ALDH) which is reported to be a stem cell and a cancer-initiating cell marker in many tissues, including colon (*211*). We performed two experiments for each cell line, that are reported in Fig. 4.14 and 4.15, incubating SW948 and SW48 NC and ST with ALDEFLUOR reagent or DEAB (a specific ALDH inhibitor) for negative control. We observed that the majority of SW948 cells were positive

to ALDH compared to the control sample (with DEAB) (Fig. 4.14), but without relevant differences due to ST6Gal-I overexpression.

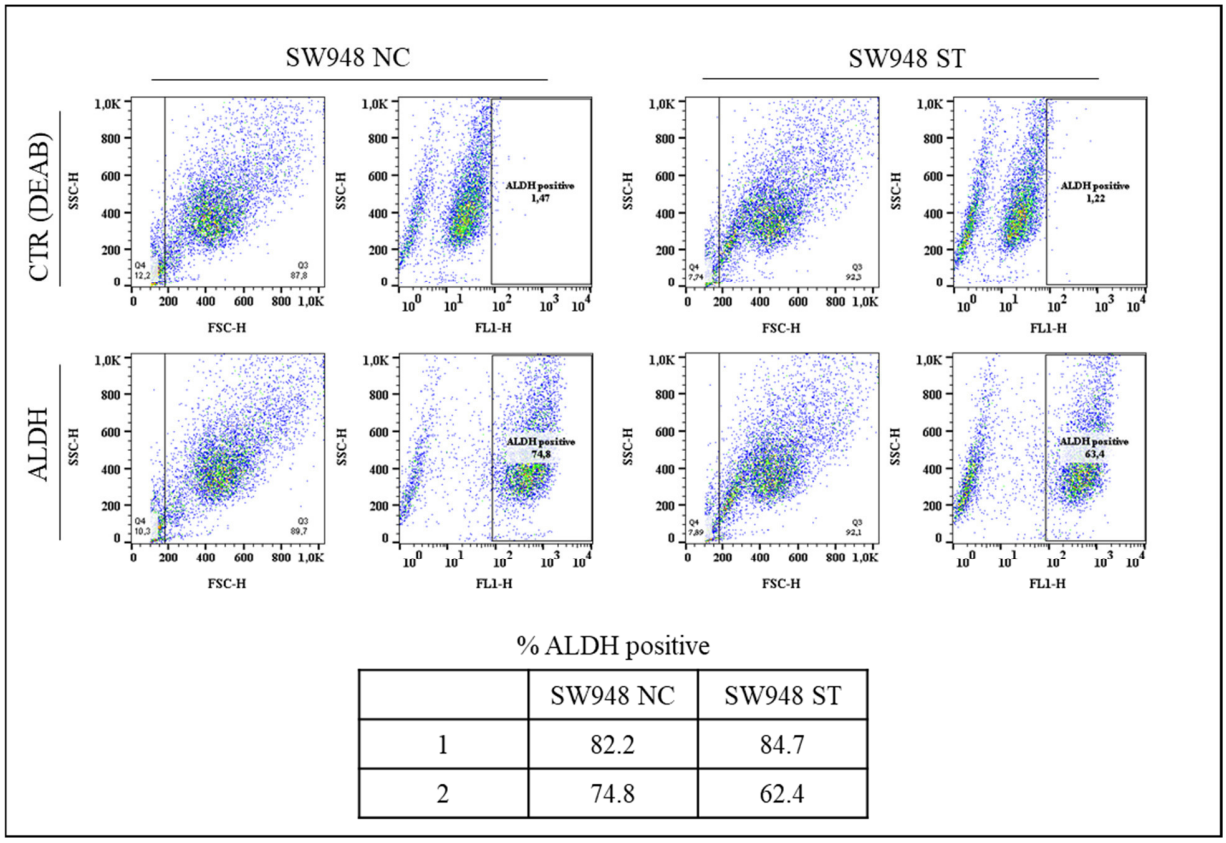

% ALDH positive

	SW948 NC	SW948 ST
1	82.2	84.7
2	74.8	62.4

Fig. 4.14 The majority of SW948 cells resulted positive for ALDH compared to the control with DEAB. SW948 NC and ST cells did not present any significant difference. SW948 NC and ST were incubated with ALDH with and without DEAB (inhibitor of ALDH) for 30 minutes at 37°C. A gate to identify ALDH positive cells was drown according to the cell population in the control sample in a dot plot SSC/FL1. The table reports the percentage of ALDH positive cells in two independent experiments.

Nevertheless, when we performed the experiment with SW48, we saw that the percentage of ALDH positive cells was much lower compared to SW948, indicating that only a limited portion of cells presented high ALDH activity and thus cancer stem cells characteristics. Moreover, we observed that the SW48 ST cells presented a lower number of ALDH positive cells compared to NC, even though the difference was not statistically significant (Fig. 4.15). These results suggest the presence of potential cancer stem cells in SW948 and SW48 cell lines, although ALDH staining failed to

reveal differences due to ST6Gal-I overexpression. Therefore, the presence of cancer stem cells in relation with ST6Gal-I overexpression must be further investigated.

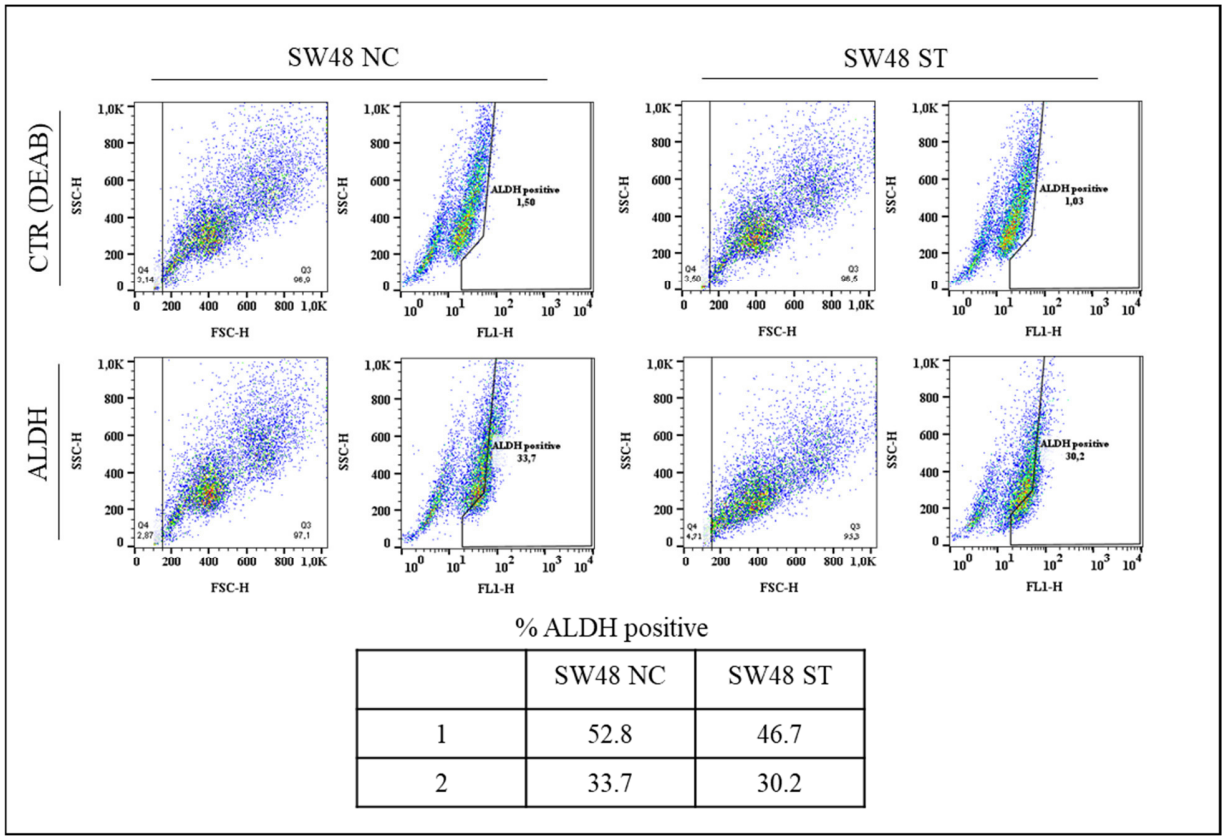

% ALDH positive

	SW48 NC	SW48 ST
1	52.8	46.7
2	33.7	30.2

Fig. 4.15 Only a portion of SW48 cells resulted positive for ALDH compared to the control with DEAB. SW48 ST presented a lower percentage of ALDH positive cells compared to NC, but the difference did not reach statistical significance. SW48 NC and ST were incubated with ALDH with and without DEAB (inhibitor of ALDH) for 30 minutes at 37°C. A gate to identify ALDH positive cells was drown according to the cell population in the control sample in a dot plot SSC/FL1. The table reports the percentage of ALDH positive cells in two independent experiments.

5. DISCUSSION

In this study, we aimed to elucidate the role of ST6Gal-I in colorectal cancer and better characterise its pro- or anti-tumour potential. In fact, many *in vivo* and *in vitro* experiments highlight the importance of ST6Gal-I in tumour development and progression (*97, 99, 104-106*), while other studies report a more pronounced malignancy in its absence (*109, 113-116, 121*). To clarify the role of ST6Gal-I in clinic we performed an evaluation of ST6Gal-I mRNA expression in correlation with clinical data using the TCGA public database that includes a high number of cancer patients. We observed that the median value of ST6Gal-I expression was similar between normal and cancer tissue in contrast to what observed previously by many studies at the protein level (*33, 93-97*) although in a limited number of patients. However, the level of ST6Gal-I mRNA expression was extremely variable among patients, allowing to investigate correlations between ST6Gal-I mRNA level and clinical parameters. We observed that low levels of ST6Gal-I mRNA expression correlated with high MSI, supporting data showing that high SNA reactivity was correlated with a microsatellite-stable phenotype (*98*). In the same direction goes the observation that low ST6Gal-I expression is correlated with BRAF mutation, in fact it has been reported that BRAF is commonly mutated in MSI colon cancer (*212*). On the other hand, ST6Gal-I mRNA expression did not correlate with clinical stage, mutation in KRAS, APC and TP53, response to therapy and overall survival. These findings are in contrast with previous data reporting a worse prognosis for CRC patients presenting high ST6Gal-I and or SNA reactivity (*96, 97*). However, data in TCGA database are based only on mRNA expression and not on enzyme activity that has been reported to increase in CRC tissue compared with normal mucosa (*189*).

From previous experiments performed by our group and from literature data, we hypothesised that the role of each glycosyltransferase in cancer progression can be cell-type specific, depending on the genetic and transcriptional background of the specific cancer specimen and to many factors that can regulate glycosyltransferase activity, including the presence of the donor and acceptor substrates. Therefore, we studied two cell models that overexpressed ST6Gal-I from cell lines lacking the endogenous form of the enzyme both derived from colon cancers but representing the two principal mechanisms for carcinogenesis in colon. In fact, SW948 and SW48 cell lines have

been isolated from CRCs originated through chromosomal instability or microsatellite instability, respectively. To confirm the overexpression of the enzyme we evaluated the presence of the mRNA, the protein itself and the reactivity to the lectin SNA that detects the presence of ST6Gal-I product. In this regard we noticed a discrepancy between the level of mRNA and protein expression in NC cells and the reactivity to SNA. This can be partially explained considering that NC cells present a low but detectable level of enzymatic activity and that the higher level of activity of SW48 NC, compared with SW948 NC, is consistent with higher reactivity to SNA in immunofluorescence and FACS analysis. In addition, we failed to observe a differential SNA reactivity between SW948 and SW48 NC and ST in western blot with denaturing and reducing conditions, while we obtained a consistent difference between NC and ST in both SW948 and SW48 in native conditions with the addition of 1% Triton-X100 in the sample mix. This could suggest the requirement of the glycoproteins in their native structure for SNA recognition of the ligand. Moreover, it is noteworthy that lectins' specificity for their ligands is considerably lower than that of antibodies In particular, SNA lectin can recognize, together with the sialic acid linked via α2,6 linkage to Gal, also that α2,6- linked to GalNAc (sialyl-Tn), whose addition is catalysed by ST6GalNAc-I. Thus, a low level of SNA reactivity can be present even in cell lines lacking ST6Gal-I.

From a transcriptomic analysis of our cell models, we noticed that the gene modulation induced by ST6Gal-I expression was very different in the two cell lines, with SW948 presenting a higher number of altered genes compared to SW48. Moreover, none of the differentially expressed genes resulted modulated in both cell lines. These demonstrates that the impact of ST6Gal-I overexpression is cell type specific.

In SW948 and SW48 cells, we reported several genes differently modulated by ST6Gal-I that we selected for validation by real time RT-PCR, based on their potential role in cancer. Not all of them were confirmed to be modulated using real time PCR. This suggests that even though transcriptomic analysis is a very useful and powerful tool to identify modulated genes in a particular context, its results always need to be verified. The two techniques provided consistent results for the upregulation of OLFM4, SH3GL2, FOLR1, TGFβ2, MYEOV and downregulation

of FMOD and KLK6 in SW948, while in SW48 cell we observed only three downregulated genes: MAP1B, MT4 and WNT16.

OLFM4 resulted to be the most up-regulated in SW948 ST cells. OLFM4 is a secreted glycoprotein overexpressed in both primary (*193, 213*), and liver metastasis (*214*) of colon tumours. OLFM4 is also considered a marker of stem cells(*215*), in fact its expression is localized in colon crypts where the stem cell niche is located (*214*). OLFM4 is regulated by the transcription factor NFκB and it seems to play a role in resistance to apoptosis (*216*). In fact, it binds to GRIM-19 a protein known to facilitate apoptosis induced by a combination of interferon β and retinoic acid treatment (*217*). Interestingly, it interacts with cell surface proteins, such as cadherins, therefore suggesting a role in cell adhesion. It has been reported that OLFM4 deletion in a pancreatic cancer model reduced cell proliferation, in contrast to previous data showing that overexpression of OLFM4 reduced cell proliferation in prostate cancer (*218*) or did not affect proliferation in a colon cancer cell line (*219*). On the other hand, OLFM4 deletion induced colon adenocarcinoma formation in mice heterozygous for *Apc* inactivation (a model for intestinal tumorigenesis) because of its negative regulation of the Wnt/β-catenin pathway (*194*). Altogether, these studies indicate that OLFM has a double-edge role, probably dependent on the cell context.

A second gene up-regulated in SW948 ST cell is SH3GL2 (or endophilin I), which is involved in clathrin-mediated endocytosis (*220*). It has been reported that this protein regulates EGFR endocytosis and degradation in laryngeal carcinoma (*221*), non-small cell lung cancer (*222*), head and neck squamous cell carcinoma (*223*) and urothelial carcinoma (*224*), therefore this gene is considered a tumour-suppressor and is frequently down-regulated in these and other malignancies. In glioblastoma cells, SH3GL2 is down-regulated through the action of mir-330 with a consequent activation of the ERK and PI3K/AKT signalling pathway (*195*). Moreover, loss of SH3GL2 promotes the migration and invasion of glioblastoma cells through activation of the STAT3/MMP2 signalling pathway (*225*). In addition, in breast cancer cells the overexpression of SH3GL2 reduced tumour growth promoting the release of cytochrome C from mitochondria and, thus, promoting apoptosis (*226*). However, its role in colorectal cancer has not been investigated yet.

FOLR1 is overexpressed in tumours, mainly from epithelial origin. It has been reported that it increases cell proliferation by activating Erk 1/2, c-Jun and c-Fos pathway (*196*). It is

overexpressed in lung adenocarcinoma, in non-small cell lung cancer and in metastatic lymph nodes from lung primary tumours (*227-229*). In breast cancer, the overexpression of FOLR1 is associated with increased risk of recurrence in triple-negative cancer, therefore it could be useful as a marker for this type of malignancy (*196, 230*). Moreover, FOLR1 is overexpressed in tumours from female genital tract such as cervical cancer (*196*), endometrium carcinoma and uterine adenocarcinoma (*231*) and ovarian cancer with aggressive phenotype (*232*). The presence of FOLR1 in sera from patients with ovarian cancer has been proposed as an early diagnosis marker(*233*). There are no published evidences of FOLR1 overexpression in colorectal cancer compared to normal mucosa (*234*), although TCGA data report an average values of 5 and 157 in normal and cancer tissue, respectively. It has been reported that its expression increases the efficacy of 5-fluoro-2'-deoxyuridine (FdUrd) treatment (*197*).

TGFβ2 is a secreted cytokine part of the TGFβ superfamily. They bind various TGF-beta receptors leading to recruitment and activation of SMAD family transcription factors regulating gene expression. One of the gene transcribed after TGFβ signalling is p21 which halts the cell cycle inhibiting CDK2 activity (*235*). In fact, one of the most known function of TGFβ family is to inhibit epithelial cells proliferation (*236*). However, more recently TGFβ signalling pathway has been considered as both a tumour suppressor and a cancer promoter (*237*), in fact it seems to inhibit the proliferation of normal epithelial and tumour cells at early stages of the disease and to cause the opposite effect on malignant and stroma cells in more advanced tumours (*238*). This switch is operated by a mechanism still not elucidated, probably concerning mutation in mediators of the tumour-suppressive pathway enhancing the tumour-promoting one (i.e. mutations on SMAD proteins occurs in 10% of CRC) (*239*). Increased secretion of TGFβ by the tumours exerts an effect on both the microenvironment and the tumour itself. In fact, it creates the permissive stroma that support tumour growth and spread, but also induces on cancer cell epithelial to mesenchymal transition (EMT) and appearance of stem cell–like traits (*240*). In particular, in colorectal cancer, TGFβ2 is overexpressed in advanced tumours and correlates with poor prognosis (*198*).

MYEOV (myeloma overexpressed) is localized at chromosome 11q13, a frequent site for chromosomal rearrangements in various carcinomas, moreover it is co-expressed with Cyclin1 and overexpressed in many malignancies (*241*), including neuroblastoma cell lines (*242*), cervical

lymph node metastasis of oral squamous cell carcinoma (*243*), oesophageal carcinoma cell lines(*244*) and in primary plasma cell leukaemia (*245*). Moreover, in colorectal cancer cells it induces migration and invasion (*199, 246*).

FMOD and KLK6 resulted downregulated in our analysis. FMOD, fibromodulin protein, is a collagen fibrillogenesis modulator. It is highly expressed in cancer stroma resulting in a dense extracellular matrix that functions as a tumour barrier (*200*). Moreover, it has been reported that FMOD is involved in angiogenesis in small cell lung cancer as a result of increased expression of angiogenic factors (*247*), is essential for glioma cells migration through its ability to induce filamentous actin stress fibre formation (*248*) and is overexpressed in prostate cancer (*249*).

KLK6, or kallikrein 6, is a serine protease member of the S1 family of protein peptidase. It is overexpressed in many malignancies, including breast (*250*), ovarian (*251*) and prostate cancer (*252*), and in melanoma and head and neck cancer (*253*). It has been reported to be upregulated also in colorectal cancer and in metastatic lymph nodes in association with poor prognosis (*254, 255*). In fact, several studies report that it is regulated by oncogenic Ras and that it can enhance colon cancer cells migration (*201*) and metastasis formation (*254*). On the basis of these studies it is not possible to predict a clear oncogenic or tumour-suppressor role of ST6Gal-I in SW948 cells. In fact, ST6Gal-I overexpression resulted in four up-regulated tumour-promoting genes (OLFM4, TGFβ2, MYEOV and FOLR1), but on the other hand two tumour-promoting genes were downregulated (FMOD and KLK6) while one tumour-suppressor gene (SH3GL2) was up-regulated.

In SW48 cells, results from microarray analysis and real time-PCR were consistent only for three downregulated genes: MAP1B, MT4 and WNT16. MAP1B is a microtubule-associated protein that contributes to migration and invasion in gastric cancer cells (*203*). Moreover, it is involved in resistance to mTOR inhibitors in glioblastoma cells (*256*) and is considered a novel paraneoplastic marker for neurological diseases with a predictive value for small cell lung carcinoma (*257*). However, it has been reported that MAP1B is part of a signature of methylated genes that define the small portion of CpG islands methylated phenotype (CIMP) in microsatellite stable (MSS) colon cancer (*258*). MT4 is a membrane type matrix metalloproteinase and plays an important role in cancer cell invasion and metastasis. In fact, it is highly expressed in lipid rafts of a metastatic

colon cancer cell line (*204*), in melanoma cell lines and tissue samples (*259*), in breast, oral and gastric cancer (*260-262*). WNT16 is part of the Wnt signalling pathway and is involved in cell proliferation. WNT16 is overexpressed in many tumours, including gastric and cervical cancer (*205, 263*) and promotes resistance to chemotherapy in prostate tumour (*206*). Moreover, it is produced from the tumour microenvironment and promotes the advancing of malignancies (*264*). All together, these data suggest that in SW48 the overexpression of ST6Gal-I promotes the down-regulation of tumour-promoting genes. However, the extent of its tumour suppressive potential results limited considering the small number of genes modulated by its overexpression.

The phenotypic changes induced by the overexpression of ST6Gal-I in SW948 and SW48 cells were not overlapping and sometimes they were divergent. We found that SW948 ST cells formed less colonies but of larger size when grown in adhesion-independent conditions. This means that only a minority of the population had the potential to grow in these conditions, but these cells were provided with accelerated proliferation. This could suggest the presence of a limited portion of cancer stem cells in SW948 ST compared to NC, but our data obtained with ALDH staining do not confirm this hypothesis. In the scratch wound test, we observed an accelerated closure of the wound by SW948 ST, due to their higher propensity to grow in monolayer compared to NC cells. This finding is consistent with what previously observed by our group in clones of SW948 cells transfected with rat ST6Gal-I (*109*). Two genes putatively involved in adhesion and motility: CNTN5 (*265*) and PHACTR3 (*266*) which displayed up-regulation in SW948 ST could be responsible for this phenotype, although we did not find differences in the capacity to invade Matrigel. In the cell type SW48, ST6Gal-I expression results in very different phenotypic effects. In fact, SW48 ST cells displayed reduced ability to close the scratch wound and poorer capacity to invade Matrigel compared to their negative control and no difference was observed in adherence-independent growth. Among the transcriptomic data which could explain this phenotype is the down-regulation in ST cells of two genes involved in cell motility and invasion: MAP1B and MT4.

Resistance to apoptosis is one of the hallmarks of cancer. We evaluated the propensity of SW948 and SW48 transduced cells to undergo apoptosis after treatment with TPEN, which induces the activation of the intrinsic pathway. We obtained different results in the two cell lines. In SW948 cells, the overexpression of ST6Gal-I caused an acceleration of apoptotic response induced by

TPEN. Moreover, data from the protein array indicated that in SW948 ST the markers associated with apoptosis and stress pathways were detectable also in absence of the apoptotic stimulus, thus suggesting a cellular environment more prone to undergo apoptosis. By contrast, in SW48 cells we did not observe any difference in the apoptotic kinetics between NC and ST and only marginal differences with the antibody protein array. These results support the idea of a cell-type specific effect of ST6Gal-I and point towards an acceleration of the apoptotic process in the SW948 cell line, in apparent conflict with studies reporting that ST6Gal-I has an important role in protection from apoptosis. In fact, the sialylation of β1-integrin, that binds galectin 3 which sometimes induces apoptosis (*133*), of the TNFR1, the receptor of TNF-α (*134*), and of the Fas-death receptor (*135*) prevents the binding with their ligands and the induction of apoptosis. However, these receptors only activate the apoptosis via the extrinsic pathway. Consequently, their impairment is due to their inability to bind the ligand, not to a modification of the apoptosis machinery. In a very recent study, it has been reported that ST6Gal-I protects cancer cells of pancreatic or ovarian origin from the apoptotic effects of serum growth factors withdrawal (*136*). The most likely interpretation for this discrepancy with our data is the strong cell type specificity of these phenotypic traits.

A differential ST6Gal-I expression apparently results in a slightly higher constitutive FAK phosphorylation, even in the absence of EGF or HGF treatment, but only in SW948 cells. Other tyrosine residues do not appear to be differentially phosphorylated. Overall, these results are consistent with the observed properties of SW948 ST cells in the scratch wound test.

6. CONCLUDING REMARKS

The data obtained in this work comprehensively suggest that the overexpression of ST6Gal-I can impact on the gene expression of the cell. This is not obvious if one considers that glycosylation is a secondary gene product, which modifies mainly glycoproteins located on the cell surface. It is reasonable to hypothesize that differentially α2,6-sialylated cell surface molecules, including growth factor receptors, display differential ability to trigger a signal transduction cascade towards the nucleus, resulting in modulation of cell transcription. This effect on gene transcription, though, is strictly cell-type specific due to the differences in the number and type of modulated genes that we observed by transcriptomic analysis in the two cell lines examined. The subtle but evident phenotypic changes in ST6Gal-I expressing cells can consequently be explained by two partially overlapping mechanisms: a direct modulation of cell membrane receptors (for example the strength of the binding of integrins to their substrates) and the modulation of gene expression. Although transcriptomic and phenotypic analysis of ST6Gal-I expressing cells does not allow to clearly establish whether this modification has a general effect of promoting or inhibiting malignancy, there is no doubt that the effect is strongly cell-type specific. According to this view, it is not surprising that literature data report sometimes conflicting observations. Current results showing phenotypic changes of moderate entity, are consistent with what we deduced from TCGA database. In fact, ST6Gal-I expression in colorectal cancer has no impact on survival, response to therapy or tumour stage, indicating the lack of a close association between ST6Gal-I expression level and malignancy. Furthermore, mice knockout for ST6Gal-I present normal development and a grossly normal phenotype with only defects in IgM production (*118*) and granulopoiesis (*119*). In addition, in a mouse model of breast cancer, ST6Gal-I KO leads to the development of more differentiated tumours with lower FAK signalling without effects on tumour growth (*120*).

However, in cancer biology even subtle differences can be important in regulating cell behaviour and consequently the clinical course of the disease. For this reason, the role of ST6Gal-I in malignancy deserves further investigations.

7. BIBLIOGRAPHY

1. K. W. Moremen *et al.* Vertebrate protein glycosylation: diversity, synthesis and function. *Nat Rev Mol Cell Biol* **13**, 448-462 (2012).
2. K. Ohtsubo *et al.* Glycosylation in cellular mechanisms of health and disease. *Cell* **126**, 855-867 (2006).
3. A. Varki. Biological roles of glycans. *Glycobiology* **27**, 3-49 (2017).
4. G. Vidarsson *et al.* IgG subclasses and allotypes: from structure to effector functions. *Front Immunol* **5**, 520 (2014).
5. J. Jaeken. Congenital disorders of glycosylation. *Handb Clin Neurol* **113**, 1737-1743 (2013).
6. I. Brockhausen *et al.* Site directed processing: role of amino acid sequences and glycosylation of acceptor glycopeptides in the assembly of extended mucin type O-glycan core 2. *Biochim Biophys Acta* **1790**, 1244-1257 (2009).
7. P. Stanley. Golgi glycosylation. *Cold Spring Harb Perspect Biol* **3**, (2011).
8. I. Brockhausen *et al.*, in *Essentials of Glycobiology,* A. Varki *et al.*, Eds. (Cold Spring Harbor (NY), 2009).
9. M. Welti. Regulation of dolichol-linked glycosylation. *Glycoconj J* **30**, 51-56 (2013).
10. A. S. Ramirez *et al.* Chemo-enzymatic synthesis of lipid-linked GlcNAc2Man5 oligosaccharides using recombinant Alg1, Alg2 and Alg11 proteins. *Glycobiology*, 1-8 (2017).
11. P. Burda *et al.* Ordered assembly of the asymmetrically branched lipid-linked oligosaccharide in the endoplasmic reticulum is ensured by the substrate specificity of the individual glycosyltransferases. *Glycobiology* **9**, 617-625 (1999).
12. M. Aebi. N-linked protein glycosylation in the ER. *Biochim Biophys Acta* **1833**, 2430-2437 (2013).
13. A. Herscovics. Importance of glycosidases in mammalian glycoprotein biosynthesis. *Biochim Biophys Acta* **1473**, 96-107 (1999).
14. F. Dall'Olio *et al.* N-glycomic biomarkers of biological aging and longevity: a link with inflammaging. *Ageing Res Rev* **12**, 685-698 (2013).
15. H. Kitagawa *et al.* Cloning and expression of human Gal beta 1,3(4)GlcNAc alpha 2,3-sialyltransferase. *Biochem. Biophys. Res. Commun* **194**, 375-382 (1993).
16. K. Sasaki *et al.* Expression cloning of a novel Gal beta (1-3/1-4) GlcNAc alpha 2,3- sialyltransferase using lectin resistance selection. *J. Biol. Chem* **268**, 22782-22787 (1993).
17. T. Okajima *et al.* Molecular cloning of a novel alpha2,3-sialyltransferase (ST3Gal VI) that sialylates type II lactosamine structures on glycoproteins and glycolipids. *J. Biol. Chem* **274**, 11479-11486 (1999).
18. J. Weinstein *et al.* Primary structure of β-galactoside α 2,6-sialyltransferase. Conversion of membrane-bound enzyme to soluble forms by cleavage of the NH_2-terminal signal anchor. *J. Biol. Chem* **262**, 17735-17743 (1987).
19. S. Takashima *et al.* Characterization of the Second Type of Human β-Galactoside α2,6-Sialyltransferase (ST6Gal II), Which Sialylates Galβ1,4GlcNAc Structures on Oligosaccharides Preferentially. Genomic Analysis of Human Sialyltransferase Genes. *J Biol. Chem* **277**, 45719-45728 (2002).
20. M. A. Krzewinski-Recchi *et al.* Identification and functional expression of a second human β-galactoside α2,6-sialyltransferase, ST6Gal II. *Eur. J Biochem* **270**, 950-961 (2003).
21. V. Lombard *et al.* The carbohydrate-active enzymes database (CAZy) in 2013. *Nucleic Acids Res* **42**, D490-495 (2014).

22. J. Bauer *et al.* Sialic acids in biological and therapeutic processes: opportunities and challenges. *Future Med Chem* **7**, 2285-2299 (2015).
23. A. Harduin-Lepers *et al.* The human sialyltransferase family. *Biochimie* **83**, 727-737 (2001).
24. F. Dall'Olio *et al.* Sialyltransferases in cancer. *Glycoconj. J* **18**, 841-850 (2001).
25. F. Dall'Olio *et al.* Sialosignaling: Sialyltransferases as engines of self-fueling loops in cancer progression. *Biochim. Biophys. Acta* **1840**, 2752-2764 (2014).
26. A. Harduin-Lepers *et al.* Sialyltransferases functions in cancers. *Front Biosci. (Elite. Ed)* **4**, 499-515 (2012).
27. S. Kitazume-Kawaguchi *et al.* The relationship between ST6Gal I Golgi retention and its cleavage-secretion. *Glycobiology* **9**, 1397-1406 (1999).
28. E. C. Svensson *et al.* Organization of the β-galactoside α 2,6-sialyltransferase gene. Evidence for the transcriptional regulation of terminal glycosylation. *J. Biol. Chem* **265**, 20863-20868 (1990).
29. U. Grundmann *et al.* Complete cDNA sequence encoding human β-galactoside α-2,6-sialyltransferase. *Nucleic Acids Res* **18**, 667 (1990).
30. X. Wang *et al.* Chromosome mapping and organization of the human β-galactoside α 2,6-sialyltransferase gene. Differential and cell-type specific usage of upstream exon sequences in B-lymphoblastoid cells. *J. Biol. Chem* **268**, 4355-4361 (1993).
31. D. A. Aas-Eng *et al.* Characterization of a promoter region supporting transcription of a novel human β-galactoside α-2,6-sialyltransferase transcript in HepG2 cells. *Biochim. Biophys. Acta* **1261**, 166-169 (1995).
32. I. Stamenkovic *et al.* The B cell antigen CD75 is a cell surface sialytransferase. *J. Exp. Med* **172**, 641-643 (1990).
33. F. Dall'Olio *et al.* β-galactoside α2,6 sialyltransferase in human colon cancer: contribution of multiple transcripts to regulation of enzyme activity and reactivity with *Sambucus nigra* agglutinin. *Int. J. Cancer* **88**, 58-65 (2000).
34. L. Xu *et al.* Transcriptional regulation of human beta-galactoside α2,6-sialyltransferase (hST6Gal I) gene in colon adenocarcinoma cell line. *Biochem. Biophys. Res. Commun* **307**, 1070-1074 (2003).
35. J. Ferlay *et al.* Cancer incidence and mortality worldwide: sources, methods and major patterns in GLOBOCAN 2012. *Int J Cancer* **136**, E359-386 (2015).
36. P. Galiatsatos *et al.* Familial adenomatous polyposis. *Am J Gastroenterol* **101**, 385-398 (2006).
37. V. Kumar *et al.*, *Robbins basic pathology*. (Elsevier/Saunders, Philadelphia, PA, ed. 9th, 2013), pp. xii, 910 p.
38. M. S. Pino *et al.* The chromosomal instability pathway in colon cancer. *Gastroenterology* **138**, 2059-2072 (2010).
39. L. Shen *et al.* Integrated genetic and epigenetic analysis identifies three different subclasses of colon cancer. *Proc Natl Acad Sci U S A* **104**, 18654-18659 (2007).
40. J. M. Bae *et al.* Molecular Subtypes of Colorectal Cancer and Their Clinicopathologic Features, With an Emphasis on the Serrated Neoplasia Pathway. *Arch Pathol Lab Med* **140**, 406-412 (2016).
41. C. R. Boland *et al.* Microsatellite instability in colorectal cancer. *Gastroenterology* **138**, 2073-2087 e2073 (2010).
42. Y. J. Kim *et al.* Perspectives on the significance of altered glycosylation of glycoproteins in cancer. *Glycoconj J* **14**, 569-576 (1997).
43. S. Hakomori *et al.* Glycosphingolipids as tumor-associated and differentiation markers. *J Natl Cancer Inst* **71**, 231-251 (1983).
44. R. Kannagi *et al.* Current relevance of incomplete synthesis and neo-synthesis for cancer-associated alteration of carbohydrate determinants--Hakomori's concepts revisited. *Biochim Biophys Acta* **1780**, 525-531 (2008).

45. S. S. Pinho *et al.* Glycosylation in cancer: mechanisms and clinical implications. *Nat Rev Cancer* **15**, 540-555 (2015).
46. D. J. Gill *et al.* Initiation of GalNAc-type O-glycosylation in the endoplasmic reticulum promotes cancer cell invasiveness. *Proc Natl Acad Sci U S A* **110**, E3152-3161 (2013).
47. N. T. Marcos *et al.* Role of the human ST6GalNAc-I and ST6GalNAc-II in the synthesis of the cancer-associated sialyl-Tn antigen. *Cancer Res* **64**, 7050-7057 (2004).
48. M. Leivonen *et al.* STn and Prognosis in Breast Cancer. *Oncology* **61**, 299-305 (2001).
49. S. Julien *et al.* Stable expression of sialyl-Tn antigen in T47-D cells induces a decrease of cell adhesion and an increase of cell migration. *Breast Cancer Res. Treat* **90**, 77-84 (2005).
50. B. M. Sandmaier *et al.* Evidence of a cellular immune response against sialyl-Tn in breast and ovarian cancer patients after high-dose chemotherapy, stem cell rescue, and immunization with Theratope STn-KLH cancer vaccine. *J. Immunother* **22**, 54-66 (1999).
51. I. Brockhausen *et al.* Pathways of mucin O-glycosylation in normal and malignant rat colonic epithelial cells reveal a mechanism for cancer-associated Sialyl-Tn antigen expression. *Biol. Chem* **382**, 219-232 (2001).
52. I. Brockhausen *et al.* Mechanisms underlying aberrant glycosylation of MUC1 mucin in breast cancer cells. *Eur. J. Biochem* **233**, 607-617 (1995).
53. P. A. Videira *et al.* ST3Gal.I sialyltransferase relevance in bladder cancer tissues and cell lines. *BMC Cancer* **9**, 357 (2009).
54. J. A. Ferreira *et al.* Overexpression of tumour-associated carbohydrate antigen sialyl-Tn in advanced bladder tumours. *Mol. Oncol* **7**, 719-731 (2013).
55. L. Lima *et al.* Response of high-risk of recurrence/progression bladder tumours expressing sialyl-Tn and sialyl-6-T to BCG immunotherapy. *Br. J. Cancer* **109**, 2106-2114 (2013).
56. P. F. Severino *et al.* Expression of sialyl-Tn sugar antigen in bladder cancer cells affects response to Bacillus Calmette Guerin (BCG) and to oxidative damage. *Oncotarget* **8**, 54506-54517 (2017).
57. Y. C. Liu *et al.* Sialylation and fucosylation of epidermal growth factor receptor suppress its dimerization and activation in lung cancer cells. *Proc. Natl. Acad. Sci. U. S. A* **108**, 11332-11337 (2011).
58. I. O. Potapenko *et al.* Glycan gene expression signatures in normal and malignant breast tissue; possible role in diagnosis and progression. *Mol Oncol* **4**, 98-118 (2010).
59. Y. Sato *et al.* Early recognition of hepatocellular carcinoma based on altered profiles of alpha-fetoprotein. *N Engl J Med* **328**, 1802-1806 (1993).
60. J. W. Dennis *et al.* β 1-6 branching of Asn-linked oligosaccharides is directly associated with metastasis. *Science* **236**, 582-585 (1987).
61. M. Demetriou *et al.* Reduced contact-inhibition and substratum adhesion in epithelial cells expressing GlcNAc-transferase V. *J. Cell Biol* **130**, 383-392 (1995).
62. H. B. Guo *et al.* Specific posttranslational modification regulates early events in mammary carcinoma formation. *Proc Natl Acad Sci U S A* **107**, 21116-21121 (2010).
63. M. Granovsky *et al.* Suppression of tumor growth and metastasis in Mgat5-deficient mice. *Nat. Med* **6**, 306-312 (2000).
64. M. Yoshimura *et al.* Suppression of lung metastasis of B16 mouse melanoma by N-acetylglucosaminyltransferase III gene transfection. *Proc. Natl. Acad. Sci. U. S. A* **92**, 8754-8758 (1995).
65. S. Nakamori *et al.* Involvement of carbohydrate antigen sialyl Lewis^{x} in colorectal cancer metastasis. *Dis. Colon Rectum* **40**, 420-431 (1997).
66. F. Dall'Olio *et al.* Mechanisms of cancer-associated glycosylation changes. *Front Biosci* **17**, 670-699 (2012).
67. D. Marrelli *et al.* Preoperative positivity of serum tumor markers is a strong predictor of hematogenous recurrence of gastric cancer. *J Surg Oncol* **78**, 253-258 (2001).

68. N. Hiraiwa *et al.* Transactivation of the fucosyltransferase VII gene by human T-cell leukemia virus type 1 Tax through a variant cAMP-responsive element. *Blood* **101**, 3615-3621 (2003).
69. N. Matsuura *et al.* Gene expression of fucosyl- and sialyl-transferases which synthesize sialyl Lewis^{x}, the carbohydrate ligands for E-selectin, in human breast cancer. *Int. J. Oncol* **12**, 1157-1164 (1998).
70. A. Togayachi *et al.* Up-regulation of Lewis enzyme (Fuc-TIII) and plasma-type α1,3fucosyltransferase (Fuc-TVI) expression determines the augmented expression of sialyl Lewis x antigen in non-small cell lung cancer. *Int. J. Cancer* **83**, 70-79 (1999).
71. M. Trinchera *et al.* The biosynthesis of the selectin-ligand sialyl Lewis x in colorectal cancer tissues is regulated by fucosyltransferase VI and can be inhibited by an RNA interference-based approach. *Int. J. Biochem. Cell Biol* **43**, 130-139 (2011).
72. N. T. Marcos *et al.* Helicobacter pylori induces β3GnT5 in human gastric cell lines, modulating expression of the SabA ligand sialyl-Lewis x. *J. Clin. Invest* **118**, 2325-2336 (2008).
73. S. Groux-Degroote *et al.* B4GALNT2 gene expression controls the biosynthesis of Sd^{a} and sialyl Lewis X antigens in healthy and cancer human gastrointestinal tract. *Int. J. Biochem. Cell Biol* **53**, 442-449 (2014).
74. C. Sato *et al.* Disialic, oligosialic and polysialic acids: distribution, functions and related disease. *J Biochem* **154**, 115-136 (2013).
75. K. J. Colley *et al.* Polysialic acid: biosynthesis, novel functions and applications. *Crit Rev Biochem Mol Biol* **49**, 498-532 (2014).
76. G. P. Bhide *et al.* Sialylation of N-glycans: mechanism, cellular compartmentalization and function. *Histochemistry and Cell Biology* **147**, 149-174 (2017).
77. A. E. Maarouf *et al.*, in *Structure and Function of the Neural Cell Adhesion Molecule NCAM,* V. Berezin, Ed. (Springer New York, New York, NY, 2010), pp. 137-147.
78. A. Tsuchiya *et al.* Polysialic acid/neural cell adhesion molecule modulates the formation of ductular reactions in liver injury. *Hepatology* **60**, 1727-1740 (2014).
79. F. Tanaka *et al.* Prognostic significance of polysialic acid expression in resected non- small cell lung cancer. *Cancer Res* **61**, 1666-1670 (2001).
80. H. Hildebrandt *et al.* Polysialic acid on the neural cell adhesion molecule correlates with expression of polysialyltransferases and promotes neuroblastoma cell growth. *Cancer Res* **58**, 779-784 (1998).
81. R. A. Falconer *et al.* Polysialyltransferase: a new target in metastatic cancer. *Curr. Cancer Drug Targets* **12**, 925-939 (2012).
82. G. Zeng *et al.* Cloning and transcriptional regulation of genes responsible for synthesis of gangliosides. *Curr Drug Targets* **9**, 317-324 (2008).
83. S. Groux-Degroote *et al.* Gangliosides: Structures, Biosynthesis, Analysis, and Roles in Cancer. *ChemBioChem* **18**, 1146-1154 (2017).
84. S. Julien *et al.* How Do Gangliosides Regulate RTKs Signaling? *Cells* **2**, 751-767 (2013).
85. A. Cazet *et al.* Consequences of the expression of sialylated antigens in breast cancer. *Carbohydr. Res* **345**, 1377-1383 (2010).
86. X. Wang *et al.* Carbohydrate-carbohydrate binding of ganglioside to integrin α5 modulates α5β1function. *J Biol. Chem* **276**, 8436-8444 (2001).
87. A. Cazet *et al.* GD3 synthase expression enhances proliferation and tumor growth of MDA-MB-231 breast cancer cells through c-Met activation. *Mol. Cancer Res* **8**, 1526-1535 (2010).
88. A. Cazet *et al.* The ganglioside GD2 induces the constitutive activation of c-Met in MDA-MB-231 breast cancer cells expressing the GD3 synthase. *Glycobiology* **22**, 806-816 (2012).
89. K. Hamamura *et al.* Functional activation of Src family kinase yes protein is essential for the enhanced malignant properties of human melanoma cells expressing ganglioside GD3. *J. Biol. Chem* **286**, 18526-18537 (2011).

90. P. D. Bos *et al.* Genes that mediate breast cancer metastasis to the brain. *Nature* **459**, 1005-1009 (2009).
91. F. Dall'Olio *et al.* Expression of α 2,6-sialylated sugar chains in normal and neoplastic colon tissues. Detection by digoxigenin-conjugated *Sambucus nigra* agglutinin. *Eur. J. Histochem* **37**, 257-265 (1993).
92. T. Sata *et al.* Expression of α2,6-linked sialic acid residues in neoplastic but not in normal human colonic mucosa. A lectin-gold cytochemical study with *Sambucus nigra* and *Maackia amurensis* lectins. *Am. J. Pathol* **139**, 1435-1448 (1991).
93. F. Dall'Olio *et al.* Increased CMP-NeuAc:Galβ1,4GlcNAc-R α 2,6 sialyltransferase activity in human colorectal cancer tissues. *Int. J. Cancer* **44**, 434-439 (1989).
94. P. Gessner *et al.* Enhanced activity of CMP-NeuAc:Gal β 1-4GlcNAc:α 2,6-sialyltransferase in metastasizing human colorectal tumor tissue and serum of tumor patients. *Cancer Lett* **75**, 143-149 (1993).
95. A. Gangopadhyay *et al.* Differential expression of α2,6-sialyltransferase in colon tumors recognized by a monoclonal antibody. *Hybridoma* **17**, 117-123 (1998).
96. M. J. Vierbuchen *et al.* Quantitative lectin-histochemical and immunohistochemical studies on the occurrence of α(2,3)- and α(2,6)-linked sialic acid residues in colorectal carcinomas. Relation to clinicopathologic features. *Cancer* **76**, 727-735 (1995).
97. M. Lise *et al.* Clinical correlations of α2,6-sialyltransferase expression in colorectal cancer patients. *Hybridoma* **19**, 281-286 (2000).
98. J. Gebert *et al.* Colonic carcinogenesis along different genetic routes: glycophenotyping of tumor cases separated by microsatellite instability/stability. *Histochem. Cell Biol* **138**, 339-350 (2012).
99. M. Dalziel *et al.* Ras oncogene induces β-galactoside α2,6-sialyltransferase (ST6Gal I) via a RalGEF-mediated signal to its housekeeping promoter. *Eur. J. Biochem* **271**, 3623-3634 (2004).
100. E. C. Seales *et al.* Ras oncogene directs expression of a differentially sialylated, functionally altered β1 integrin. *Oncogene* **22**, 7137-7145 (2003).
101. Y. Zhao *et al.* alpha2,6-Sialylation mediates hepatocellular carcinoma growth in vitro and in vivo by targeting the Wnt/beta-catenin pathway. *Oncogenesis* **6**, e343 (2017).
102. D. Pousset *et al.* Increased α2,6 sialylation of N-glycans in a transgenic mouse model of hepatocellular carcinoma. *Cancer Res* **57**, 4249-4256 (1997).
103. F. Dall'Olio *et al.* Expression of β-galactoside α2,6 sialyltransferase and of α2,6-sialylated glycoconjugates in normal human liver, hepatocarcinoma, and cirrhosis. *Glycobiology* **14**, 39-49 (2004).
104. A. Wei *et al.* ST6Gal-I overexpression facilitates prostate cancer progression via the PI3K/Akt/GSK-3beta/beta-catenin signaling pathway. *Oncotarget*, (2016).
105. C. C. Hsieh *et al.* Elevation of beta-galactoside alpha2,6-sialyltransferase 1 in a fructoseresponsive manner promotes pancreatic cancer metastasis. *Oncotarget* **8**, 7691-7709 (2017).
106. Q. Meng *et al.* Knockdown of ST6Gal-I inhibits the growth and invasion of osteosarcoma MG-63 cells. *Biomed. Pharmacother* **72**, 172-178 (2015).
107. S. Lin *et al.* Cell Surface α2,6-Sialylation Affects Adhesion of Breast Carcinoma Cells. *Exp. Cell Res* **276**, 101-110 (2002).
108. E. C. Seales *et al.* Hypersialylation of β1 integrins, observed in colon adenocarcinoma, may contribute to cancer progression by up-regulating cell motility. *Cancer Res* **65**, 4645-4652 (2005).
109. M. Chiricolo *et al.* Phenotypic changes induced by expression of β-galactoside α2,6 sialyltransferase I in the human colon cancer cell line SW948. *Glycobiology* **16**, 146-154 (2006).
110. F. M. Shaikh *et al.* Tumor cell migration and invasion are regulated by expression of variant integrin glycoforms. *Exp. Cell Res* **314**, 2941-2950 (2008).

111. Y. Zhuo *et al.* Emerging Role of α2,6-Sialic Acid as a Negative Regulator of Galectin Binding and Function. *J. Biol. Chem* **286**, 5935-5941 (2011).
112. Y. Zhuo *et al.* Sialylation of β1 integrins blocks cell adhesion to galectin-3 and protects cells against galectin-3-induced apoptosis. *J. Biol. Chem* **283**, 22177-22185 (2008).
113. H. Yamamoto *et al.* α2,6-Sialyltransferase gene transfection into a human glioma cell line (U373 MG) results in decreased invasivity. *J. Neurochem* **68**, 2566-2576 (1997).
114. H. Yamamoto *et al.* α2,6-Sialylation of cell-surface N-glycans inhibits glioma formation in vivo. *Cancer Res* **61**, 6822-6829 (2001).
115. H. Yamamoto *et al.* The expression of CMP-NeuAc: Gal β 1,4GlcNAc α 2,6 sialyltransferase [EC 2.4.99.1] and glycoproteins bearing α 2,6- linked sialic acids in human brain tumours. *Glycoconj. J* **12**, 848-856 (1995).
116. G. Dawson *et al.* Transfection of 2,6 and 2,3-sialyltransferase genes and GlcNAc-transferase genes into human glioma cell line U-373 MG affects glycoconjugate expression and enhances cell death. *J. Neurochem* **89**, 1436-1444 (2004).
117. P. Antony *et al.* Epigenetic inactivation of ST6GAL1 in human bladder cancer. *BMC. Cancer* **14**, 901 (2014).
118. T. Hennet *et al.* Immune regulation by the ST6Gal sialyltransferase. *Proc Natl Acad Sci U S A* **95**, 4504-4509 (1998).
119. M. Nasirikenari *et al.* Altered granulopoietic profile and exaggerated acute neutrophilic inflammation in mice with targeted deficiency in the sialyltransferase ST6Gal I. *Blood* **108**, 3397-3405 (2006).
120. M. Hedlund *et al.* α2-6-Linked sialic acids on N-glycans modulate carcinoma differentiation in vivo. *Cancer Res* **68**, 388-394 (2008).
121. D. O. Croci *et al.* Glycosylation-Dependent Lectin-Receptor Interactions Preserve Angiogenesis in Anti-VEGF Refractory Tumors. *Cell* **156**, 744-758 (2014).
122. M. J. Schultz *et al.* ST6Gal-I sialyltransferase confers cisplatin resistance in ovarian tumor cells. *J. Ovarian. Res* **6**, 25 (2013).
123. H. Ma *et al.* Reversal Effect of ST6GAL 1 on Multidrug Resistance in Human Leukemia by Regulating the PI3K/Akt Pathway and the Expression of P-gp and MRP1. *PLoS. One* **9**, e85113 (2014).
124. J. J. Park *et al.* Sialylation of epidermal growth factor receptor regulates receptor activity and chemosensitivity to gefitinib in colon cancer cells. *Biochem. Pharmacol* **83**, 849-857 (2012).
125. M. Nakano *et al.* Identification of glycan structure alterations on cell membrane proteins in desoxyepothilone B resistant leukemia cells. *Mol. Cell Proteomics* **10**, M111 (2011).
126. W. J. Lee *et al.* Organ-specific gene expressions in C57BL/6 mice after exposure to low-dose radiation. *Radiat. Res* **165**, 562-569 (2006).
127. M. Lee *et al.* Protein sialylation by sialyltransferase involves radiation resistance. *Mol. Cancer Res* **6**, 1316-1325 (2008).
128. D. Hanahan *et al.* The hallmarks of cancer. *Cell* **100**, 57-70 (2000).
129. A. Pena-Blanco *et al.* Bax, Bak and beyond - mitochondrial performance in apoptosis. *FEBS J*, (2017).
130. L. Coultas *et al.* The role of the Bcl-2 protein family in cancer. *Semin Cancer Biol* **13**, 115-123 (2003).
131. T. J. Sayers. Targeting the extrinsic apoptosis signaling pathway for cancer therapy. *Cancer Immunol Immunother* **60**, 1173-1180 (2011).
132. https://images.novusbio.com/design/trail.png.
133. Y. Zhuo *et al.* Sialylation of beta1 integrins blocks cell adhesion to galectin-3 and protects cells against galectin-3-induced apoptosis. *J Biol Chem* **283**, 22177-22185 (2008).

134. Z. Liu *et al.* ST6Gal-I regulates macrophage apoptosis via alpha2-6 sialylation of the TNFR1 death receptor. *J Biol Chem* **286**, 39654-39662 (2011).
135. A. F. Swindall *et al.* Sialylation of the Fas death receptor by ST6Gal-I provides protection against Fas-mediated apoptosis in colon carcinoma cells. *J Biol Chem* **286**, 22982-22990 (2011).
136. C. M. Britain *et al.* The Glycosyltransferase ST6Gal-I Protects Tumor Cells against Serum Growth Factor Withdrawal by Enhancing Survival Signaling and Proliferative Potential. *J Biol Chem* **292**, 4663-4673 (2017).
137. J. N. Contessa *et al.* Inhibition of N-linked glycosylation disrupts receptor tyrosine kinase signaling in tumor cells. *Cancer Res* **68**, 3803-3809 (2008).
138. I. G. Ferreira *et al.* Glycosylation as a Main Regulator of Growth and Death Factor Receptors Signaling. *Int J Mol Sci* **19**, (2018).
139. J. W. Dennis *et al.* Adaptive regulation at the cell surface by N-glycosylation. *Traffic* **10**, 1569-1578 (2009).
140. S. L. Organ *et al.* An overview of the c-MET signaling pathway. *Ther Adv Med Oncol* **3**, S7-S19 (2011).
141. C. A. Bradley *et al.* Targeting c-MET in gastrointestinal tumours: rationale, opportunities and challenges. *Nat Rev Clin Oncol* **14**, 562-576 (2017).
142. M. Kong-Beltran *et al.* The Sema domain of Met is necessary for receptor dimerization and activation. *Cancer Cell* **6**, 75-84 (2004).
143. G. Kozlov *et al.* Insights into function of PSI domains from structure of the Met receptor PSI domain. *Biochem Biophys Res Commun* **321**, 234-240 (2004).
144. R. Paumelle *et al.* Hepatocyte growth factor/scatter factor activates the ETS1 transcription factor by a RAS-RAF-MEK-ERK signaling pathway. *Oncogene* **21**, 2309-2319 (2002).
145. G. H. Xiao *et al.* Anti-apoptotic signaling by hepatocyte growth factor/Met via the phosphatidylinositol 3-kinase/Akt and mitogen-activated protein kinase pathways. *Proc Natl Acad Sci U S A* **98**, 247-252 (2001).
146. M. Garcia-Guzman *et al.* Met-induced JNK activation is mediated by the adapter protein Crk and correlates with the Gab1 - Crk signaling complex formation. *Oncogene* **18**, 7775-7786 (1999).
147. C. Boccaccio *et al.* Induction of epithelial tubules by growth factor HGF depends on the STAT pathway. *Nature* **391**, 285-288 (1998).
148. A. Y. Hui *et al.* Src and FAK mediate cell-matrix adhesion-dependent activation of Met during transformation of breast epithelial cells. *J Cell Biochem* **107**, 1168-1181 (2009).
149. H. Yoon *et al.* Understanding the roles of FAK in cancer: inhibitors, genetic models, and new insights. *J Histochem Cytochem* **63**, 114-128 (2015).
150. B. Linggi *et al.* ErbB receptors: new insights on mechanisms and biology. *Trends Cell Biol* **16**, 649-656 (2006).
151. D. J. Arndt-Jovin *et al.* Structure-function relationships of ErbB RTKs in the plasma membrane of living cells. *Cold Spring Harb Perspect Biol* **6**, a008961 (2014).
152. R. Roskoski, Jr. ErbB/HER protein-tyrosine kinases: Structures and small molecule inhibitors. *Pharmacol Res* **87**, 42-59 (2014).
153. M. Scaltriti *et al.* The epidermal growth factor receptor pathway: a model for targeted therapy. *Clin Cancer Res* **12**, 5268-5272 (2006).
154. R. Roskoski, Jr. The ErbB/HER family of protein-tyrosine kinases and cancer. *Pharmacol Res* **79**, 34-74 (2014).
155. T. J. Yeatman. A renaissance for SRC. *Nat Rev Cancer* **4**, 470-480 (2004).
156. S. C. Wang *et al.* Nuclear translocation of the epidermal growth factor receptor family membrane tyrosine kinase receptors. *Clin Cancer Res* **15**, 6484-6489 (2009).
157. J. J. Park *et al.* Sialylation of epidermal growth factor receptor regulates receptor activity and chemosensitivity to gefitinib in colon cancer cells. *Biochem Pharmacol* **83**, 849-857 (2012).

158. Y. C. Liu *et al.* Sialylation and fucosylation of epidermal growth factor receptor suppress its dimerization and activation in lung cancer cells. *Proc Natl Acad Sci U S A* **108**, 11332-11337 (2011).
159. H. Y. Yen *et al.* Effect of sialylation on EGFR phosphorylation and resistance to tyrosine kinase inhibition. *Proc Natl Acad Sci U S A* **112**, 6955-6960 (2015).
160. D. O. Croci *et al.* Glycosylation-dependent lectin-receptor interactions preserve angiogenesis in anti-VEGF refractory tumors. *Cell* **156**, 744-758 (2014).
161. J. Qian *et al.* alpha2,6-hyposialylation of c-Met abolishes cell motility of ST6Gal-I-knockdown HCT116 cells. *Acta Pharmacol Sin* **30**, 1039-1045 (2009).
162. J. Lu *et al.* beta-Galactoside alpha2,6-sialyltranferase 1 promotes transforming growth factor-beta-mediated epithelial-mesenchymal transition. *J Biol Chem* **289**, 34627-34641 (2014).
163. C. L. Zhang *et al.* Stem cells in cancer therapy: opportunities and challenges. *Oncotarget* **8**, 75756-75766 (2017).
164. K. Takahashi *et al.* Induction of pluripotent stem cells from adult human fibroblasts by defined factors. *Cell* **131**, 861-872 (2007).
165. S. Yamanaka. Induced pluripotent stem cells: past, present, and future. *Cell Stem Cell* **10**, 678-684 (2012).
166. J. Deng *et al.* Targeted bisulfite sequencing reveals changes in DNA methylation associated with nuclear reprogramming. *Nat Biotechnol* **27**, 353-360 (2009).
167. R. Radpour. Tracing and targeting cancer stem cells: New venture for personalized molecular cancer therapy. *World J Stem Cells* **9**, 169-178 (2017).
168. M. Baumann *et al.* Exploring the role of cancer stem cells in radioresistance. *Nat Rev Cancer* **8**, 545-554 (2008).
169. L. Ricci-Vitiani *et al.* Colon cancer stem cells. *J Mol Med (Berl)* **87**, 1097-1104 (2009).
170. M. J. Munro *et al.* Cancer stem cells in colorectal cancer: a review. *J Clin Pathol*, (2017).
171. L. Ricci-Vitiani *et al.* Identification and expansion of human colon-cancer-initiating cells. *Nature* **445**, 111-115 (2007).
172. L. Du *et al.* CD44 is of functional importance for colorectal cancer stem cells. *Clin Cancer Res* **14**, 6751-6760 (2008).
173. L. Hao *et al.* Expression and clinical significance of SALL4 and beta-catenin in colorectal cancer. *J Mol Histol* **47**, 117-128 (2016).
174. S. Ardalan Khales *et al.* SALL4 as a new biomarker for early colorectal cancers. *J Cancer Res Clin Oncol* **141**, 229-235 (2015).
175. H. D. Tuy *et al.* ABCG2 expression in colorectal adenocarcinomas may predict resistance to irinotecan. *Oncol Lett* **12**, 2752-2760 (2016).
176. X. W. Ding *et al.* ABCG2: a potential marker of stem cells and novel target in stem cell and cancer therapy. *Life Sci* **86**, 631-637 (2010).
177. F. M. Corvinus *et al.* Persistent STAT3 activation in colon cancer is associated with enhanced cell proliferation and tumor growth. *Neoplasia* **7**, 545-555 (2005).
178. L. Lin *et al.* STAT3 is necessary for proliferation and survival in colon cancer-initiating cells. *Cancer Res* **71**, 7226-7237 (2011).
179. P. Dalerba *et al.* Phenotypic characterization of human colorectal cancer stem cells. *Proc Natl Acad Sci U S A* **104**, 10158-10163 (2007).
180. M. Shimokawa *et al.* Visualization and targeting of LGR5(+) human colon cancer stem cells. *Nature* **545**, 187-192 (2017).
181. S. Deng *et al.* Distinct expression levels and patterns of stem cell marker, aldehyde dehydrogenase isoform 1 (ALDH1), in human epithelial cancers. *PLoS One* **5**, e10277 (2010).
182. Y. Deng *et al.* ALDH1 is an independent prognostic factor for patients with stages II-III rectal cancer after receiving radiochemotherapy. *Br J Cancer* **110**, 430-434 (2014).

183. K. Hasehira *et al.* Structural and quantitative evidence for dynamic glycome shift on production of induced pluripotent stem cells. *Mol Cell Proteomics* **11**, 1913-1923 (2012).
184. Y. C. Wang *et al.* Specific lectin biomarkers for isolation of human pluripotent stem cells identified through array-based glycomic analysis. *Cell Res* **21**, 1551-1563 (2011).
185. H. Tateno *et al.* Glycome diagnosis of human induced pluripotent stem cells using lectin microarray. *J Biol Chem* **286**, 20345-20353 (2011).
186. Y. C. Wang *et al.* Glycosyltransferase ST6GAL1 contributes to the regulation of pluripotency in human pluripotent stem cells. *Sci Rep* **5**, 13317 (2015).
187. A. F. Swindall *et al.* ST6Gal-I protein expression is upregulated in human epithelial tumors and correlates with stem cell markers in normal tissues and colon cancer cell lines. *Cancer Res* **73**, 2368-2378 (2013).
188. M. J. Schultz *et al.* The Tumor-Associated Glycosyltransferase ST6Gal-I Regulates Stem Cell Transcription Factors and Confers a Cancer Stem Cell Phenotype. *Cancer Res* **76**, 3978-3988 (2016).
189. F. Dall'Olio *et al.* Beta-galactoside alpha2,6 sialyltransferase in human colon cancer: contribution of multiple transcripts to regulation of enzyme activity and reactivity with Sambucus nigra agglutinin. *Int J Cancer* **88**, 58-65 (2000).
190. D. J. Taatjes *et al.* Post-Golgi apparatus localization and regional expression of rat intestinal sialyltransferase detected by immunoelectron microscopy with polypeptide epitope-purified antibody. *J. Biol. Chem* **263**, 6302-6309 (1988).
191. N. Malagolini *et al.* Exposure of α2,6-sialylated lactosaminic chains marks apoptotic and necrotic death in different cell types. *Glycobiology* **19**, 172-181 (2009).
192. P. Chomczynski *et al.* Single-step method of RNA isolation by acid guanidinium thiocyanate-phenol-chloroform extraction. *Anal Biochem* **162**, 156-159 (1987).
193. S. Koshida *et al.* Specific overexpression of OLFM4(GW112/HGC-1) mRNA in colon, breast and lung cancer tissues detected using quantitative analysis. *Cancer Sci* **98**, 315-320 (2007).
194. W. Liu *et al.* Olfactomedin 4 deletion induces colon adenocarcinoma in ApcMin/+ mice. *Oncogene* **35**, 5237-5247 (2016).
195. Y. Yao *et al.* MiR-330-mediated regulation of SH3GL2 expression enhances malignant behaviors of glioblastoma stem cells by activating ERK and PI3K/AKT signaling pathways. *PLoS One* **9**, e95060 (2014).
196. P. S. Ginter *et al.* Folate Receptor Alpha Expression Is Associated With Increased Risk of Recurrence in Triple-negative Breast Cancer. *Clin Breast Cancer* **17**, 544-549 (2017).
197. H. Tsukihara *et al.* Folic Acid-Metabolizing Enzymes Regulate the Antitumor Effect of 5-Fluoro-2'-Deoxyuridine in Colorectal Cancer Cell Lines. *PLoS One* **11**, e0163961 (2016).
198. A. C. Tsamandas *et al.* The potential role of TGFbeta1, TGFbeta2 and TGFbeta3 protein expression in colorectal carcinomas. Correlation with classic histopathologic factors and patient survival. *Strahlenther Onkol* **180**, 201-208 (2004).
199. A. C. Moss *et al.* ETV4 and Myeov knockdown impairs colon cancer cell line proliferation and invasion. *Biochem Biophys Res Commun* **345**, 216-221 (2006).
200. P. O. Olsson *et al.* Fibromodulin deficiency reduces collagen structural network but not glycosaminoglycan content in a syngeneic model of colon carcinoma. *PLoS One* **12**, e0182973 (2017).
201. R. S. Henkhaus *et al.* Kallikrein 6 is a mediator of K-RAS-dependent migration of colon carcinoma cells. *Biol Chem* **389**, 757-764 (2008).
202. J. Wu *et al.* Depletion of JMJD5 sensitizes tumor cells to microtubule-destabilizing agents by altering microtubule stability. *Cell Cycle* **15**, 2980-2991 (2016).

203. W. F. Gou *et al.* ING5 suppresses proliferation, apoptosis, migration and invasion, and induces autophagy and differentiation of gastric cancer cells: a good marker for carcinogenesis and subsequent progression. *Oncotarget* **6**, 19552-19579 (2015).
204. L. Nimri *et al.* Restoration of caveolin-1 expression suppresses growth, membrane-type-4 metalloproteinase expression and metastasis-associated activities in colon cancer cells. *Mol Carcinog* **52**, 859-870 (2013).
205. S. E. Norollahi *et al.* Regulatory Fluctuation of WNT16 Gene Expression Is Associated with Human Gastric Adenocarcinoma. *J Gastrointest Cancer*, (2017).
206. Y. Sun *et al.* Treatment-induced damage to the tumor microenvironment promotes prostate cancer therapy resistance through WNT16B. *Nat Med* **18**, 1359-1368 (2012).
207. A. Mojtahedi *et al.* Evaluation of apoptosis induction using PARP cleavage on gastric adenocarcinoma and fibroblast cell lines by different strains of Helicobacter pylori. *Pak J Biol Sci* **10**, 4097-4102 (2007).
208. E. B. Traenckner *et al.* Phosphorylation of human I kappa B-alpha on serines 32 and 36 controls I kappa B-alpha proteolysis and NF-kappa B activation in response to diverse stimuli. *EMBO J* **14**, 2876-2883 (1995).
209. J. Yang *et al.* Pro-survival effects by NF-kappaB, Akt and ERK(1/2) and anti-apoptosis actions by Six1 disrupt apoptotic functions of TRAIL-Dr4/5 pathway in ovarian cancer. *Biomed Pharmacother* **84**, 1078-1087 (2016).
210. Y. Sanchez *et al.* Conservation of the Chk1 checkpoint pathway in mammals: linkage of DNA damage to Cdk regulation through Cdc25. *Science* **277**, 1497-1501 (1997).
211. A. Volonte *et al.* Cancer-initiating cells from colorectal cancer patients escape from T cell-mediated immunosurveillance in vitro through membrane-bound IL-4. *J Immunol* **192**, 523-532 (2014).
212. M. Kloor *et al.* Clinical significance of microsatellite instability in colorectal cancer. *Langenbecks Arch Surg* **399**, 23-31 (2014).
213. F. Quesada-Calvo *et al.* OLFM4, KNG1 and Sec24C identified by proteomics and immunohistochemistry as potential markers of early colorectal cancer stages. *Clin Proteomics* **14**, 9 (2017).
214. Q. Yang *et al.* Immuno-proteomic discovery of tumor tissue autoantigens identifies olfactomedin 4, CD11b, and integrin alpha-2 as markers of colorectal cancer with liver metastases. *J Proteomics* **168**, 53-65 (2017).
215. L. G. van der Flier *et al.* OLFM4 is a robust marker for stem cells in human intestine and marks a subset of colorectal cancer cells. *Gastroenterology* **137**, 15-17 (2009).
216. K. K. Kim *et al.* Up regulation of GW112 Gene by NF kappaB promotes an antiapoptotic property in gastric cancer cells. *Mol Carcinog* **49**, 259-270 (2010).
217. X. Zhang *et al.* GW112, a novel antiapoptotic protein that promotes tumor growth. *Cancer Res* **64**, 2474-2481 (2004).
218. L. Chen *et al.* Olfactomedin 4 suppresses prostate cancer cell growth and metastasis via negative interaction with cathepsin D and SDF-1. *Carcinogenesis* **32**, 986-994 (2011).
219. W. Liu *et al.* Reduced hGC-1 protein expression is associated with malignant progression of colon carcinoma. *Clin Cancer Res* **14**, 1041-1049 (2008).
220. F. Simpson *et al.* SH3-domain-containing proteins function at distinct steps in clathrin-coated vesicle formation. *Nat Cell Biol* **1**, 119-124 (1999).
221. C. Shang *et al.* SH3GL2 gene participates in MEK-ERK signal pathway partly by regulating EGFR in the laryngeal carcinoma cell line Hep2. *Med Sci Monit* **16**, BR168-173 (2010).
222. S. Dasgupta *et al.* SH3GL2 is frequently deleted in non-small cell lung cancer and downregulates tumor growth by modulating EGFR signaling. *J Mol Med (Berl)* **91**, 381-393 (2013).
223. G. P. Maiti *et al.* Overexpression of EGFR in head and neck squamous cell carcinoma is associated with inactivation of SH3GL2 and CDC25A genes. *PLoS One* **8**, e63440 (2013).

224. S. Majumdar *et al.* Loss of Sh3gl2/endophilin A1 is a common event in urothelial carcinoma that promotes malignant behavior. *Neoplasia* **15**, 749-760 (2013).
225. Y. Zhu *et al.* Loss of SH3GL2 promotes the migration and invasion behaviours of glioblastoma cells through activating the STAT3/MMP2 signalling. *J Cell Mol Med* **21**, 2685-2694 (2017).
226. A. Kannan *et al.* Mitochondrial Reprogramming Regulates Breast Cancer Progression. *Clin Cancer Res* **22**, 3348-3360 (2016).
227. B. R. Driver *et al.* Folate Receptor alpha Expression Level Correlates With Histologic Grade in Lung Adenocarcinoma. *Arch Pathol Lab Med* **140**, 682-685 (2016).
228. T. Kato *et al.* Nanoparticle targeted folate receptor 1-enhanced photodynamic therapy for lung cancer. *Lung Cancer* **113**, 59-68 (2017).
229. H. Shi *et al.* A current review of folate receptor alpha as a potential tumor target in non-small-cell lung cancer. *Drug Des Devel Ther* **9**, 4989-4996 (2015).
230. B. M. Necela *et al.* Folate receptor-alpha (FOLR1) expression and function in triple negative tumors. *PLoS One* **10**, e0122209 (2015).
231. S. Senol *et al.* Folate receptor alpha expression and significance in endometrioid endometrium carcinoma and endometrial hyperplasia. *Int J Clin Exp Pathol* **8**, 5633-5641 (2015).
232. S. Notaro *et al.* Evaluation of folate receptor 1 (FOLR1) mRNA expression, its specific promoter methylation and global DNA hypomethylation in type I and type II ovarian cancers. *BMC Cancer* **16**, 589 (2016).
233. F. Leung *et al.* Validation of a Novel Biomarker Panel for the Detection of Ovarian Cancer. *Cancer Epidemiol Biomarkers Prev* **25**, 1333-1340 (2016).
234. S. A. Farkas *et al.* DNA methylation and expression of the folate transporter genes in colorectal cancer. *Tumour Biol* **36**, 5581-5590 (2015).
235. P. Lampropoulos *et al.* TGF-beta signalling in colon carcinogenesis. *Cancer Lett* **314**, 1-7 (2012).
236. J. Massague. TGF-beta signal transduction. *Annu Rev Biochem* **67**, 753-791 (1998).
237. R. Derynck *et al.* TGF-beta signaling in tumor suppression and cancer progression. *Nat Genet* **29**, 117-129 (2001).
238. L. M. Wakefield *et al.* Beyond TGFbeta: roles of other TGFbeta superfamily members in cancer. *Nat Rev Cancer* **13**, 328-341 (2013).
239. M. Villalba *et al.* Role of TGF-beta in metastatic colon cancer: it is finally time for targeted therapy. *Cell Tissue Res* **370**, 29-39 (2017).
240. S. Penuelas *et al.* TGF-beta increases glioma-initiating cell self-renewal through the induction of LIF in human glioblastoma. *Cancer Cell* **15**, 315-327 (2009).
241. R. A. de Almeida *et al.* Control of MYEOV protein synthesis by upstream open reading frames. *J Biol Chem* **281**, 695-704 (2006).
242. J. Takita *et al.* Aberrations of NEGR1 on 1p31 and MYEOV on 11q13 in neuroblastoma. *Cancer Sci* **102**, 1645-1650 (2011).
243. K. Sugahara *et al.* Combination effects of distinct cores in 11q13 amplification region on cervical lymph node metastasis of oral squamous cell carcinoma. *Int J Oncol* **39**, 761-769 (2011).
244. J. Brown *et al.* Genomic imbalances in esophageal carcinoma cell lines involve Wnt pathway genes. *World J Gastroenterol* **17**, 2909-2923 (2011).
245. N. Coccaro *et al.* MYEOV gene overexpression in primary plasma cell leukemia with t(11;14)(q13;q32). *Oncol Lett* **12**, 1460-1464 (2016).
246. G. Lawlor *et al.* MYEOV (myeloma overexpressed gene) drives colon cancer cell migration and is regulated by PGE2. *J Exp Clin Cancer Res* **29**, 81 (2010).
247. Z. Ao *et al.* Tumor angiogenesis of SCLC inhibited by decreased expression of FMOD via downregulating angiogenic factors of endothelial cells. *Biomed Pharmacother* **87**, 539-547 (2017).
248. B. Mondal *et al.* Integrative functional genomic analysis identifies epigenetically regulated fibromodulin as an essential gene for glioma cell migration. *Oncogene* **36**, 71-83 (2017).

249. N. Reyes *et al.* The small leucine rich proteoglycan fibromodulin is overexpressed in human prostate epithelial cancer cell lines in culture and human prostate cancer tissue. *Cancer Biomark* **16**, 191-202 (2016).
250. A. Mange *et al.* An integrated cell line-based discovery strategy identified follistatin and kallikrein 6 as serum biomarker candidates of breast carcinoma. *J Proteomics* **142**, 114-121 (2016).
251. N. Ahmed *et al.* Clinical relevance of kallikrein-related peptidase 6 (KLK6) and 8 (KLK8) mRNA expression in advanced serous ovarian cancer. *Biol Chem* **397**, 1265-1276 (2016).
252. L. Stone. Prostate cancer: In a SNP: KLK6 mutations in aggressive disease. *Nat Rev Urol* **14**, 326-327 (2017).
253. J. Thierauf *et al.* Expression of Kallikrein-Related Peptidase 6 in Primary Mucosal Malignant Melanoma of the Head and Neck. *Head Neck Pathol* **11**, 314-320 (2017).
254. E. Sells *et al.* Specific microRNA-mRNA Regulatory Network of Colon Cancer Invasion Mediated by Tissue Kallikrein-Related Peptidase 6. *Neoplasia* **19**, 396-411 (2017).
255. L. Ohlsson *et al.* Lymph node tissue kallikrein-related peptidase 6 mRNA: a progression marker for colorectal cancer. *Br J Cancer* **107**, 150-157 (2012).
256. D. R. Laks *et al.* A Molecular Cascade Modulates MAP1B and Confers Resistance to mTOR Inhibition in Human Glioblastoma. *Neuro Oncol*, (2017).
257. A. Gadoth *et al.* Microtubule-associated protein 1B: Novel paraneoplastic biomarker. *Ann Neurol* **81**, 266-277 (2017).
258. M. Ferracin *et al.* The methylator phenotype in microsatellite stable colorectal cancers is characterized by a distinct gene expression profile. *J Pathol* **214**, 594-602 (2008).
259. B. Hieronimus *et al.* Expression and Characterization of Membrane-Type 4 Matrix Metalloproteinase (MT4-MMP) and its Different Forms in Melanoma. *Cell Physiol Biochem* **42**, 198-210 (2017).
260. M. T. Brazao-Silva *et al.* Metallothionein gene expression is altered in oral cancer and may predict metastasis and patient outcomes. *Histopathology* **67**, 358-367 (2015).
261. A. Truong *et al.* Dynamics of internalization and recycling of the prometastatic membrane type 4 matrix metalloproteinase (MT4-MMP) in breast cancer cells. *FEBS J* **283**, 704-722 (2016).
262. Y. Wang *et al.* Expression and clinical significance of matrix metalloproteinase-17 and -25 in gastric cancer. *Oncol Lett* **9**, 671-676 (2015).
263. M. Y. Liu *et al.* Identification of key genes associated with cervical cancer by comprehensive analysis of transcriptome microarray and methylation microarray. *Oncol Lett* **12**, 473-478 (2016).
264. Y. Sun *et al.* SFRP2 augments WNT16B signaling to promote therapeutic resistance in the damaged tumor microenvironment. *Oncogene* **35**, 4321-4334 (2016).
265. Y. Kamei *et al.* Human NB-2 of the contactin subgroup molecules: chromosomal localization of the gene (CNTN5) and distinct expression pattern from other subgroup members. *Genomics* **69**, 113-119 (2000).
266. S. Worch *et al.* Genomic organization and expression pattern of scapinin (PHACTR3) in mouse and human. *Cytogenet Genome Res* **115**, 23-29 (2006).